Active and Passive Precision Grip Responses to

Unexpected Perturbations

by

Michael De Gregorio

A Dissertation Presented in Partial Fulfillment
of the Requirements for the Degree
Doctor of Philosophy

Approved July 2013 by the
Graduate Supervisory Committee:

Veronica J. Santos, Chair
Panagiotis K. Artemiadis
Marco Santello
Thomas Sugar
Stephen I. Helms Tillery

ARIZONA STATE UNIVERSITY

August 2013

ABSTRACT

The development of advanced, anthropomorphic artificial hands aims to provide upper extremity amputees with improved functionality for activities of daily living. However, many state-of-the-art hands have a large number of degrees of freedom that can be challenging to control in an intuitive manner. Automated grip responses could be built into artificial hands in order to enhance grasp stability and reduce the cognitive burden on the user. To this end, three studies were conducted to understand how human hands respond, passively and actively, to unexpected perturbations of a grasped object along and about different axes relative to the hand. The first study investigated the effect of magnitude, direction, and axis of rotation on precision grip responses to unexpected rotational perturbations of a grasped object. A robust "catch-up response" (a rapid, pulse-like increase in grip force rate previously reported only for translational perturbations) was observed whose strength scaled with the axis of rotation. Using two haptic robots, we then investigated the effects of grip surface friction, axis, and direction of perturbation on precision grip responses for unexpected translational and rotational perturbations for three different hand-centric axes. A robust catch-up response was observed for all axes and directions for both translational and rotational perturbations. Grip surface friction had no effect on the stereotypical catch-up response. Finally, we characterized the passive properties of the precision grip-object system via robot-imposed impulse perturbations. The hand-centric axis associated with the greatest translational stiffness was different than that for rotational stiffness. This work expands our

understanding of the passive and active features of precision grip, a hallmark of human dexterous manipulation. Biological insights such as these could be used to enhance the functionality of artificial hands and the quality of life for upper extremity amputees.

# DEDICATION

This work could not have been completed without the love and support of the soon-to-be Mrs. Charise De Gregorio. Thank you for being there for me when I thought this was impossible, and for constantly reminding me that I am in a forest and shouldn't focus on only one tree.

In memoriam of Kevin Bair.

"The flame that burns twice as bright burns half as long." - Lao Tzu

# ACKNOWLEDGMENTS

Over the past five years I have worked hard toward this culminating moment. However, **none** of this work would have been possible without the following people:

Dr. Veronica Santos, you have been a mentor in the fullest extent of the word. Thank you for your patience, your advice, your time, and your faith in me. Without you, I would not be where I am today, and this document would certainly not exist.

Dr. Panagiotis Artemiadis, Dr. Marco Santello, Dr. Thomas Sugar, and Dr. Stephen Helms Tillery, thank you for your expertise and support. Your direction was essential in shaping this work.

Fellow members of the ASU Biomechatronics lab, thank you for being a sounding board for crazy ideas. If any of you need a committee member, just let me know.

The material presented in herein is based upon work supported by the National Science Foundation under Grant No. 0954254 and the ASU Ira A. Fulton Schools of Engineering. Any opinions, findings, and conclusions or recommendations expressed in this material are those of the author(s) and do not necessarily reflect the views of the National Science Foundation.

For their help with the work presented in Chapter 3, the author would like to acknowledge Dr. Kevin Keenan for guidance in the EMG analysis, Dr. Marco Santello, Dr. Stephen Helms Tillery, and Dr. Qiushi Fu for technical feedback, and Kevin Bair, Nicholas Fette, and Ryan Manis for data collection and processing.

For their help with the work presented in Chapters 4 and 5, the author would like to acknowledge Dr. Panagiotis Artemiadis for guidance in the stiffness classification analysis, Dr. Marco Santello for the use of equipment and laboratory space, Dr. Qiushi Fu for assistance with the phantom set up, and Juan Soto for data collection.

## TABLE OF CONTENTS

CHAPTER Page

CHAPTER Page

CHAPTER Page

LIST OF TABLES

TABLE Page

LIST OF FIGURES

FIGURE Page

# CHAPTER 1

# INTRODUCTION

With the advent of anthropomorphic robotic and prosthetic hands come both the promise of increased functionality of artificial hands and the non-trivial challenges of controlling a large number of degrees of freedom. Engineers can reduce the cognitive burden on the operators of artificial hands by designing automated grip responses into the control of the hand itself. Of course, care must be taken so as not to undermine the independence of the human operator. If implemented well, automated grip responses (artificial reflexes) could intervene in a manner that is transparent to the user and buys time for processing and two-way communication between the operator and the manipulator.

Building intelligence into artificial systems has long been an approach in the field of robotics. In the 1980s, roboticists proposed a reflexive control architecture that directly linked sensing and actuation in artificial systems (Bekey & Tomovic, 1986). “Grasp pre-shaping” is a good example of how visual feedback on object shape has been used to implement pre-programmed grasp postures (Allen, Ciocarlie, Goldfeder, & Dang, 2009; Santello, Flanders, & Soechting, 1998). While automated pre-shaping could aid in the initial grasp of an object, on-line grasp adjustments such as changes in digit placement or fingertip force vectors may still be necessary to account for erroneous digit placement or perturbations of the grasped object. Much effort has been put into developing dynamic tactile sensors (the reader is referred to (Argall & Billard, 2010; M. H. Lee & Nicholls, 1999; Yousef, Boukallel, & Althoefer, 2011)) and control algorithms that will enable on-line adjustments of fingertip forces using real-time feedback from tactile sensors.

We are particularly interested in on-line grasp adjustments during precision grip, which is fundamental to the human ability to grasp and manipulate objects. In precision grip, or opposition pinch, the grasped object is “pinched between the flexor aspects of the fingers and the opposing thumb” (Napier, 1956). Grasp stability using a two-fingered precision grip is achieved through force closure, which only requires two soft finger contacts for an object in 3D having six degrees of freedom (Prattichizzo & Trinkle, 2008). Assuming minimal changes in digit center of pressure location, grasp stability will depend critically on each digit’s 3D force vector and its relationship to the friction cone determined by the grasped object and the fingerpad skin. Most of this chapter will, therefore, focus on the spatial and temporal coordination of fingertip forces during precision grip.

While biomimicry is not a necessity for engineered solutions to artificial grasp, it is difficult to ignore the ease with which the human hand can manipulate objects. Much inspiration for grasp control algorithms can be taken from neurophysiology studies on human grasp. This chapter begins with a brief overview of key findings from a subset of prior precision grip studies. For more comprehensive reviews, the reader is referred to (R. S. Johansson & Flanagan, 2009; R. S. Johansson, 1996; Roland S. Johansson & Flanagan, 2008). The chapter will conclude with results from a study that, to our knowledge, is the first to investigate grip responses to unexpected torque loads and to show characteristic, yet axis-dependent, "catch-up responses" for conditions other than pure linear slip (De Gregorio & Santos, 2013a). The catch-up response will be described in further detail in Section I.B.2.

**Influence of intrinsic object properties on fingertip forces.**

An object's physical properties (extrinsic and intrinsic) can influence fingertip forces on the object during grasp and manipulation (R. S. Johansson, 1996). Examples of extrinsic object properties include the orientation and motion of the object. Examples of intrinsic object properties include weight, mass distribution, size, texture, frictional condition, shape, surface curvature, and fragility (R. S. Johansson, 1996). A subset of intrinsic object properties and their parametric influences on fingertip force control is addressed here.

**Weight.** In 1984, Westling and Johansson conducted an experiment in which each subject held an object in midair using a precision grip. Experimenters were able to pseudorandomly alter the weight of an object having symmetric grip surfaces without changing its visual appearance (Westling & Johansson, 1984). Subjects performed tasks in which they lifted the object from a table, held the object stationary in midair, and then replaced the object to the table (lift-hold-replace) or lifted the object, held the object in midair, and then allowed the object to slip from their fingertips (lift-hold-slip).

Fingertip forces were reported in normal and tangential components relative to the grip surface. Grip force was defined as the compressive force normal to the grip surface and load force referred to the lifting force tangential to the grip surface for the vertically oriented object. Parallel coordination of grip forces and load forces on the object is believed to be a general control strategy for achieving grasp stability, regardless of grasp configuration or task (R. S. Johansson, 1996). For instance, when subjects were tasked with holding objects of various weights, the static grip forces employed during the static grasp of the object in midair changed in proportion to the weight of the object (Kinoshita, Bäckström, Flanagan, & Johansson, 1997; Westling & Johansson, 1984).

**Frictional condition between object and skin.** The preceding discussion on the influence of object weight on fingertip forces would not be complete without an analysis of the frictional condition between the object and the fingerpad skin. In the same set of experiments previously described, Westling and Johansson also varied frictional conditions by exchanging pairs of grip surfaces (sandpaper, suede, or silk) (Westling & Johansson, 1984). Static grip force changed in proportion to the inverse of the coefficient of static friction at the finger-object interface. That is, static grip force increased as the surface became more slippery. While the relationship between static grip force and weight remained approximately linear, the slope of this linear relationship increased as the surface became more slippery (Westling & Johansson, 1984).

Slip force was defined as the minimum grip force necessary to prevent slip, as determined via trials during which subjects purposefully reduced grip forces until slip occurred (Westling & Johansson, 1984). The relationship between the tangential load force and the normal slip force was determined by the coefficient of friction for the object-skin contact condition. Thus, slip forces would increase as slipperiness increased. Subject-specific safety margins for prevention of slip were defined as the difference between actual grip forces and the slip forces. The safety margin increased with slip force and was, therefore, higher for more slippery surfaces (Westling & Johansson, 1984). Safety margins were relatively low such that excessive grip forces were avoided (R. S. Johansson & Westling, 1984; Westling & Johansson, 1984). It has been postulated that "the manipulative task is apparently underwritten by a program to prevent slips" (R. S. Johansson & Westling, 1988).

**Shape.** Object shape was varied in a 1997 study by Jenmalm and Johansson (P. Jenmalm & Johansson, 1997). The test object had symmetric grip surfaces and was designed such that the angle of the grip surface relative to the vertical plane could be varied from -40° (tapered downward) to 30° (tapered upward) in 10° increments. The grip surfaces were vertical and parallel for the 0° case.

Fingertip forces were reported in horizontal and vertical components. Horizontal forces were not always normal to the grip surface (except for the 0° case), but they were always pointed towards the object's midline. Horizontal forces increased as surface angle increased and the object tapered upward (P. Jenmalm & Johansson, 1997). This relationship held prior to object lift-off and during the static grasp of the object in midair. Vertical forces were relatively independent of surface angle. Interestingly, the components of force normal and tangential to the grip surface maintained an approximately constant ratio regardless of surface angle. As a result, the safety margin for the prevention of linear slip was independent of surface angle (P. Jenmalm & Johansson, 1997).

**Surface curvature.** In 1998, Goodwin et al. conducted an experiment in which curvature of the grip surface was varied for a task requiring object tilt (Goodwin, Jenmalm, & Johansson, 1998). The test object had two symmetric grip surfaces and was designed such that surface curvature could be varied (concave, flat, or convex). Subjects were instructed to grasp the test object and tilt the base of the object up and away from the body using elbow flexion and radial flexion of the wrist. Unlike the prior studies discussed here which addressed linear slip caused by forces tangential to the grip surface, this study addressed *rotational slip* (Kinoshita et al., 1997) caused by tangential torques at the fingertips about an axis perpendicular to the grip surface. Such torques resulted from rotation of the grasped object about the *grip axis* (line connecting the two fingertips).

Rotary slip tests were performed in order to determine the slip force, or grip force below which rotational slip would occur (Goodwin et al., 1998). Interestingly, the experimenters differentiated the importance of each digit by defining a critical digit as the digit that employed the greater of the two slip forces. Any decrease in grip force by this critical digit would lead to undesired rotational slip of the object. Safety margins for prevention of rotational slip were defined as the difference between actual grip forces and the slip force of the critical digit for that trial. It was found that safety margin increased as surface curvature increased and the surface became more convex (Goodwin et al., 1998). However, the relative safety margin, the safety margin expressed as a fraction of grip force, was actually less dependent upon surface curvature (Goodwin et al., 1998; P. Jenmalm, Dahlstedt, & Johansson, 2000) and more dependent upon torque load (Goodwin et al., 1998). Interestingly, the magnitude of the safety margin for rotational slips (Goodwin et al., 1998) was comparable to that for linear slips (Westling & Johansson, 1984).

Grip force for the tilting task had an approximately linear relationship with surface curvature (higher grip forces for more convex surfaces) (Goodwin et al., 1998). Regardless of surface curvature, grip force increased linearly with torsional load throughout the tilting movement (Goodwin et al., 1998). As the object was tilted further upward, the tangential torque at the fingertips increased, and higher grip forces were applied. A similar experiment that varied surface curvature for a lifting task, as opposed to a tilting task, concluded that surface curvature moderately affected slip force but not grip force for linear slips (Per Jenmalm, Goodwin, & Johansson, 1998). It is important to note that the effects of surface curvature on grip forces were greater for tasks in which rotational slip was imminent (tangential torque loads dominated) (Goodwin et al., 1998; P. Jenmalm et al., 2000) as compared to those when linear slip was imminent (linear force loads dominated) (Per Jenmalm et al., 1998).

## Influence of anticipation on fingertip forces

The discussion of anticipation effects on fingertip forces is limited here. For lengthier discussions on the importance of prediction of motor commands and sensory events with respect to control strategies during purposeful object manipulation, the reader is referred to (Flanagan, Bowman, & Johansson, 2006; Roland S. Johansson & Flanagan, 2008; Wing & Flanagan, 1998).

### Anticipated, self-imposed perturbations in bimanual tasks.

Anticipatory or preparatory motor responses are particularly useful when the subject has an expectation or prediction about the grasping task. This is the case for voluntary movements and when perturbations are imposed by subjects themselves, as with a bimanual task. In 1988, Johansson and Westling conducted a study in which subjects grasped a pair of vertical grip plates that were attached to a cup into which balls of various weights could be dropped from different heights (R. S. Johansson & Westling, 1988). In some trials, subjects dropped the ball themselves using the contralateral, non-dominant hand. In other trials, the experimenter dropped the ball such that the load perturbation was unexpected (R. S. Johansson & Westling, 1988). Subjects wore ear phones and had minimal audio feedback. Except for control trials in which subjects had visual feedback, subjects closed their eyes for all trials. Another set of control trials was conducted during which the experimenter interfered with the task by catching the ball dropped by subjects before the ball landed in the cup.

When subjects dropped the ball, grip forces increased after the ball was released in anticipation of the impending impact of the ball with the cup. Grip forces began to increase 150 ms before impact and continued 100 ms after load force peaked (R. S. Johansson & Westling, 1988). This preparatory motor response occurred whether or not the experimenter interfered with the impact of the ball and whether or not visual cues were available. The preparatory grip force magnitude increased with more slippery frictional conditions. The preparatory grip force rate scaled with the weight of the ball and the weight of the grip apparatus. The duration of the grip force increase scaled with the height through which the ball dropped (R. S. Johansson & Westling, 1988).

When the experimenter dropped the ball, there were no preparatory motor responses by subjects. Rather, a reactive grip force response was triggered by the impact of the ball with the cup and began 70-80 ms after the onset of impact (R. S. Johansson & Westling, 1988). As with the preparatory grip force response, the triggered grip force magnitude scaled with the weight of the ball. However, the magnitude of the grip force increase was larger when the experimenter dropped the ball than when subjects dropped the ball. Regardless of who dropped the ball, both grip and load forces increased in parallel (R. S. Johansson & Westling, 1988).

**“Active” objects with unpredictable properties.** Thus far, the fingertip force adaptations described were observed during experiments in which subjects grasped passive objects whose intrinsic physical properties were constant and predictable. For such passive objects, sensorimotor memories could be used to make predictions about the objects for feedforward adjustments of fingertip force. In the early 1990s, Johansson and colleagues conducted a series of experiments (Flanagan et al., 2006; P. Jenmalm et al., 2000; Per Jenmalm et al., 1998) with active objects that exerted unpredictable pulling loads having different force amplitudes (R S Johansson, Riso, Häger, & Bäckström, 1992) and rates (Roland S. Johansson, Häger, & Riso, 1992). The manipulandum consisted of a pair of grip plates that could be pulled in the distal direction by a motor to impose a loading phase (ramped increase in force load), plateau phase (constant force load), and unloading phase (ramped decrease in force load) (R S Johansson et al., 1992). Subjects were instructed to restrain the object upon detection of the pulling load without visual feedback. For the static load phase, the safety margins for the prevention of linear slip appeared similar for passive and active objects (R S Johansson et al., 1992).

As with passive objects, grip force changed with load force during restraint of the active objects. With passive objects, grip and load forces were initiated and scaled in parallel and the grip force rate had a bell-shaped profile (R. S. Johansson & Westling, 1988). With active objects, however, the grip force changes were delayed due to the unpredictable nature of the force loading and unloading (R S Johansson et al., 1992). The grip force rate had a biphasic profile and featured a rapid initial increase in grip force (a pulse-like *"catch-up response"* in grip force rate) that was followed by a period of steadily increasing grip force (a secondary "tracking response" in grip force rate) if the distal load continued to increase after the catch-up response (R S Johansson et al., 1992). The catch-up response allowed the delayed grip force to quickly catch up to the unexpected load force and maintain a sufficient safety margin for the prevention of linear slip. For a constant load force rate, features of the catch-up response such as latency (approximately 140 ms after onset of loading), shape, size, and duration (200-250 ms) were independent of load force amplitude (R S Johansson et al., 1992). When load force rate was varied, the amplitude of the catch-up response increased with load force rate and the grip response latency decreased with load force rate (Roland S. Johansson et al., 1992). Interestingly, the duration of the catch-up response was 200 ms, regardless of the load force rate (Roland S. Johansson et al., 1992). The stereotypical features of the catch-up response, in particular its fixed duration, suggested that the catch-up response was a centrally programmed, default grip response that was released as a unit in response to unexpected increases in load (R S Johansson et al., 1992; Roland S. Johansson et al., 1992). These findings supported prior observations of stereotypical evoked grip force responses (consistent response latencies of 60-90 ms and durations of 100-200 ms) that appeared to be automatic and not consciously mediated (Cole & Abbs, 1988). When finger sensibility was impaired via digital anesthesia, the tracking response disappeared, suggesting that the tracking response is a grip response mechanism that relies critically on cutaneous afferent input to make online grip force adjustments (R. S Johansson, Häger, & Bäckström, 1992).

In 1993, Cole and Johansson used the same active object as in the prior series of experiments (R S Johansson et al., 1992; R. S Johansson et al., 1992; Roland S. Johansson et al., 1992), but also varied frictional condition at the finger-object interface (Cole & Johansson, 1993). The loading profile featured a ramped increase, plateau phase, and ramped decrease in force applied in the distal direction (Cole & Johansson, 1993). The intertrial or preload grip force was defined as the grip force at the onset of the load perturbation. The preload grip force scaled with the inverse of the coefficient of friction (Cole & Johansson, 1993). The more slippery the grip surface, the greater the preload grip force. As in prior studies (R S Johansson et al., 1992; Roland S. Johansson et al., 1992), the grip force profile featured a catch-up and secondary tracking response (Cole &

Johansson, 1993). Features of the catch-up response such as onset latency, shape, and duration were independent of frictional condition (Cole & Johansson, 1993). It was found that the preload grip force greatly affected the scaling of the catch-up and tracking responses, possibly to avoid unnecessarily large or dangerously small safety margins for linear slip at the peak load force (Cole & Johansson, 1993). Since the preload grip force contributes to the overall grip response, increases in this grip force baseline value resulted in decreases in the catch-up and/or tracking responses. Thus, it was postulated that initial state information such as frictional condition could "globally" affect the grip response to unexpected pulling loads by adjusting a "central scaling factor" or "gain" for the load-to-grip sensorimotor transformation (Cole & Johansson, 1993). Larger preload grip forces and, thus, higher safety margins at the start of the trial were employed after slip (Per Jenmalm et al., 1998; R S Johansson & Cole, 1994) and when digital anesthesia was used (Häger-Ross & Johansson, 1996).

**Influence of load direction on fingertip forces.**

Multiple studies have reported that fingertip force responses evoked by unanticipated loads are affected by the direction of the loading (Häger-Ross, Cole, & Johansson, 1996; Häger-Ross & Johansson, 1996; Jones & Hunter, 1992). In a 1992 study, Jones and Hunter reported directional effects of translation loads on the magnitude of the grip force (Jones & Hunter, 1992). Specifically, subjects used larger grip forces for distal loads that pulled away from the palm than for proximal loads that pushed towards the palm. It was postulated that the frictional condition at the finger-object interface was a function of loading direction due to the anisotropic properties of glabrous skin (Jones & Hunter, 1992).

In 1996, Häger-Ross et al. specifically investigated the effects of load direction relative to gravity and hand orientation (Häger-Ross et al., 1996). Subjects had to restrain an active object with two parallel, symmetric grip surfaces with the ulnar side of the hand facing either downward or upward. A motor was used to apply unpredictable loads in the distal, proximal, radial, and ulnar directions. Depending on hand orientation, the radial and ulnar load directions would be in the direction of gravity or opposed to gravity. Regardless of hand orientation, grip force response latencies were shorter for what were referred to as the “dangerous directions”: distal loads as opposed to proximal loads, and directions with gravity instead of against gravity (Häger-Ross et al., 1996). These findings were consistent with another study that varied load direction and support conditions for the hand and forearm (Häger-Ross & Johansson, 1996). Interestingly, the latencies for cutaneous afferent responses were similar for the distal and proximal load directions and, yet, the grip force response latencies were shorter for distal loads (Häger-Ross et al., 1996). It was postulated that load directions relative to both gravity (with or against) and hand geometry (away or towards the palm) serve as “intrinsic task variables” for the central control of grasp stability when faced with unpredictable loads (Häger-Ross et al., 1996). The fact that grip force response latencies and magnitudes were independent of load direction when digital sensibility was impaired suggests that digital sensory inputs play critical roles in reactive grip control (Häger-Ross & Johansson, 1996).

## Influence of sensory feedback on fingertip forces

**Visual feedback.** Visual cues play a critical role in anticipatory parameter control (R. S. Johansson, 1996), a control policy which proposes that fingertip forces are adapted to intrinsic object properties (e.g., shape (P. Jenmalm & Johansson, 1997), size (Gordon, Forssberg, Johansson, & Westling, 1991), weight (Gordon, Westling, Cole, & Johansson, 1993), surface curvature (P. Jenmalm et al., 2000)) in anticipation of force requirements based on prior experience. During grasp experiments in which object shape (grip surface angle) was varied, it was found that visual feedback was used to adjust fingertip force in a feedforward manner from the onset of horizontal force generation (P. Jenmalm & Johansson, 1997). Furthermore, the grip surface angle from the previous trial had no effect on the forces applied in the current trial when visual feedback was available, regardless of whether cutaneous afferent feedback was intact or not (P. Jenmalm & Johansson, 1997).

In a different study that varied the size and weight of objects, visual cues about object size influenced the scaling of fingertip forces during the loading phase even before additional somatosensory cues related to actual object weight became available with object lift-off (Gordon et al., 1991). Subjects usef prior experience, as with common everyday objects, to scale fingertip forces after visually identifying the object and estimating the object’s weight (Gordon et al., 1993). When size and weight were covaried and object density remained constant, visual cues about size were used as indirect measures of weight for anticipatory fingertip force scaling (Gordon et al., 1991).

**Digital feedback.** Digital sensibility plays a critical role in both the shaping of anticipatory grip adjustments that are informed by sensorimotor memories and the shaping of evoked or reactive grip responses to unpredictable load perturbations (Cole & Abbs, 1988; R. S Johansson et al., 1992). Discrete event, sensory-driven control has been proposed as a control policy, used in addition to anticipatory parameter control, that uses discrete mechanical events encoded in the spatiotemporal patterns of sensory inputs to trigger pre-programmed corrective grip responses (R. S. Johansson, 1996). Due to their proximity to the finger-object interface, tactile receptors innervating the glabrous skin are believed to be particularly important for the adaptation of fingertip forces to intrinsic object properties (R. S. Johansson, 1996). It has even been said that "it appears that tactile afferents of the skin in contact with the object are the only species of receptor in the hand capable of triggering and initially scaling an appropriate change in grip force in response to an imposed change in load force" (Macefield & Johansson, 1996).

Multiple studies have addressed the importance of cutaneous afferent feedback to the adaptation of fingertip forces to variations in the frictional condition at the finger-object interface. A 1984 study using a lift-hold-replace task showed that the adaptation of grip forces and load forces to frictional condition was dependent upon input from cutaneous afferents (R. S. Johansson & Westling, 1984). Specifically, afferents innervating the glabrous skin areas that directly contacted the object were important for detecting "local" slip events and estimating the frictional condition (R. S. Johansson & Westling, 1984). It is believed that fast-adapting FA I units are primarily responsible for triggering and initially scaling the automatic, reactive grip force responses to ramped increases in load forces (R.S. Johansson & Westling, 1987; Macefield, Häger-Ross, & Johansson, 1996).

In the absence of visual cues, cutaneous afferent feedback about object shape (P. Jenmalm & Johansson, 1997) and surface curvature (P. Jenmalm et al., 2000) influenced fingertip forces soon after object contact. When grip surface angle was varied, fingertip force adjustments to the new surface angle emerged approximately 100 ms after object contact (P. Jenmalm & Johansson, 1997). When subjects had to rely on cutaneous afferent feedback alone, fingertip forces prior to the 100 ms timepoint were influenced by the previous trial. When surface curvature was varied, fingertip force adjustments to the new surface curvature emerged 100-200 ms after object contact (P. Jenmalm et al., 2000). Again, initial fingertip forces were influenced by the force conditions of the previous trial. Once the new surface curvature was detected, tactile cues were used to adapt fingertip forces in a feedforward manner (P. Jenmalm et al., 2000). While both visual and tactile feedback have been associated with feedforward adjustments of fingertip force (P. Jenmalm et al., 2000; P. Jenmalm & Johansson, 1997), tactile feedback is especially critical for anticipatory grip force adjustments to frictional conditions (Edin, Westling, & Johansson, 1992; R.S. Johansson & Westling, 1987).

Nondigital sensory input from joint receptors, intrinsic and extrinsic hand muscles, and skin strain sensors located away from the fingertips may also contribute to grip responses. Häger-Ross and Johansson observed catch-up responses despite the use of three different support conditions (hand support, forearm support, no support) used to vary the transmission of the perturbations at the fingertips to other segments of the hand and forearm (Häger-Ross & Johansson, 1996). Nonetheless, it is believed that digital inputs are the principal sensory inputs used during reactive grip control (Cole & Abbs, 1988; Häger-Ross & Johansson, 1996; R. S Johansson et al., 1992; R.S. Johansson & Westling, 1987; Macefield et al., 1996; Macefield & Johansson, 1996; Westling & Johansson, 1987). Anesthetization of both digits in a precision grip weakened the effect of load rate on catch-up response strength, increased grip response latencies, and, in some cases, caused the absence of a grip force response altogether (R. S Johansson et al., 1992).

**Overview of experiments**

This dissertation is comprised of three separate studies. Chapter 2 investigates human precision grip responses to unexpected rotationally-dominant step perturbations. Specifically, Chapter 2 discusses the joint kinematics associated with rotational perturbations and describes the characteristics of the catch-up response elicited by the perturbations.

Chapter 3 delves further into the catch-up response and describes precision grip responses to pure translational and pure rotational perturbations imposed by two haptic robots along and about all three hand-centric axes (distal-proximal, radial-ulnar, and grip). The effects of different grip surface friction conditions across the two digits is also studied.

Chapter 4 characterizes the passive properties of the precision grip-object system. Using robot-imposed impulse perturbations, the rotational and translational stiffness of the system were investigated. Chapter 5 concludes with a summary of key contributions of this research and future directions.

# CHAPTER 2

# KINEMATICS AND KINETICS OF PRECISION GRIP RESPONSES TO UNEXPECTED PERTURBATIONS

## INTRODUCTION

When objects in precision grip were perturbed by unpredictable pulling loads, a rapid initial increase in grip force rate, in the form of a “pulse-like” *catch-up response* (R S Johansson et al., 1992), allowed the delayed reactive grip force to catch up to the unexpected load force and maintain a safety margin against linear slip (R. S. Johansson & Westling, 1988). Features of the catch-up response such as onset latency, shape, and duration were independent of load force amplitude (R S Johansson et al., 1992) and frictional condition (Cole & Johansson, 1993). When load force rate increased, strength of the catch-up response increased and onset latency decreased while duration of the catch-up response remained 200ms (Roland S. Johansson et al., 1992). The stereotypical features of the catch-up response suggested it was a centrally-programmed, default grip response that was released as a unit in response to unexpected loading (R S Johansson et al., 1992; R. S Johansson et al., 1992; Roland S. Johansson et al., 1992). These findings supported observations of evoked, automatic reactive grip responses (Cole & Abbs, 1988).

Studies involving self-imposed rotational perturbations suggested that slip conditions may scale grip responses. While linear slip is caused by forces tangential to the grip surface, rotational slip is caused by torques about the axis perpendicular to the grip surface (Kinoshita et al., 1997). However, prior experiments on rotational slip used voluntary tasks such as lifting and holding (P. Jenmalm et al., 2000), lifting and tilting (Goodwin et al., 1998), or releasing one's grasp to allow tilting (Kinoshita et al., 1997). These studies focused only on torque loads about the "grip axis" which connects the two fingertips.

The objectives of this study were twofold: to determine if a catch-up response is elicited by *unexpected rotational perturbations*, and, if so, to determine if features of the catch-up response (onset latency, shape, duration, strength) are dependent on the direction, strength, and/or axis of the perturbation. To our knowledge, this is the first study to investigate grip responses to unexpected torque loads and to show characteristic, yet axis-dependent, catch-up responses for conditions other than pure linear slip.

## MATERIALS AND METHODS

**Experiment.** Eighteen consenting, healthy, right-handed subjects aged 19-38years (nine male, nine female) participated in the study under a protocol approved by the Arizona State University Institutional Review Board.

A motion-capture system (MX-T40 cameras, Vicon) and 3mm diameter hemispherical markers (Mocap Solutions) were used to collect kinematic data at 200 Hz from the thumb and index finger of each subject's dominant hand and an instrumented object (Fig. 2.1A). Surface electromyography (EMG) was used to measure the activity of the first dorsal interosseous (FDI) muscle (EMG 100C, BIOPAC Systems).

The instrumented object had two flat, parallel grip surfaces spaced 39mm apart. Fingertip forces and torques were measured independently for the thumb and index finger at 1.8kHz by six degree-of-freedom force/torque transducers (Nano-25, ATI Industrial Automation) housed within the object, whose total mass was 194g with the transducers. The aluminum grip plates were covered by a single layer of masking tape in order to minimize reflectivity during motion capture.

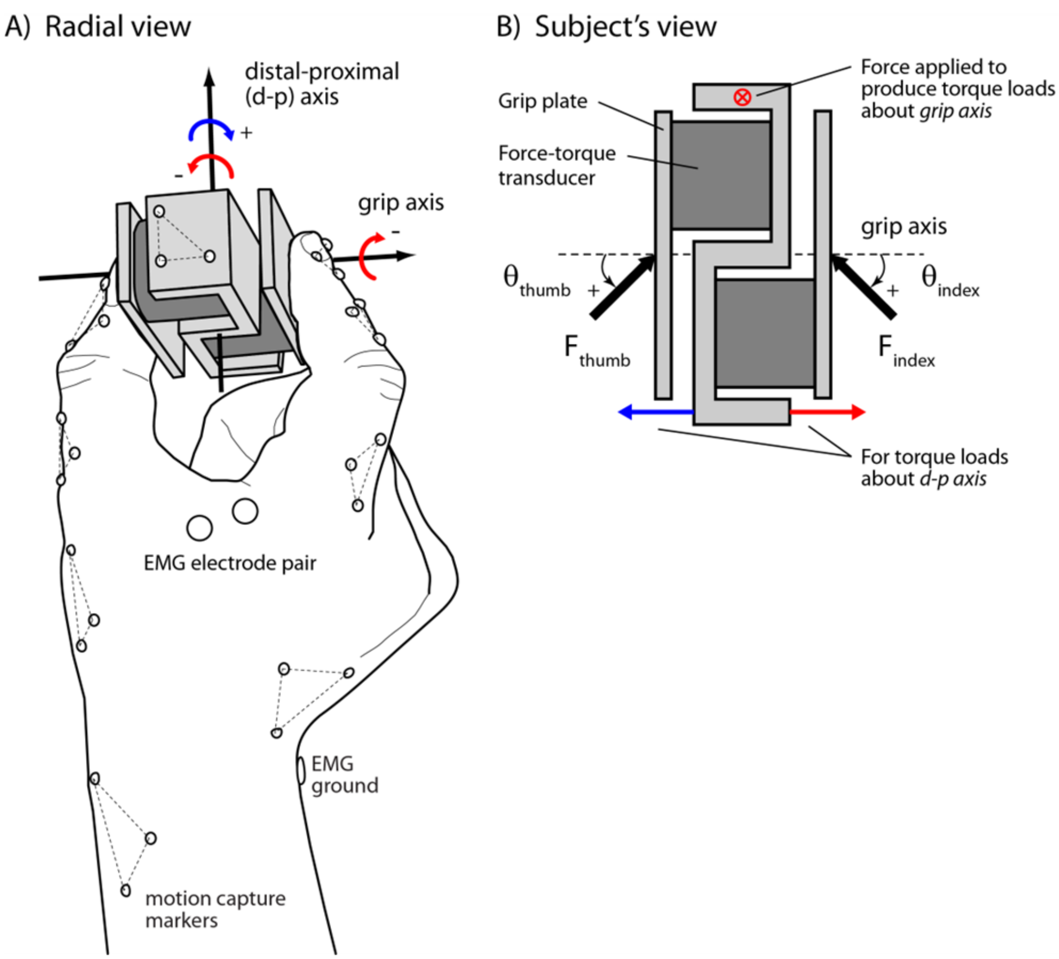


*Figure 2.1. Experimental set-up.* (A) A radial view of the subject's hand is shown with triads of retro-reflective markers (indicated by dotted lines) that were used to track the motion of the thumb, index finger, and instrumented object. Surface EMG was used to record first dorsal interosseous activity. Directions of rotation

(red = negative, blue = positive) were defined with respect to each of two hand-referenced, object-fixed axes: distal-proximal and grip axes. (B) A view from the perspective of the subject of the object shows the locations of the attachment points used to impose rotational perturbations with a cable, mass, and pulley system. The angle $\theta$ of the fingertip force vector was measured relative to the grip surface normal in the plane containing the grip axis. (Adapted from (De Gregorio & Santos, 2013a).)

Rotational perturbations were imposed about two axes which were defined relative to the subject's hand, fixed relative to the object, and passed through the object's center of mass (Fig. 2.1A): the distal-proximal ("d-p") axis away from and towards the subject's palm, and the grip axis. Positive and negative rotations were imposed about the d-p axis while only a negative rotation was imposed about the grip axis such that the top of the object tilted away from the subject's palm. Perturbations were imposed using a mass and pulley system attached to the object via lightweight, inextensible fishing line (200 lbf braided line, PowerPro). An unexpected, step torque load was imposed during each 5 sec trial by dropping a mass (100g or 150g) vertically by 5cm at a random time and leaving the mass hanging. No significant swinging of the mass was observed. *Object-moments* (externally-applied torque loads) were imposed by attaching the fishing line to points 34.3mm above or below the object's center of mass (Fig. 2.1B, Table 2.1). Each subject sat upright with the dominant arm supported by a tabletop, elbow flexed, and forearm parallel to the tabletop and perpendicular to the subject's frontal plane. With each subject's dominant hand and wrist unsupported at the end of the table, a vacuum positioning pillow (Versa Form, Sammons Preston) and velcro strap constrained the subject's forearm to the tabletop. Hand pronation and supination were restricted while wrist flexion/extension and radio-ulnar deviation were not.

At the start of each 5-trial experimental block, subjects were handed the instrumented object and instructed to hold the object upright using a precision grip with the thumb and index finger each centered on its own grip plate and directly opposed to one another, with the other digits curled towards their palm as if making a fist (Fig. 2.1A). The instructions given to subjects were to hold the object with just enough force to keep it aloft, return the object to its initial orientation as soon as a randomly-timed perturbation was detected, avoid dropping the object, and notify the researcher if he/she felt fatigued. To minimize visual cues about the perturbation, subjects were instructed to look towards a fixed location away from the object and investigator. There were no auditory cues for the perturbation.

Presented to subjects in the order shown in Table 2.1, six experimental blocks used combinations of levels for three factors: axis of rotation (d-p, grip axis), direction of rotation (positive, negative), and object-moment magnitude (small, large). After each block, subjects received a mandatory 30sec rest period during which the object was taken from the subject and prepared for the next block. No practice trials were allowed.

**Data analysis.** Motion capture data were processed with MATLAB

(Mathworks) after using Vicon Nexus software to ensure complete marker sets. Object kinematics were used to determine the onset of object perturbation (defined as “t=0sec”), verify the predominance of rotational motion in each perturbation, and synchronize trials. Angular deviations of the object from its initial upright orientation were measured about the axis of interest (Fig. 2.1A) and averaged across trials for each block on a subject-specific basis. Extracted from mean data, the peak angular deviation of the object was defined as the maximum magnitude of rotation of the object from its initial orientation.

FDI surface EMG data were full-wave rectified, filtered using a fourth-order, 50Hz low-pass Chebyshev filter (Hodges & Bui, 1996), and normalized using maximum voluntary contraction data collected at the start of the experiment. For each subject, all trials for a given block were averaged to ensure that trends in muscle activation were consistent. Conservative activation threshold values were set at three standard deviations of the baseline noise prior to the onset of object perturbation (averaged over each subject-specific block). The FDI was deemed active if EMG activity (averaged over a single block) remained above threshold for a continuous period of at least 50ms (Hodges & Bui, 1996). Visual inspection verified that the activation thresholds resulted in reliable threshold crossings (Di Fabio, 1987). The time to initial FDI activation (time of the first upward threshold crossing relative to the onset of object perturbation) was used as the *onset latency of the catch-up response*. Due to poor connectivity, EMG data is only presented for 15-17 subjects, depending on the perturbation conditions.

Fingertip force and torque data were filtered using a fourth order, 30Hz low-pass Butterworth filter (Jordan & Newell, 2004). Force data for individual trials were averaged for each block on a subject-specific basis to ensure consistent extraction of key features (Cole & Johansson, 1993; Edin et al., 1992; Goodwin et al., 1998; P. Jenmalm et al., 2000). Normal force rates were obtained from first-order differences of normal forces for each individual trial while accounting for sampling rate, averaging those data for each block on a subject-specific basis, and smoothing with a moving boxcar average having a width of 50ms. Extracted from mean data, peak normal force was used to mark the end of the catch-up response in order to determine the duration of the catch-up response, and peak normal force rate was used to define the *strength of the catch-up response*.

**Statistical analysis.** The data could not be transformed into normal distributions using square-root, log, or inverse sine functions. Thus, we used the Kruskal-Wallis test (nonparametric analogue to the one-way ANOVA) with an alpha level of 0.05 to evaluate the independent effects of three factors: axis of rotation (d-p, grip), direction of rotation (positive, negative), and object-moment magnitude (small, large) (Table 2.1), and to test whether quantities of interest could be pooled across digits. Summary data are reported as either median ranges or median ± median absolute deviation (MAD) unless otherwise specified.

Table 2.1.

*Experimental Block Conditions*

| Experimental block # | Experimental factors: Axis of rotation | Direction of rotation | Object-moment magnitude (OMM) [mN-m] |
|---|---|---|---|
| 1 | Distal-proximal | Positive | 33.6 |
| 2 | | | 50.5 |
| 3 | | Negative | 50.5 |
| 4 | | | 33.6 |
| 5 | Radial-ulnar | Positive | 6.7 |
| 6 | | | 10.0 |
| 7 | | Negative | 10.0 |
| 8 | | | 6.7 |
| 9 | Grip | Negative | 33.6 |
| 10 | | | 50.5 |

## RESULTS

For rotations about the d-p axis, the object was twisted clockwise or counter-clockwise as viewed from the subject's perspective (Fig. 2.1). For rotations about the grip axis, the top of the object was tilted away from the subject's palm. Subjects could halt the tilting, but were unable to restore the object to its initial upright orientation.

**Joint angles.** A kinematic analysis for perturbations about the d-p axis revealed that abduction/adduction responses were elicited in the thumb and index finger in addition to flexion/extension (Figs. 2.2 and 2.3). Peak index finger joint angles were synchronized with peak object rotation angles (~65-80 ms after perturbation) while thumb joint angles lagged behind (De Gregorio, Bair, &

Santos, 2009). However, the time from perturbation onset to peak angular deviation of the object ranged from 130 to 278 ms (averaged across all trials for each perturbation direction and magnitude).

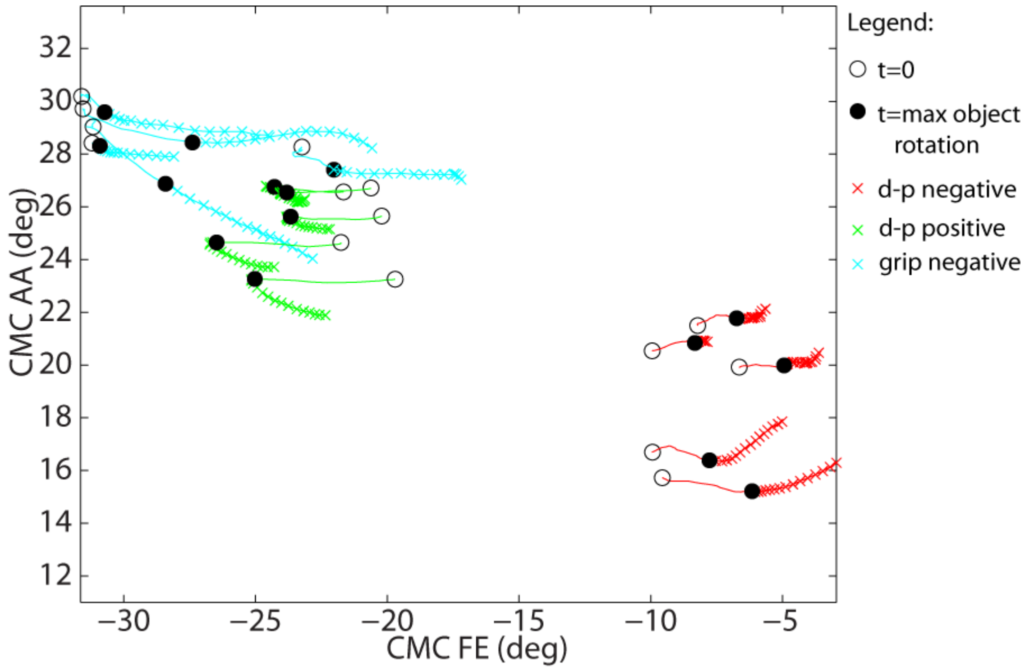


*Figure 2.2. Thumb carpometacarpal (CMC) joint angles for adduction/abduction (AA) and flexion/extension (FE) for the 50.5 N-mm case.* Open circles indicate the onset of the perturbation. Closed circles indicate the time of maximum object rotation. X's are shown for the 0-75 ms window following the time of maximum object rotation. Data are shown for a representative subject.

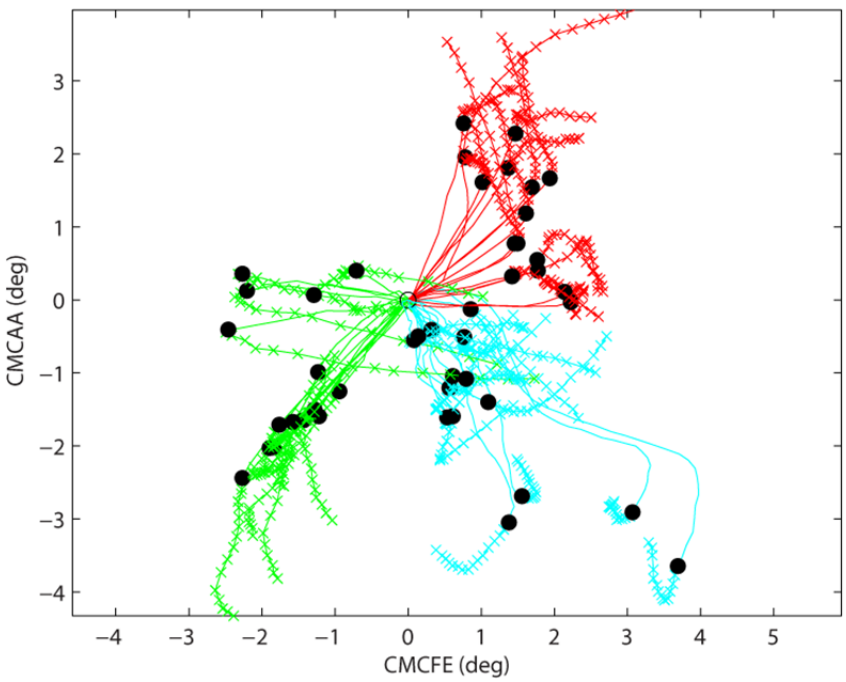


*Figure 2.3. Thumb carpometacarpal (CMC) joint angles for adduction/abduction (AA) and flexion/extension (FE) for the 50.5 N-mm case (change from initial posture).* Open circles indicate the onset of the perturbation. Closed circles indicate the time of maximum object rotation. X's are shown for the 0-75 ms window following the time of maximum object rotation. Red, green, and cyan indicate d-p negative, d-p positive, and grip negative experimental conditions. Data are shown for three subjects.

**Catch-up response.** Shortly after the onset of perturbation, FDI became active and a unimodal catch-up response began (Fig. 2.4), during which digit normal forces increased and decreased in parallel. The period from the onset of perturbation (“a”, Fig. 2.4) until FDI activation (“b”, Fig. 2.4) was considered as the passive phase, and was characterized by smooth, unimodal tangential fingertip forces immediately after the onset of perturbation (Fig. 2.5). The large ± MAD ranges after FDI activation were consistent with an increase in neuromuscular activity.

An active unimodal catch-up response was clearly observed in the normal force rates for all subjects, both digits, and all blocks (representative block shown in Fig. 2.4, multiple blocks shown in Fig. 2.6). The catch-up response began with FDI activation (“b”, Fig. 2.4) and ended with peak normal force (“d”, Fig. 2.4). FDI activity began 71-89ms after the onset of perturbation (Fig. 2.7, Table 2.2), the time to peak normal force was 283-319ms after the onset of perturbation, and the duration of the catch-up response was 217-231ms (Table 2.2). Time to peak normal force rate (127-152ms, Table 2.2), onset latency, and duration of the catch-up response were not affected by any experimental factor: axis of rotation, direction of rotation, or object-moment magnitude.

For all subjects, digits, and object-moment magnitudes, the strength of the catch-up response and peak normal force were greatest for rotational perturbations about the grip axis (Figs. 2.6 and 2.8, Table 2.2), which tilted the top of the object away from the subject’s palm and induced rotational slip. Strength of the catch-up response and peak normal force were 31-55N/s and 6-7N greater for rotations about the grip axis than for rotations about the d-p axis, respectively. Strength of the catch-up response was not affected by direction of rotation and was only affected by object-moment magnitude for one type of rotation (positive rotations about the d-p axis, Fig. 2.8).

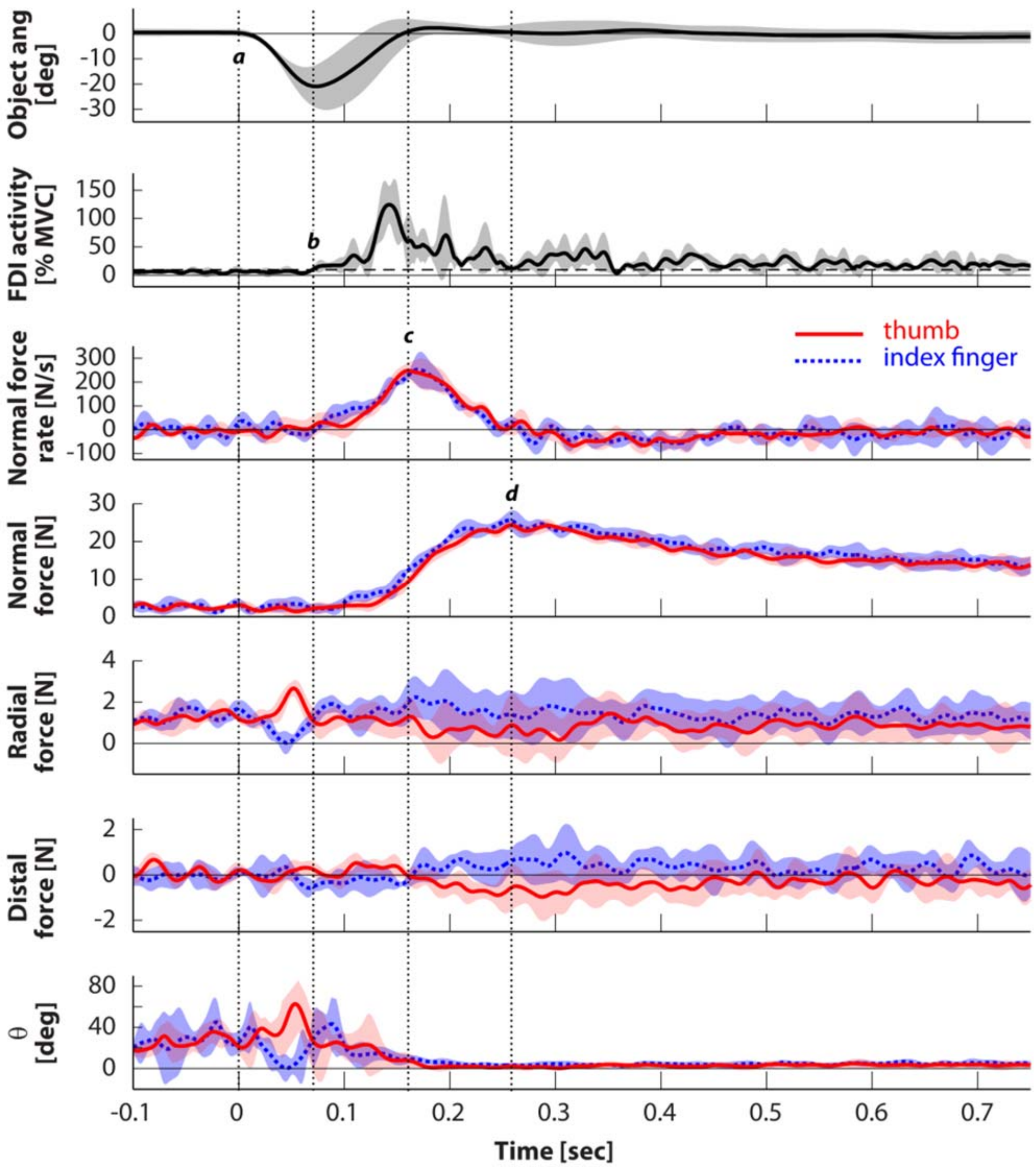


*Figure 2.4. Object angle, FDI activity, and fingertip forces, rates, and angles as a function of time.* Mean data are reported for a representative subject for a single block of experiments (large object-moment magnitude, negative rotation about the distal-proximal axis) for angle of deviation of the object, FDI activity (normalized by maximum voluntary contraction), normal force rate, normal, distal, and radial force components, and angle $\theta$ of the fingertip force vector relative to the grip

surface normal. The thumb (mean = solid red line) and index finger (mean = dotted blue line) data could be pooled. The shaded region (red and blue for thumb and index finger, respectively) around each mean trace represents ± SEM across five trials. Vertical dotted lines indicate times for: *a* onset of perturbation; *b* start of the catch-up response (time to FDI activation); *c* strength of catch-up response (peak normal force rate); and *d* end of the catch-up response (peak normal force). Each digit's fingertip forces are reported relative to an object-fixed reference frame in terms of normal components (+ refers to compressive forces along the grip axis) and tangential components (+ refers to forces in the radial direction that point towards the top of the object or to forces in the distal direction that point away from the subject along the d-p axis). A distinct unimodal catch-up response was observed in the normal force rate data for each digit. (Adapted from (De Gregorio & Santos, 2013a).)

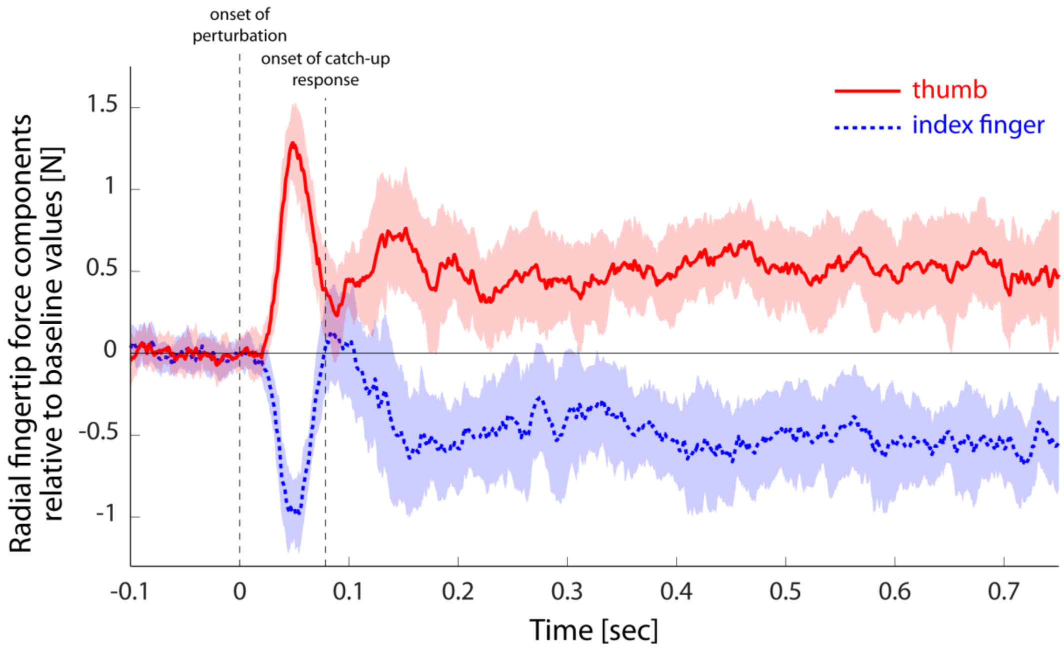


*Figure 2.5. Variability in radial fingertip force components.* For clarity, radial force components relative to baseline values (prior to perturbation) are shown in order to account for trial-to-trial variations in baseline fingertip forces. Trends are shown for negative rotations about the distal-proximal axis, for all 18 subjects, for both object-moment magnitudes (n = 35 trials total), and both the thumb (solid red line) and index finger (dotted blue line). Thick lines represent median values and shaded regions represent the ± MAD ranges. Radial force components exhibited the least variability from the onset of perturbation (dashed vertical line at t=0 sec) to first dorsal interosseous activation at 83.9 ± 12.8 ms (dashed vertical line marking the onset of the catch-up response). (Reprinted with permission from (De Gregorio & Santos, 2013a).)

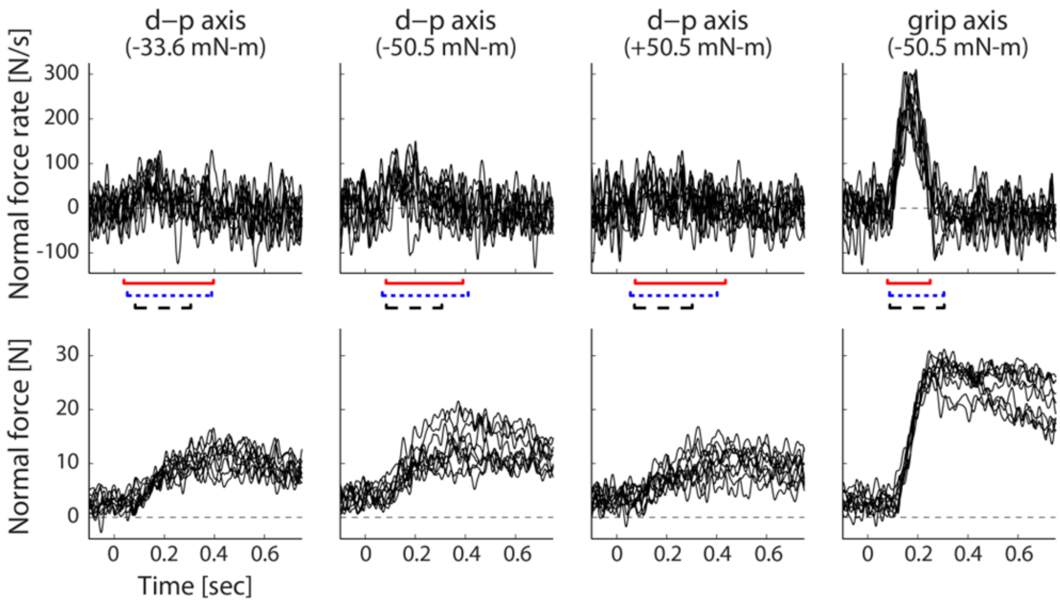


*Figure 2.6. Normal force rate and normal force as a function of time for different blocks.* Unimodal catch-up responses were observed in the normal force rates for all object-moment magnitudes, rotation directions, and rotation axes. Individual trial data (n = 5 trials) for one subject are shown here for both digits and five blocks. Catch-up responses were strongest for rotations about the grip axis. Positive normal forces correspond to compressive forces along the grip axis. Solid red and dotted blue lines beneath the normal force rates plots indicate the duration of the catch-up response for the thumb and index finger, respectively. Median values from Table 2.1 are indicated by dashed black lines. (Adapted from (De Gregorio & Santos, 2013a).)

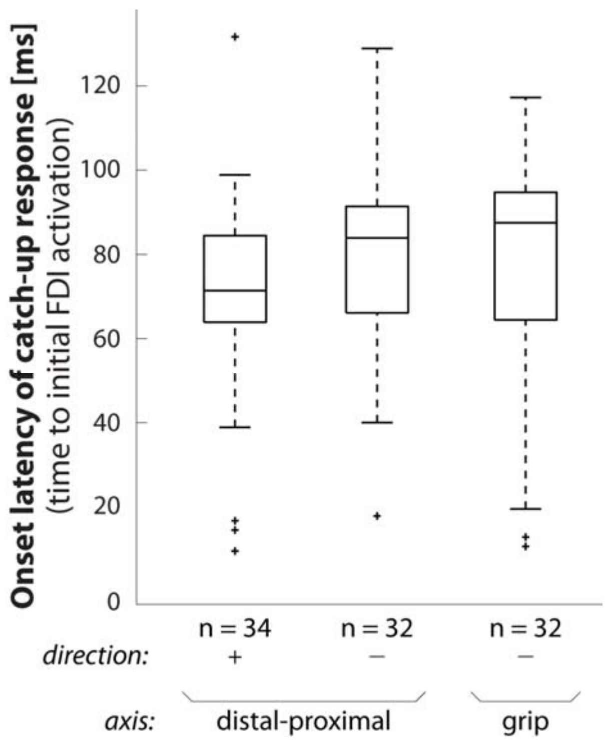


*Figure 2.7. Onset latency of the catch-up response (time to first dorsal interosseous activation).* The box plots show the time to first dorsal interosseous (FDI) activation which was used to mark the start of the catch-up response. FDI was considered to be active if the surface EMG signal crossed a threshold of 3 SD of the baseline noise and remained above threshold for at least 50 ms. Short latency values resulted from the fact that we report time to *first* activation according to our conservative activation criteria even though FDI activity may have briefly fallen below the activation threshold afterwards. Each box plot consists of data pooled across the small and large object-moment magnitudes for each rotation condition (from left to right: *n*=[34, 32, 32] mean values total). Each box plot indicates the 25th, 50th, and 75th percentiles. The whiskers indicate the 10th and 90th percentiles. Outliers (indicated by "+") had values that were more than 1.5 times the interquartile range from the top or the bottom of the box.

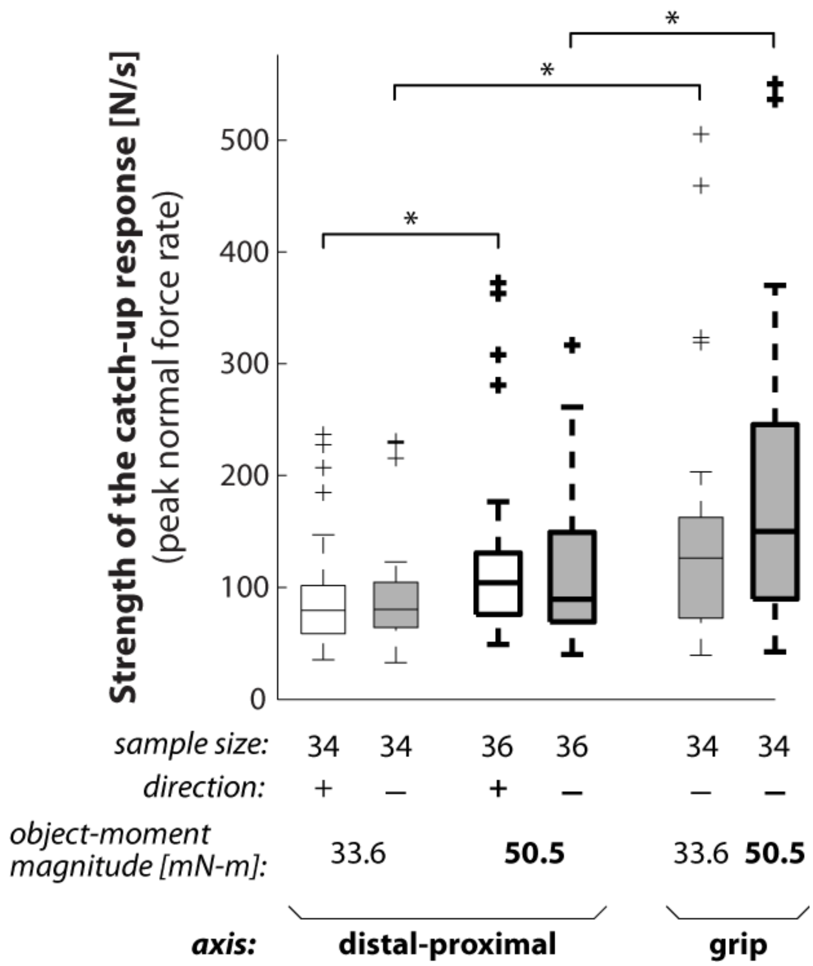


*Figure 2.8. Strength of the Catch-up response (peak normal force rate).* Each column represents strength of the catch-up response pooled across the thumb and index finger for 18 subjects. Thicker box plots are used for large object-moment magnitudes. Shaded boxplots are used for negative rotations. Catch-up responses were strongest for rotations about the grip axis. Asterisks indicate statistically significantly differences across groups. Each box plot indicates the 25th, 50th, and 75th percentiles. The whiskers indicate the 10th and 90th percentiles. Outliers (indicated by "+") had values that were more than 1.5 times the interquartile range from the top or the bottom of the box.

## DISCUSSION

**Adduction and abduction play a role in correction of rotational perturbations.** The kinematic responses for the thumb and index finger to rotational perturbations involve both adduction/abduction and flexion/extension motions. The joint angle data clustered according to specific perturbation axis and direction combinations (Fig. 2.2). .

As observed in this study, rotational perturbations to grasped objects involve adduction/abduction joints in addition to flexion/extension joints. This finding suggests that control of adduction and abduction joints should also be considered when developing grip response controllers for anthropomorphic artificial hands that include these degrees of freedom. Furthermore, if tactile and/or proprioceptive feedback, such as joint angles, were available in an artificial hand system, these data could be used to invoke a context-appropriate grip response.

**Existence of the catch-up response for rotational perturbations.** Prior studies described the catch-up response as a means by which subjects maintained a stable grasp when unexpected translational loads were imposed and linear slip was imminent (Cole & Johansson, 1993; Häger-Ross et al., 1996; Häger-Ross & Johansson, 1996; R S Johansson et al., 1992; Roland S. Johansson et al., 1992). We have shown that a characteristic unimodal catch-up response is also elicited in response to unexpected rotational perturbations that induce conditions other than linear slip. The catch-up response was observed for all subjects, both digits, and irrespective of three experimental factors: object-moment magnitude, axis of rotation, and direction of rotation (Fig. 2.6). Peak normal force and strength of the catch-up response were generally unaffected by torque load or direction of rotation, suggesting that strength of the catch-up response may be similarly robust to torque magnitude as it is to force magnitude (R S Johansson et al., 1992).

Due to the perturbation method (Fig. 2.1B), the external perturbations were not pure rotations but rather combinations of rotation and translation. Nonetheless, a kinematic analysis confirmed that rotational effects were predominant for the (0, 100ms) period immediately following the perturbation. Future experiments will utilize haptic devices to impose purely rotational perturbations, randomize experimental conditions, and include rotations about a radial-ulnar axis. A direct comparison of intra-subject grip responses to pure rotational slip and pure linear slip is also planned.

**Robust timing of the catch-up response.** The temporal characteristics of the catch-up response were robust to experimental conditions. The durations of the catch-up response (217-231ms, Table 2.2) were consistent with previously reported durations of 200-250ms for unexpected linear slip (R S Johansson et al., 1992). Onset latency of the catch-up response (71-89ms, Fig. 2.6, Table 2.2) overlapped with the 50-100ms range reported for grip force responses to natural slips (R.S. Johansson & Westling, 1987) and was not far from the 50-70ms range reported for the latency of a “phasic burst of muscle activity” after the onset of an unexpected force perturbation (Cole & Abbs, 1988). Prior studies reported catch-up response onset latencies of 80±9ms (mean±std) (R S Johansson et al., 1992), and 62±9ms and 74±9ms for catch-up responses to distal and proximal loads, respectively (Häger-Ross et al., 1996).

The consistent shape and timing of the catch-up response to rotational perturbations across experimental conditions supports the existence of pre-programmed grip responses that ensure early stabilization of the grasped object (R S Johansson et al., 1992; Roland S. Johansson et al., 1992; Wing & Flanagan, 1998). Onset latency was based on FDI activation, but was based on changes in normal force rates in other studies (Häger-Ross et al., 1996; R S Johansson et al., 1992). While exact onset threshold criteria for normal force rates were not provided in the literature, the time to FDI activation was essentially coincident with the initial increase in normal force rate (Fig. 2.4 in this work; Fig. 3 in Johansson et al. 1992c).

**Axis of rotation affects catch-up response strength.** Axis of rotation relative to the hand had the greatest effect on the catch-up response. Peak normal force and strength of the catch-up response were greatest for rotations about the grip axis (Fig. 2.6, Table 2.2). Peak normal forces ranged from 12.5-19.2N (Table 2.2) and, yet, the time to achieve the peak normal force was consistent (283-319ms, Table 2.2). The robust timing suggests that the effects of axis of rotation manifested as changes in strength of the catch-up response.

Changes in the axis of rotation fundamentally changed the loading and slip conditions as well as the contributions of the digits to the passive resistance of the perturbations. With no part of the hand to physically oppose rotations about the grip axis, the rotational slip conditions resulted in the largest peak and time to peak angular deviations, and the strength of the catch-up response may have been scaled up to counter rotational slip, in particular (Fig. 2.6, Table 2.2). Rotations about the grip axis are particularly troublesome because of the incompatibility of fingertip force/torque capabilities with the axis of rotation, which passes through both fingertips by definition. Normal grip forces are aligned with the axis of rotation and fingertips cannot actively produce tangential torques in the plane of the fingerpad. The smoothness of tangential forces suggests that passive resistance contributes to at least the first 50ms of the measured forces (Fig. 2.5). Along with natural limits on joint motion and skin stretch, viscoelastic fingerpads (Pawluk & Howe, 1999) and passive joint torques (Kuo & Deshpande, 2010) resist perturbations.

The fact that catch-up responses were strongest for rotations about the grip axis (Fig. 5, Table 2.2) is consistent with prior observations that grip forces are more closely regulated for rotational slip than linear slip (Goodwin et al., 1998; P. Jenmalm et al., 2000), and that grip responses to unanticipated loads vary with load (and slip) direction, with conservative grip responses being associated with “dangerous [loading] directions,” such as away from the palm or in the direction of gravity (Häger-Ross et al., 1996). In particular, stronger grip forces (Häger-Ross et al., 1996; Jones & Hunter, 1992) and shorter grip response latencies (Häger-Ross & Johansson, 1996) were observed in response to force loads away from the palm, although we did not observe axis-dependent effects on grip response latency.

The idea that motion away from the hand constitutes a “dangerous direction” (Häger-Ross et al., 1996) applies to translational perturbations, but is not meaningful for rotational perturbations which lead to simultaneous motion towards and away from the hand. We propose that the grip axis is a “dangerous axis” relative to the d-p axis, where critical differences exist in the conditions for slip and passive resistance of the digits. Hand posture and orientation of the perturbation with respect to joints may also be factors (Häger-Ross & Johansson, 1996). Rotations about the d-p axis might be resisted by the stiffnesses of entire digits while rotations about the grip axis might be resisted primarily by fingerpads. Furthermore, subjects were instructed to curl the middle, ring, and little fingers, which likely pre-tensioned the flexor digitorum profundus to resist flexion of the index finger.

The finding that grip responses to unexpected rotational perturbations can be axis-dependent has direct implications on the kinematic and kinetic control of anthropomorphic, high degree-of-freedom artificial hands. We previously showed that rotational perturbations elicited simultaneous adduction/abduction and flexion/extension of the thumb carpometacarpal joint (De Gregorio & Santos, 2010). While the “catch-up response” appears to reflect a “grip harder” strategy, the act of gripping “harder” is not necessarily the result of pure flexion for human or artificial hands.

**Passive and active phases of the grip response.** As with any unexpected loading of a hand-object system, grip responses will be comprised of a combination of passive and active components. While the non-invasive techniques used in this study preclude discussions regarding the neural pathways involved in the grip responses, some conclusions can be drawn about periods of the response which clearly precede the onset of FDI activity, as measured via surface EMG. The passive dynamics of the hand-object system are likely reflected in the reaction forces at the digit-object interface. The smooth, uniform changes in radial, tangential forces suggests that passive resistance contributes to at least the first 50 ms of the measured fingertip forces (Fig. 2.5). This was true for all subjects, both digits, and regardless of object-moment magnitude or direction of rotation about the d-p axis. After the FDI became active, the changes in radial forces exhibited increased variability about the median and were likely dominated by active muscle responses (Fig. 2.5).

Responses to perturbations may also have been influenced by joint stiffness and digital yield as affected by hand posture (Häger-Ross & Johansson, 1996; R. S Johansson et al., 1992), and orientation of the perturbation with respect to joints. Subjects were instructed to curl the middle, ring, and little fingers, which likely pre-tensioned the flexor digitorum profundus to resist flexion of the index finger. Rotations about the d-p axis might be resisted by the stiffnesses of entire digits while rotations about the grip axis might be resisted primarily by fingerpads. Passive resistance to perturbations could have arisen from natural limits on joint motion and skin stretch, viscoelastic musculoskeletal structures (Zajac, 1989) and fingerpads (Pawluk & Howe, 1999)), as well as passive joint torques (Kuo & Deshpande, 2010; S.-W. Lee, Chen, & Kamper, 2009). The temporal overlap and relative contributions of the passive and active components of the grip response remain unclear and require further investigation.

**Independent control of fingertip force vectors.** Edin et al. showed that digits could be independently controlled for a task in which subjects used a precision grip with symmetric contact points to lift an object having different frictional conditions at the parallel, vertical grip surfaces (Edin et al., 1992). Specifically, the ratios of normal force to tangential force were found to be independent across the thumb and index finger (Edin et al., 1992). Fu et al. showed that digit tangential forces could be independently controlled when subjects were tasked with simultaneously lifting and minimizing roll of an object using a precision grip with directly opposed, symmetric contact points (Fu, Zhang, & Santello, 2010).

The present study supports the idea of independent digit control and, importantly, suggests that the ability to independently control fingertip forces in an asymmetric manner can be used to compensate for torque loads that necessitate asymmetric digit responses during precision grip. Fingertip force vectors were projected onto the plane containing the grip axis in order to illustrate the asymmetry in the force response across digits for negative rotations about the d-p axis (Fig. 2.9). From an analysis of the angle $\theta$ of each fingertip force vector with respect to the grip surface normal, it appears that each digit's force vectors can be controlled independently and asymmetrically.

Two distinct types of grip responses were observed across the 18 subjects that could be differentiated by whether steady-state values for the angle $\theta$ were equal ("symmetric case") or unequal ("asymmetric case"). For the asymmetric case, one digit's force vector eventually pointed the top of the object while the other digit's force vector remained essentially normal to the grip surface (Fig.

2.9A). It would appear as if one digit (index finger for negative rotations about the d-p axis) played a supportive role as a pivot point while the other digit (thumb for negative rotations about the d-p axis) played a more active role to counter the external torque.

Physics dictates that fingertip forces must create a corrective moment about the object’s center of mass to counteract an external torque load. The corrective moment can be created by modifying one’s 3D fingertip force vector and/or digit placement. While subjects were instructed to grasp the object with both digits centered on each grip plate, it is possible that some subjects grasped the object with their digits in direct opposition to one another while others did not. Our observations suggest that selective digit placement and modulation of fingertip force direction are two strategies that could be used to counter an external torque load. However, conclusive remarks about digit roles (if any) cannot be made without further analyses of digit center of pressure.

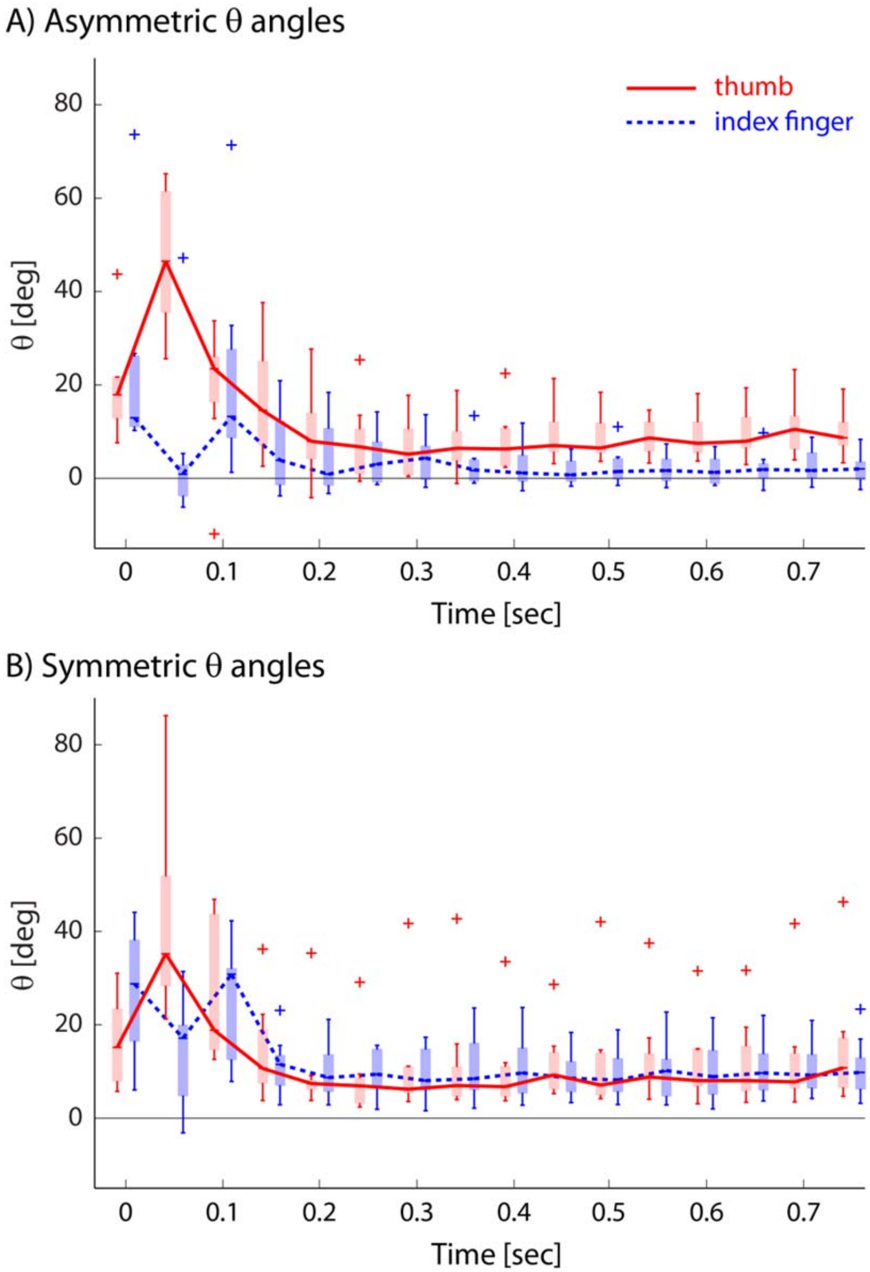


*Figure 2.9. Angle of fingertip force vector relative to the grip surface normal.* The angle $\theta$ of each fingertip force vector was measured relative to the grip surface normal in the plane containing the grip axis. Data are shown for large object-moment magnitude, negative rotations about the distal-proximal axis for two groups of subjects who were separated based on the symmetry, or lack thereof, of

forces applied by the thumb (solid red lines and boxes) and index finger (dotted blue lines and boxes) relative to the vertical centerline of the object. Boxplots are shown in 50 ms increments from perturbation onset (t = 0 sec) until 750 ms. (A) Nine subjects used asymmetric force vectors about the centerline of the object (unequal steady-state $\theta$ angles) to correct the object rotation. Steady-state thumb and index fingertip force angles became statistically significantly different around 350 ms. (B) Nine subjects used symmetric force vectors (equal steady-state $\theta$ angles). Thumb and index fingertip force angles became statistically indistinguishable from one another around 100 ms.

**FDI activation timing suggests that automatic grip responses are distinct from stretch reflexes.** Whether anticipatory or triggered by a perturbation stimulus, expressions of automatic or programmed motor responses have been found in the coordinated changes in fingertip forces during precision grip tasks (R S Johansson et al., 1992; R. S. Johansson & Westling, 1988; R. S. Johansson, 1996; Roland S. Johansson et al., 1992). It is not entirely clear which neural pathways are involved in the automatic grip responses, but reflex loops have been considered. The identification, organization, labeling, and interpretation of reflex responses remain controversial in the neurophysiology community. While the application of surface EMG to a single muscle in this study is insufficient for resolving the long-standing controversies, we can still discuss our findings in the context of what is currently known about neural pathways associated with stretch reflexes and automatic grip responses.

Surface EMG was used to investigate the timing of first dorsal interosseous activation relative to the onset of perturbation of the grasped object (Fig. 2.4). The delays between the onset of perturbation and FDI activation overlap data previously reported by others for precision grip responses to unexpected loads (Cole & Abbs, 1988; R.S. Johansson & Westling, 1987). While it is physically plausible that the motions imposed on the thumb and index finger by the external torque loads could have triggered stretch reflexes, most FDI activation latencies observed in this study (71-89 ms, Table 2.2) exceeded those reported by others for tendon jerk and stretch reflexes in muscles of the hand. Forcible stretching of the flexor pollicis longus in the thumb has been observed to elicit 25-30 ms short-latency and 40 ms long-latency muscle responses (Matthews, 1984a). Other studies have reported 25 ms tendon jerk latencies in the flexor pollicis longus and 40 ms stretch reflex responses in the flexor pollicis longus and flexor pollicis brevis in response to jerk-type perturbations of the thumb (Marsden, Merton, & Morton, 1976; Matthews, 1984b). FDI stretch reflex latencies have been described as having a short latency response of 32 ms and a long latency response of 55 ms (Thilmann, Schwarz, Töpper, Fellows, & Noth, 1991). If stretch reflexes were triggered, forces generated from long-latency stretch reflexes would likely be dwarfed by those resulting from supraspinally-mediated, automatic responses and/or voluntary responses (Bizzi, Dev, Morasso, & Polit, 1978; Brown, Rack, & Ross, 1982). In a study that applied unexpected force loads directly to an object in precision grip or to the hand itself, it was hypothesized that cutaneous mechanoreceptors in the digital pulps play a larger role in automatic grip force adjustments than stretch reflexes (Cole & Abbs, 1988).

Table 2.2.

*Object kinematics and grip response events*

| Axis: | Distal-proximal | | Grip |
|---|---|---|---|
| **Direction:** | **Positive** | **Negative** | **Negative** |
| Peak angular deviation of object [deg] | Small OMM 9.5 ± 1.9<br>Large OMM 12.7 ± 2.0 | Small OMM 11.7 ± 1.9<br>Large OMM 17.8 ± 3.8 | Small OMM 33.6 ± 5.2<br>Large OMM 40.5 ± 8.3 |
| Time to peak angular deviation of object [ms] | Small OMM 55.0 ± 0.0<br>Large OMM 65.0 ± 5.0 | Small OMM 60.0 ± 5.0<br>Large OMM 70.0 ± 5.0 | 137.5 ± 25.0 |
| **Onset latency of the catch-up response** [ms]<br>*(Time to FDI activation, "b" in Fig. 2.4)* | 71.4 ± 9.2 | 83.9 ± 12.8 | 88.6 ± 9.2 |
| **Strength of the catch-up response** [N/s]<br>*(Peak normal force rate)* | Small OMM 79.5 ± 21.9<br>Large OMM 104.2 ± 27.0 | 83.4 ± 21.8 | 134.7 ± 50.8 |
| Time to peak normal force rate [ms]<br>*("c" in Fig. 2.4)* | 127.2 ± 15.5 | 152.2 ± 28.9 | 145.8 ± 16.7 |
| Peak normal force [N] | 13.0 ± 2.9 | 12.5 ± 3.3 | 19.2 ± 8.0 |
| Time to peak normal force [ms]<br>*("d" in Fig. 2.4)* | 309.2 ± 84.7 | 319.2 ± 80.5 | 282.5 ± 45.3 |
| **Duration of the catch-up response** [ms]<br>*(from "b" to "d" in Fig. 2.4)* | 230.8 ± 74.7 | 221.9 ± 79.2 | 216.9 ± 50.8 |

## CONCLUSION

Previous studies (R S Johansson et al., 1992; R. S Johansson et al., 1992; Roland S. Johansson et al., 1992) had shown that the catch-up response existed for unexpected translational perturbations of an object in a precision grip. We imposed unexpected rotational perturbations and found that catch-up responses can also be elicited by conditions other than pure linear slip or rotational slip at the fingerpad. The early period of the grip response appeared to be dominated by passive mechanics while the later period was dominated by a characteristic active catch-up response and independent (and often asymmetric) control of fingertip forces at steady-state. The uniform timing of the catch-up response was consistent with prior studies on grip responses to translational perturbations (Cole & Abbs, 1988; R.S. Johansson & Westling, 1987). In the end, it seems that we generate a grip harder response, but that the strength this response is context-dependent. The fact that qualitatively different load and slip conditions elicited similar catch-up responses suggests that a pre-programmed increase in normal (grip) force is a hallmark of human grip responses to unexpected perturbations. The results of this study could be used to inform the design of fingertip force control strategies for artificial hands having sensors (tactile, proprioceptive) that can detect the nature of perturbations imposed on the grasped object.

Chapter 3 will describe experiments in which we used haptic robots to impart pure translational and pure rotational perturbations, and to investigate perturbations about the radial-ulnar axis. While the effects of trial-to-trial learning were not studied here explicitly, it is possible that some learning took place due to the repetitive nature of the task. The use of haptic devices helps to minimize effects of learning and anticipation, by allowing the randomization of perturbation type (translational or rotational), axis, and direction. Digit placement and center of pressure analyses will also be possible with the use of force/torque transducers that are highly sensitive at low fingertip force magnitudes. Surface EMG of additional muscles besides FDI will enable investigations of coordinated muscle activity, activation latencies, and possible co-contraction or pre-stiffening strategies.

# CHAPTER 3

# PRECISION GRIP RESPONSES TO UNEXPECTED ROTATIONAL AND TRANSLATIONAL PERTURBATIONS

## INTRODUCTION

When objects in precision grip were perturbed by unpredictable, translational pulling loads, a rapid initial increase in grip force rate, in the form of a “pulse-like” *catch-up response* (R S Johansson et al., 1992), allowed the delayed reactive grip force to catch up to the unexpected load force and maintain a safety margin against linear slip (R. S. Johansson & Westling, 1988). Features of the catch-up response such as onset latency, shape, and duration were independent of load force amplitude (R S Johansson et al., 1992) and frictional condition (Cole & Johansson, 1993). When load force rate increased, strength of the catch-up response increased and onset latency decreased while duration of the catch-up response remained 200ms (Roland S. Johansson et al., 1992). The stereotypical features of the catch-up response suggested it was a centrally-programmed, default grip response that was released as a unit in response to unexpected loading (R S Johansson et al., 1992; R. S Johansson et al., 1992; Roland S. Johansson et al., 1992). These findings supported observations of evoked, automatic reactive grip responses (Cole & Abbs, 1988).

Previous work showed the existence of the catch-up response for conditions other than pure linear slip (De Gregorio & Santos, 2013a). The temporal characteristics of the catch-up response (onset latency, duration) were robust to perturbation axis, direction, and magnitude. Further, the strength of the catch-up response scaled with axis of perturbation. In that study (Chapter 2) (De Gregorio & Santos, 2013a), unexpected perturbations applied to an instrumented object in precision grasp were rotationally dominant, but not purely rotational because of the experimental set-up. In addition, rotational perturbations were only investigated for the distal-proximal and grip axes.

The objectives of this study were to (i) investigate grip responses to pure translational and pure rotational perturbations, (ii) impose perturbations along and about all three hand-centric axes (distal-proximal, radial-ulnar, and grip), and (iii) investigate the effects of different grip surface friction conditions across the two digits.

## MATERIALS AND METHODS

**Equipment.** Ten consenting subjects (eight right-handed, two left-handed) with no history of neurological or hand impairment participated in this study approved by the Arizona State University Institutional Review Board. The subjects ranged in age from 25 to 35 years (5 male, 5 female).

An instrumented object housed two six degree-of-freedom force/torque transducers (Nano-17, ATI Industrial Automation) that were used to measure the fingertip forces and torques of the thumb and index finger independently at 2 kHz. Each sensor was rigidly attached to a steel grip plate that could be outfitted with one of two smooth surfaces with differing coefficients of friction (Kapton Polymide or PTFE) which were attached to magnetic strip backings. Magnetic backings were used to minimize the amount of time spent changing surfaces between trials, which were randomized by grip surface. The Kapton Polymide (high friction) surface had a coefficient of friction of 0.63 and the PTFE (low friction) surface had a coefficient of friction that ranged from 0.05 to 0.1 (McMaster-Carr, 2012). The grip surfaces were presented in one of three configurations: Kapton on the thumb side and Kapton on the index finger side (high-high), Kapton on the thumb side and PTFE on the index finger side (high-low), and PTFE on the thumb side and Kapton on the index finger side (low-high). A PTFE to PTFE pairing was not utilized in order to prevent subjects from dropping the object or getting fatigued through the use of large grip forces. The grip surfaces were parallel to one another and spaced 38 mm apart.

A Grass QP511 Quad Ace surface electromyography (EMG) system was used to collect data from four hand muscles (two intrinsic, two extrinsic) at 2 kHz. As seen in Figure 3.1, the four hand muscles that we investigated were the first dorsal interosseous (FDI, intrinsic, thumb and index finger), the abductor pollicis brevis (APB, intrinsic, thumb), the extensor digitorum communis (EDC, extrinsic, index finger), and the flexor pollicis longus (FPL, extrinsic, thumb).

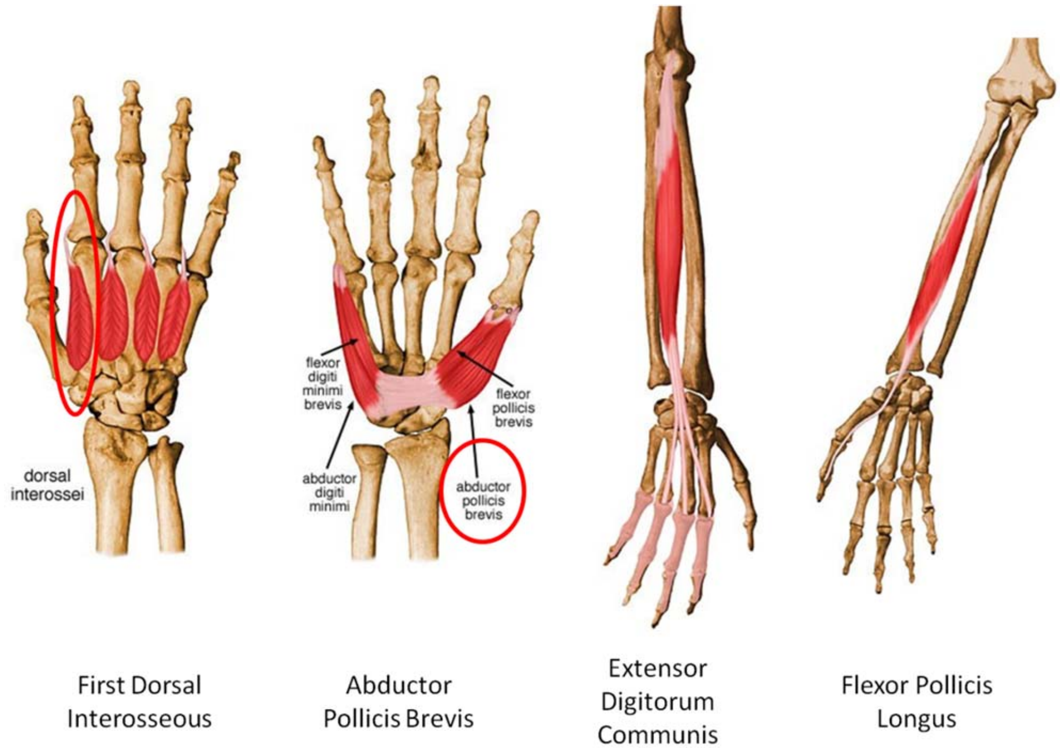


*Figure 3.1. Muscles targeted for EMG analysis.* Surface EMG was used to record from two intrinsic muscles and two extrinsic muscles. Adapted from ("UW Muscle Atlas," n.d.).

Two Phantom haptic devices (Phantom Premium 1.5, SensAble Technologies) were used to administer translational perturbations along and rotational perturbations about the principal axes (Fig. 3.2). Translational perturbations along the distal-proximal ("d-p") axis were directed away from and towards the subject's palm, perturbations along the radial-ulnar ("r-u") axis were aligned with the vertical axis of the grip plate and moved the object upward or downward, and translations along the grip axis, which connected the two finger pads, were directed into the index finger or the thumb. The Phantoms were rigidly attached to the object using one of two attachment configurations (Fig. 3.2). To ensure that perturbations would be administered in a hand-centric reference frame, the position and orientation of the object was monitored using a magnetic position and orientation sensor (Fastrak, Polhemus) recording data at 120 Hz. For each trial, position and orientation data for the object were transformed into the reference frames of the two Phantom robots such that perturbations commanded at the Phantom end-effectors would result in desired perturbations in the hand-centric reference frame.

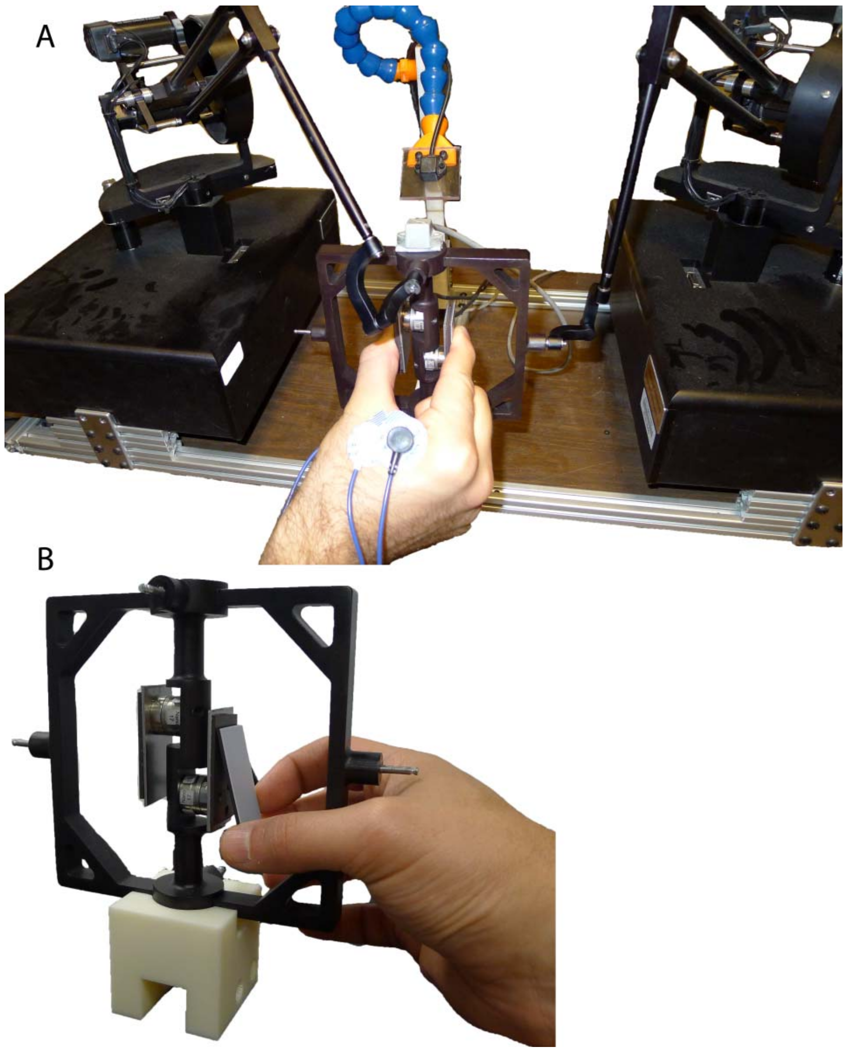


*Figure 3.2. Experimental Setup.* A: The subject grasps the 3D printed, instrumented object using a precision grip. A motion capture sensor is attached to the object and two haptic robots impart perturbations in a hand-centric reference frame. B: Different grip surfaces having magnetic backings can be quickly and easily changed.

In order to minimize the pronation, supination, adduction, and abduction of the wrist, each subject's arm and wrist were restrained by a vacuum positioning pillow (versa Form, Sammons Preston). Visual feedback was eliminated during the experimental trials by the use of powered shutter goggles. The shutter goggles remained opaque throughout the experimental session except when subjects were allowed visual feedback in order to grasp the instrumented object prior to each trial.

**Procedure.** Subjects were instructed to hold the instrumented object (Fig. 9) between the thumb and index-finger of their dominant hand with their other fingers curled into their palm. A 1.5 sec step load (force or torque) was imposed at a random time during each 5 second trial. The applied step loads were 1.47 N (150 g) and 50.5 N-mm for force and torque step loads, respectively. We used these levels in order to compare results from this study to those of our previous work (De Gregorio & Santos, 2013a) described in Chapter 2. In addition to the perturbation start time, four additional factors were randomized in order to minimize learning: type of perturbation (rotational or translational), grip surface friction (high-high, high-low, low-high), direction of perturbation (positive or negative), and axis of perturbation (d-p, r-u, or grip). The only exception was for rotational perturbations about the grip axis, which were randomized by grip surface friction and direction of perturbation, but blocked together in order to minimize the time spent reconfiguring the experimental set-up (Fig. 3.2).

Twenty three experimental blocks consisting of six randomized trials were created varying the aforementioned factors. Over the course of the 23 experimental blocks, each combination of factors was tested four times. A mandatory 30 second rest period was given between blocks. In addition, subjects were instructed to notify the researcher if additional rest was necessary to avoid fatigue. During the rest period the Phantom configuration was changed, if necessary. An example of the experimental trial order is shown in Table 3.1. Each subject was presented with the same blocks of trials, in the same order. There were no practice trials.

Table 3.1.

*Example of an Experimental Block*

| Phantom Configuration | Surface Condition (Thumb-Index) | Type | Axis | Direction |
|---|---|---|---|---|
| 1 | High-High | Rotational | R-U | Negative |
| 1 | High-High | Translational | GRIP | Positive |
| 1 | Low-High | Translational | GRIP | Negative |
| 1 | High-High | Rotational | R-U | Negative |
| 1 | High-High | Rotational | D-P | Negative |
| 1 | High-High | Rotational | R-U | Positive |

**Data Analysis.** Position and orientation data for the object were transformed into the hand-centric reference frame using MATLAB (Mathworks). These data were used to determine the onset of object perturbation (t = 0 sec) and synchronize all trials. All position data were averaged across trials of the same perturbation type (rotational or translational), perturbation axis, (d-p, r-u, or grip), perturbation direction (positive or negative), and surface condition (high-high, high-low, low-high) on a subject-specific basis.

All surface EMG data were full-wave rectified, filtered using a fourth-order, 40 Hz low-pass Chebyshev filter (Hodges & Bui, 1996), and normalized based on the maximum contraction signal recorded, including maximum voluntary contraction trials prior to the start of the experiment. Each subject's data were averaged across trials of the same type to ensure that the trends in muscle activity level were consistent. A threshold of one and a half standard deviations of the baseline noise 100 ms prior to the onset of perturbation was used to determine when a muscle was considered active. A muscle was considered active if the activity level remained above the threshold for at least 50 ms (Hodges & Bui, 1996). The validity of activation thresholds was confirmed using visual inspection to ensure that our results were reliable (Di Fabio, 1987). The time to initial FDI activation was used to determine the onset latency of the catch-up response (De Gregorio & Santos, 2013a). Due to problems with surface EMG connectivity, the EDC and FPL data from one subject were not usable.

Force and torque data were filtered using a fourth order, 30 Hz low-pass Butterworth filter (De Gregorio & Santos, 2013a). Force and torque data were averaged across trials of the same perturbation type (rotational or translational), perturbation axis, (d-p, r-u, or grip), perturbation direction (positive or negative), and surface condition (high-high, high-low, low-high) on a subject-specific basis. Normal force rates were obtained by taking the first order difference of the normal forces for each individual trial and taking the average across trials of the same type on a subject-specific basis. Peak normal force was used to mark the end of the catch-up response in order to determine the duration of catch-up response. Peak normal force rates were used to determine the strength of the catch-up response.

**Statistical Analysis.** Non parametric statistical analyses were used due to the small sample size and non-normality of the data. Specifically, we employed the Kruskal-Wallis test to evaluate the independent effects of four experimental factors: perturbation axis (d-p, r-u, or grip), direction of perturbation (positive or negative), grip surface friction (high-high, high-low, low-high), and type of perturbation (rotational or translational). Additionally, the Kruskal-Wallis analysis was used to test if data could be pooled across the thumb and index finger. Data from the two left-handed subjects were mapped to those of the eight right-handed subjects prior to pooling of the data (Table 3.2). For all analyses, the alpha level was set to 0.05. All Summary data are reported as median ± median absolute deviation (MAD), unless otherwise specified.

**RESULTS**

For translational perturbations along the d-p axis, the instrumented object was pulled away from or pushed toward the subject's palm (Fig. 3.2). For translations along the r-u axis, the object was moved vertically upward or downward in the subject's grasp. For translations along the grip axis, the object was pushed directly into either the thumb or the index finger.

For rotational perturbations about the d-p axis, the object was rotated clockwise or counter-clockwise from the subject's perspective (Fig. 3.2). For rotations about the r-u axis, the object was rotated about the vertical axis of the object and twisted between the thumb and index finger. For rotations about the grip axis, the top of the object was tilted away from the subject's palm or towards the subject's palm. Subjects were able to stop the perturbations about the grip axis, but were unable to bring the object back to the initial, upright position.

**Passive phase.** As described in (De Gregorio & Santos, 2013a), the passive phase of each trial was treated as the period after perturbation onset, but before FDI activation (Fig. 3.3). Prior to FDI activation, there was no evidence of activation of any of the other three muscles (APB, EDC, FPL).

The preload grip and tangential (r-u) forces were calculated for the first 100 ms prior to the onset of perturbation. Both the grip and tangential forces were robust to grip surface condition ($p \geq 0.405$), direction ($p \geq 0.358$) of, axis ($p \geq 0.512$) of, and type ($p \geq 0.294$) of perturbation.

**Active phase.** Shortly after the perturbation was commanded ('a' in Fig. 3.3), the FDI breached the activation threshold which marked the beginning of the active phase. The most prominent feature of the active phase is the rapid, pulse-like parallel increase in thumb and index finger normal force known as the catch-up response (De Gregorio & Santos, 2013a; R S Johansson et al., 1992). The catch-up response was observed in the normal force rates of both digits for all subjects regardless of perturbation type, axis, direction, or grip surface friction. The catch-up response began with the onset of FDI activity (Fig. 3.3, 'b') and ended with the peak normal force ('d', Fig. 3.3) (De Gregorio & Santos, 2013a). The onset of catch-up response ranged from 70-81 ms and from 68-78 ms for rotational and translational perturbations, respectively, and lasted between 221 – 291 ms for rotational perturbations and between 163 - 238 ms for translational perturbations (median values, Table 3.2). The time to peak normal force rate ranged from 254 – 296 ms and 220 – 258 ms from the onset of perturbation for rotational and translational perturbations, respectively. The time to initial FDI activation (onset latency of the catch-up response) and the catch-up response duration were both unaffected by grip surface friction (Fig. 3.4, Fig. 3.5). However, the time to peak normal force rate was affected by grip surface friction for perturbations about the grip axis in the positive direction (top of object rotates toward the palm), for which the low-high friction condition (low friction surface for the thumb, high friction surface for the index finger) resulted in a time to peak normal force rate that was 26 - 41 ms slower than for the other two grip surface friction conditions ($p = 0.031$).

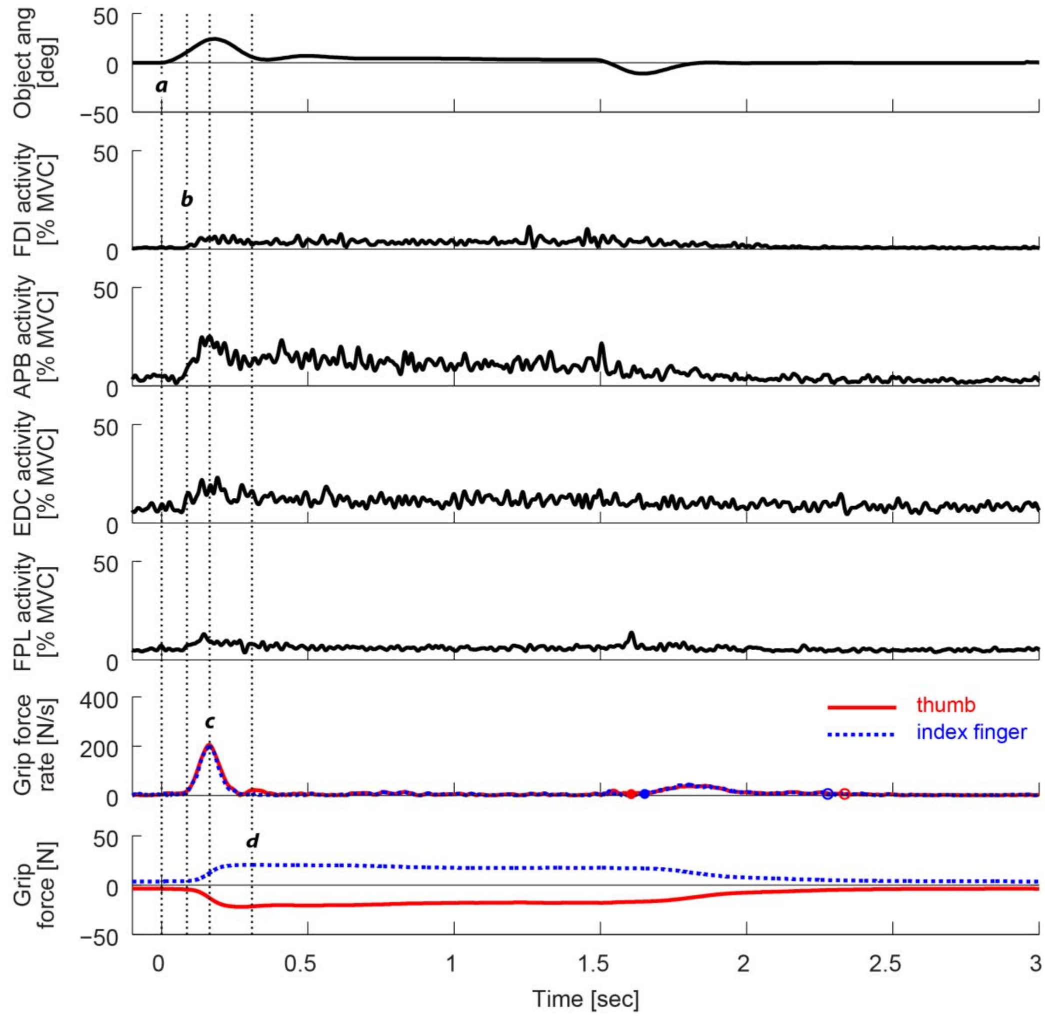


*Figure 3.3. Object angle, muscle activity, grip force, and grip force rate as a function of time.* An example trial is shown for a representative subject with the following events marked: **a** (t = 0) onset of perturbation, **b**: onset of catch-up response, **c**: peak normal force rate, **d**: end of catch-up response (peak normal force). The solid dots in the grip force rate plot indicate the onset of the grip response to the removal of the step load.

The direction of perturbation had varying effects. For the onset latency of the catch-up response, perturbation direction had an effect for rotational perturbations about the r-u axis with the high-high grip surface friction ($p = 0.009$). The catch-up response began 16 ms later for positive perturbations about the r-u axis that twisted the object towards the thumb than for negative perturbations. The duration of the catch-up response was similarly affected. For translational perturbations along the r-u axis with a high-low grip surface friction, it was found that positive perturbations upwards elicited shorter catch-up response durations ($p = 0.022$). For translational perturbations along the grip axis, duration of the catch-up response was affected by the direction of perturbation for the high-high and high-low grip surface friction conditions ($p = 0.040$, $p = 0.043$). In both cases, it was found that the duration of the catch-up response was greater for perturbations in the positive direction towards the index finger. Peak normal force rate was occurred sooner for positive rotations about the d-p axis (clockwise from the subject's point of view) for all grip surface friction conditions ($p \leq 0.013$), negative rotations about the r-u axis (clockwise when viewed from above) at the high-low grip surface friction ($p = 0.001$), and negative translations along the r-u axis (downward) for high-low and low-high grip surface friction conditions ($p \leq 0.004$).

Table 3.2.

*Grip response events.*

| Axis: | Distal-proximal | | Radial-ulnar | | Grip | |
|---|---|---|---|---|---|---|
| **Direction:** | **Positive** | **Negative** | **Positive** | **Negative** | **Positive** | **Negative** |
| Onset latency of the catch-up response [ms] *("a" in Fig. 3.3)* | Translation 69.0 ± 6 Rotation 77.0 ± 7 | Translation 78.0 ± 8 Rotation 81.0 ± 7 | Translation 75.0 ± 7 Rotation 80.0 ± 9 | Translation 76.0 ± 10 Rotation 70.0 ± 11 | Translation 68.0 ± 11 Rotation 76.0 ± 8 | Translation 69.0 ± 13 Rotation 73.0 ± 9 |
| Strength of the catch-up response [N/s] | Translation 63.9 ± 24 Rotation 47.8 ± 10 | Translation 36.5 ± 9 Rotation 48.9 ± 10 | Translation 68.4 ± 31 Rotation 51.2 ± 21 | Translation 74.8 ± 29 Rotation 49.1 ± 18 | Translation 90.2 ± 31 Rotation 55.5 ± 18 | Translation 88.9 ± 31 Rotation 55.7 ± 20 |
| Duration of the catch-up response [ms] *(from "b" to "d" in Fig. 3.3)* | Translation 194 ± 30 Rotation 225 ± 41 | Translation 192 ± 50 Rotation 221 ± 41 | Translation 163 ± 25 Rotation 244 ± 34 | Translation 212 ± 39 Rotation 245 ± 36 | Translation 238 ± 49 Rotation 275 ± 62 | Translation 178 ± 67 Rotation 291 ± 67 |
| Time to peak normal force rate [ms] *("c" in Fig. 3.3)* | Translation 250 ± 23 Rotation 257 ± 19 | Translation 247 ± 16 Rotation 287 ± 22 | Translation 232 ± 14 Rotation 271 ± 28 | Translation 258 ± 11 Rotation 254 ± 29 | Translation 220 ± 11 Rotation 296 ± 26 | Translation 224 ± 12 Rotation 286 ± 25 |
| Peak normal force [N] | Translation 13.9 ± 3.2 Rotation 15.5 ± 2.6 | Translation 12.3 ± 3.2 Rotation 14.6 ± 3.0 | Translation 13.9 ± 3.3 Rotation 15 ± 3.6 | Translation 15.5 ± 3.5 Rotation 1.5 ± 3.4 | Translation 17.3 ± 3.0 Rotation 18.4 ± 6.8 | Translation 15.6 ± 3.2 Rotation 17.0 ± 4.5 |

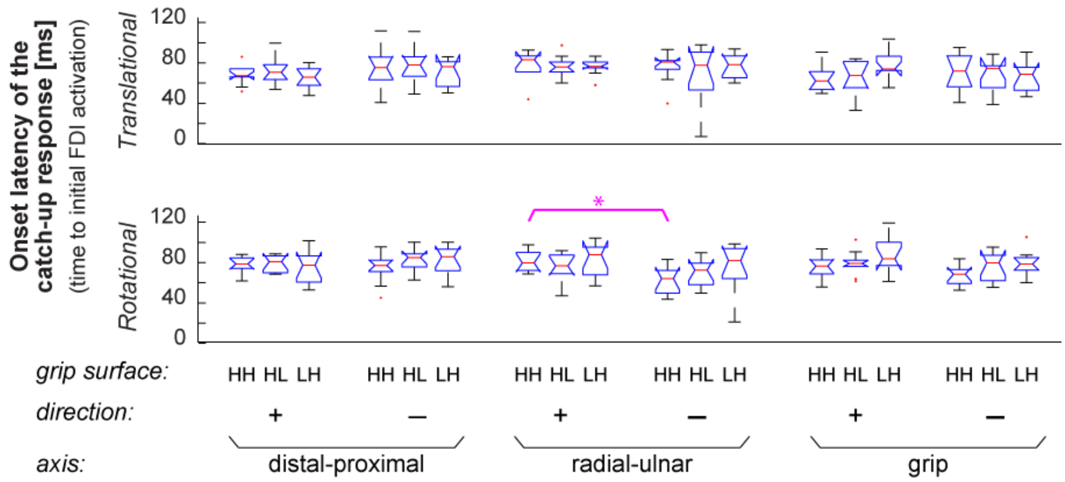


*Figure 3.4. Onset latency of the catch-up response.* The onset latency of the catch-up response is shown for translational perturbations (top) and rotational perturbations (bottom) for the different experimental conditions. The magenta asterisk indicates a statistically significant effect of perturbation direction.

The axis of perturbation had no effect on the onset latency of the catch-up response regardless of perturbation type (rotational or translational). However, the duration of the catch-up response and the time to peak normal force rate were both affected by axis of perturbation in some instances. The duration of catch-up response was affected by the axis of perturbation for the high-low ($p = 0.019$) and low-high ($p = 0.021$) grip surface friction conditions (Fig. 3.5). For both surface friction conditions, the catch-up response was shorter for rotations about the d-p axis than for those about the grip axis. Time to peak normal force rate was affected by axis of perturbation for rotational perturbations with a low-high grip surface friction ($p < 0.001$) and translational perturbations with a high-low grip surface friction ($p = 0.011$). In the rotational case, the peak normal force rate occurred later for rotations about the grip axis than for rotations about the other two axes. However, in the translational case, the peak normal force rate occurred sooner for translational perturbations along the grip axis than for those along the r-u axis.

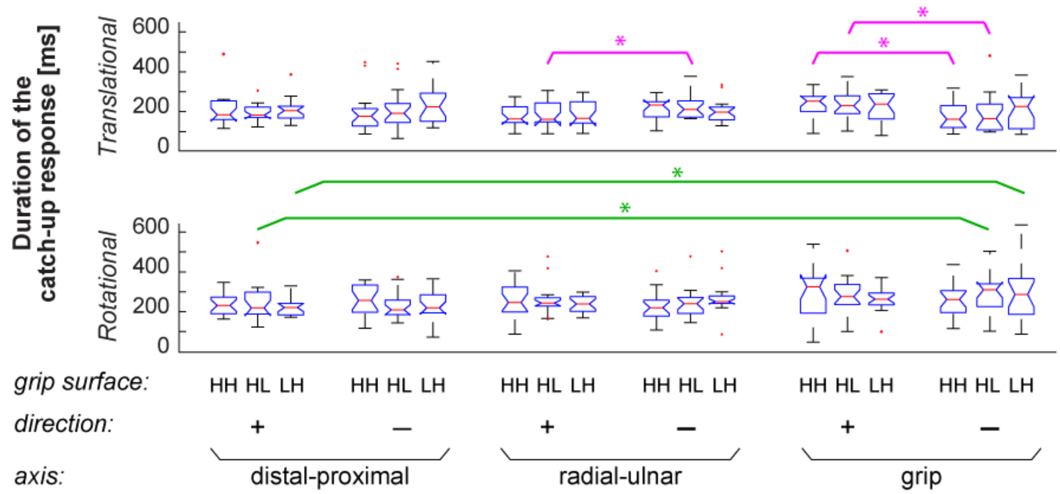


*Figure 3.5. Duration of the catch-up response.* The duration of the catch-up response is shown for translational perturbations (top) and rotational perturbations (bottom) for the different experimental conditions. The magenta asterisk indicates a statistically significant effect of perturbation direction. The green asterisk indicates a statistically significant effect of the axis of perturbation.

The onset latency of the catch-up response was affected by the type of perturbation. Specifically, the catch-up response began earlier for translational perturbations along the grip axis than for rotational perturbations about the grip axis for high-low and low-high grip surface friction conditions ($p = 0.033$ for both cases). The duration of the catch-up response was also affected by the type of perturbation ($p \leq 0.035$). For almost all axis and surface friction condition combinations, the catch-up responses lasted longer for rotational perturbations than for translational perturbations (Fig. 3.5). The only case in which perturbation type did not affect the duration of the catch-up response was for d-p axis perturbations with a low-high surface friction condition. Furthermore, the time to peak normal force rate was greater for rotational perturbations than for translational perturbations ($p \leq 0.035$), except for r-u axis perturbations with a high-high surface friction condition.

Peak normal force values ranged from 11 - 14 N and 12 - 17 N for rotational and translational perturbations, respectively. The peak normal force rates (strength of the catch-up response) ranged from 48 – 56 N/s for rotational perturbations and from 36 – 90 N/s for translational perturbations. Peak normal force and strength of the catch-up response were unaffected by surface friction condition, but were affected by other experimental factors.

The direction of perturbation had varied effects on peak normal force and strength of the catch-up response. Peak normal force was 2.5 N larger for positive rotations about the r-u axis (counter-clockwise when viewed from above) than for negative rotations for the high-low surface friction condition ($p = 0.048$). For all surface friction conditions, the strength of the catch-up response was greater for positive translational perturbations along the d-p axis (away from the palm) than for negative perturbations ($p \leq 0.027$) (Fig. 3.6).

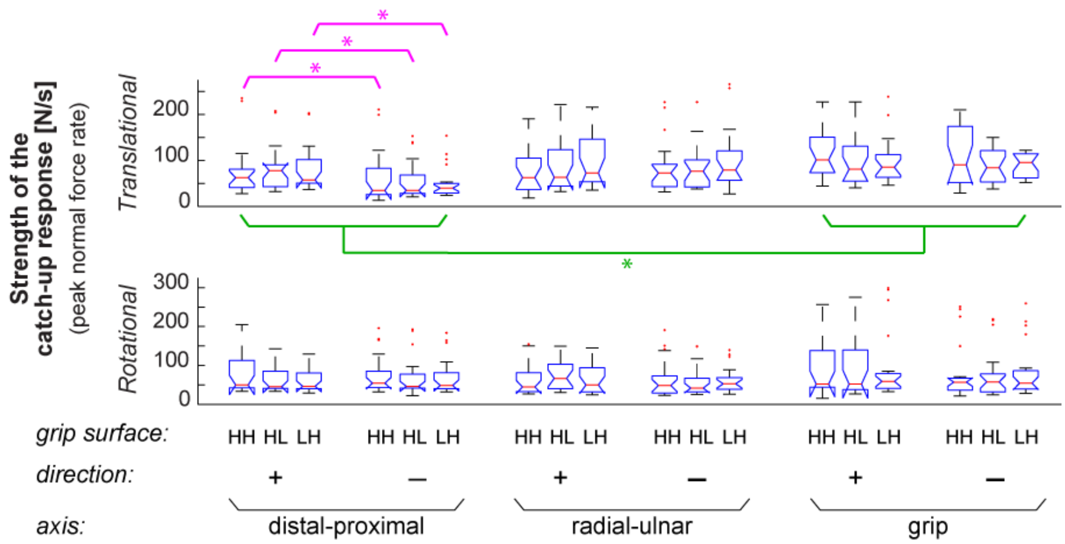


*Figure 3.6. Strength of the catch-up response.* The strength of the catch-up response is shown for translational perturbations (top) and rotational perturbations (bottom) for the different experimental conditions. The magenta asterisk indicates a statistically significant effect of perturbation direction. The green asterisk indicates a statistically significant effect of the axis of perturbation.

The axis of perturbation affected peak normal force and strength of the catch-up response for translational perturbations. At the high-high surface friction condition, translational perturbations along the grip axis elicited peak normal forces that were 2.9 N and 4.6 N larger ($p = 0.001$) than those for perturbations along the r-u and d-p axes, respectively. Peak normal forces were 3.4 N smaller for translational perturbations along the d-p axis than for perturbations along the grip axis ($p = 0.002$). The peak normal force rates were affected by the axis of perturbation for translational perturbations for all three surface friction conditions ($p \leq 0.005$). Regardless of the surface friction condition, the strength of the catch-up response was largest for translational perturbations along the grip axis and smallest for those along the d-p axis (Fig. 3.6, Table 3.2).

Peak normal force was only affected by the type of perturbation in for d-p perturbations with the high-high surface friction condition ($p = 0.005$), where the peak normal force for rotational perturbations was 18 N greater than that for translational perturbations.

The strength of the catch-up response was affected by perturbation type ($p \leq 0.047$). For all surface friction conditions, catch-up responses were stronger for translational perturbations than for rotational perturbations for the r-u and grip axes ($p \leq 0.046$). In contrast, the catch-up response was stronger for rotational perturbations than for translational perturbations for the d-p axis with the high-high surface friction condition. Strength of the catch-up response was not affected for perturbations along or about the d-p axis for high-low or low-high surface friction conditions ($p \geq 0.482$).

**Unloading phase.** At the end of each Phantom-imposed, 1.5 sec step load, the load was turned off. The sudden removal of the step load caused a decrease in subject's grip force (Fig. 3.3). The decrease in grip force began 127 - 233 ms and 188 - 227 ms after the step load was turned off for rotational and translational perturbations, respectively. As seen in Figure 3.3, the grip force rate profile of the unloading response was bell-shaped and resembled a weaker catch-up response of longer duration.

## DISCUSSION

Previous studies have defined the catch-up response as a means by which one can maintain a stable grasp in the face of unexpected translational perturbations (Cole & Johansson, 1993; Häger-Ross et al., 1996; Häger-Ross & Johansson, 1996; R S Johansson et al., 1992) or rotationally-dominant perturbations (De Gregorio & Santos, 2013b). One of the primary goals of the present study was to investigate grip responses to pure translational perturbations and pure rotational perturbations for multiple hand-centric axes. Regardless of grip surface friction, perturbation type, axis, or direction, a distinct catch-up response was elicited to ensure grasp stability. The temporal characteristics of the catch-up response (onset latency, duration) were unaffected by the experimental factors.

**Catch-up response was not affected by grip surface friction.** It was previously shown that the thumb and index finger could be independently controlled for a task in which subjects used a precision grip with symmetric contact points to lift an object having different frictional conditions (sandpaper or silk) at the parallel, vertical grip surfaces (Edin et al., 1992). One of the goals of the present study was to investigate whether grip responses to unexpected perturbations would be affected by different grip surface friction conditions across the thumb and index finger. Knowing that subjects' fingertips would be subjected to hundreds of potentially slip-inducing perturbations, we purposely avoided the use of sandpaper which might cause discomfort to subjects. Instead, two smooth surfaces were selected based on the disparity in their coefficients of friction. The coefficient of friction for Kapton Polymide ($\mu = 0.63$) was an order of magnitude greater than that for PTFE ($\mu = 0.05\text{-}0.1$) (McMaster-Carr, 2012).

It was originally hypothesized that a low friction surface (PTFE) might result in a shorter onset latency and/or greater strength of the catch-up response. It was also hypothesized that subjects would modulate their preload fingertip forces based on the grip surface friction conditions (Edin et al., 1992). Surprisingly, onset latency and strength of the catch-up response remained greatly unaffected by grip surface friction (Figs. 3.4 and 3.6). Previous studies that varied grip surface conditions altered the coefficient of friction by changing the surface roughness, typically using sandpaper and silk for high and low friction surfaces, respectively (Edin et al., 1992; R. S. Johansson & Westling, 1984; Westling & Johansson, 1984). In our study, grip surface friction was varied with negligible (if any) change to grip surface roughness. Though coefficient of friction and roughness are related, it is possible that roughness is a more salient feature of the grip surface. In order to determine whether a surface has a higher coefficient of friction than another surface, humans typically move their fingers along the surfaces (Lederman & Klatzky, 1987). However, it is possible that surface roughness could be perceived if the fingerpad was pressed statically but firmly enough into a bumpy surface. In this study, each randomly-assigned pair of grip surfaces were smooth. Subjects were not given the opportunity to haptically explore the smooth surfaces, were not given practice trials, and did not adjust their preload fingertip forces according to coefficient of friction. It is also possible that the range of coefficients of friction employed ($\mu = 0.05\text{-}0.63$) was too narrow to cause observable differences in preload fingertip forces and catch-up response characteristics.

It has been shown that, for isometric lifting tasks, subjects modulate their vertical tangential forces (fingertip force components along the r-u axis) in order to maintain a stable grasp while keeping their normal forces along the grip axis relatively constant (Edin et al., 1992). In the present study, subjects' r-u and grip axis force components were unaffected by grip surface friction during the preload period prior to the onset of perturbation ($p \geq 0.334$).

**Strength of the catch-up response.**

***Effect of perturbation axis.*** The strength of the catch-up response was only affected by axis of perturbation for translational perturbations. This was surprising, given previous findings in which rotationally-dominant perturbations scaled in strength according to the axis of perturbation (De Gregorio & Santos, 2013b). Specifically, rotations about the grip axis that caused torsional slip at the fingerpads elicited stronger catch-up responses than those about the d-p axis that could be resisted passively by fingerpads and entire digits (De Gregorio & Santos, 2013b). In the present study, median values of catch-up response strength were larger for rotational perturbations about the grip axis for all grip surface friction conditions (Fig. 3.6). However, the spread of the catch-up response strength values were such that perturbation axis did not have a statistically significant effect on strength of the catch-up response for rotational perturbations. One possibility is that inter-subject variability was too great to yield statistically significant differences. Another possibility is that the scaling of catch-up response strength observed in the prior study (De Gregorio & Santos, 2013b) could have been driven by afferent feedback associated with translational slip. That is, despite the fact that object kinematics confirmed the rotational dominance of the imposed perturbation, the hybrid perturbation (translational plus rotational) may have yielded just enough translational slip stimuli to scale the strength of the catch-up response. Just because rotation may dominate the kinematics of a perturbation does not mean that stimuli induced by a rotation will dominate grip responses generated by the nervous system.

Interestingly, for translational perturbations, catch-up responses were strongest for perturbations along the grip axis as compared to those for perturbations along the d-p and r-u axes, regardless of grip surface friction. When perturbed along the grip axis, the grasped object was pushed into one of the digits. Compression of the fingerpad in the direction of translational perturbation may have increased the finger-object contact area as well as the number of tactile afferents stimulated (Goodwin, John, & Marceglia, 1991). If tactile stimuli contribute to the strength of the catch-up response, compression of the fingerpad could result in a stronger catch-up response. However, it should be noted that translational perturbations along the grip axis simultaneously resulted in movement of the object away from the other digit. The quick decompression of the fingerpad could result in tactile stimuli associated with a sudden loss of contact with a grasped object, which might elicit a stronger catch-up response.

***Effect of perturbation direction.*** Perturbation direction affected the strength of the catch-up response for translational perturbations along the d-p axis.

The catch-up response was stronger for perturbations that pulled the grasped object away from the palm than for those that pushed the object towards the palm, regardless of grip surface friction. These findings are consistent with previous studies in which the strength of the catch-up response was greater for "dangerous" directions, away from the palm or in the direction of gravity (Häger-Ross et al., 1996; Jones & Hunter, 1992).

For translational pertubations along the r-u axis (aligned with gravity), the median values of catch-up response strength were greater for perturbations in the direction of gravity (downwards, negative r-u direction) than those for perturbations that opposed the direction of gravity (upwards, positive r-u direction) (Fig. 3.6). However, the spread of the catch-up response strength values were such that perturbation direction did not have a statistically significant effect on strength of the catch-up response.

**CONCLUSION**

In this study, we aimed to (i) investigate grip responses to pure translational and pure rotational perturbations, (ii) impose perturbations along and about all three hand-centric axes (distal-proximal, radial-ulnar, and grip), and (iii) investigate the effects of different grip surface friction conditions across the two digits. We found that the temporal characteristics of the catch-up response (onset latency, duration) were essentially robust to all experimental factors (see Appendix C), including grip surface friction. The uniform timing of the catch-up response was consistent with prior studies on grip responses to translational perturbations (Cole & Abbs, 1988; R.S. Johansson & Westling, 1987). Thus, it seems that a pre-programmed increase in normal (grip) force is the stereotypical grip response to unexpected perturbations, whether translational or rotational in nature.

The strength of the catch-up response was sometimes context-dependent. The strength of the catch-up response was only affected by the axis of perturbation for translational perturbations. Translational perturbations along the grip axis were strongest while perturbations along the d-p axis were the weakest. Yet, catch-up responses elicited by translational perturbations away from the palm (positive d-p axis) were stronger than those for perturbations towards the palm. This finding was consistent with a previous study in which the catch-up response was stronger for “dangerous” directions (away from the palm of the hand, or with gravity) (Häger-Ross et al., 1996; Jones & Hunter, 1992).

Grip surface friction had no effect on catch-up response characteristics or preload normal and tangential forces. This result was surprising, as it was hypothesized that fingertip forces would scale independently according to grip surface frictional conditions (Edin, Westling, & Johansson, 1992). It may be that roughness, not necessarily coefficient of friction alone, is a salient property of grip surfaces.

# CHAPTER 4

# TRANSLATIONAL AND ROTATIONAL STIFFNESS OF THE PRECISION GRIP – OBJECT SYSTEM

## INTRODUCTION

The active properties of precision grip responses to unexpected perturbations have been studied extensively in the literature (De Gregorio & Santos, 2013; Häger-Ross, Cole, & Johansson, 1996; R S Johansson, Riso, Häger, & Bäckström, 1992; R. S Johansson, Häger, & Bäckström, 1992; Roland S. Johansson, Häger, & Riso, 1992; Jones & Hunter, 1992) and in Chapters 2 and 3 of this dissertation. However, it is well known that passive properties of the hand also play a role in grasp stabilization, particularly during the early phase of the grip response when active responses have not yet been triggered (Fig. 2.4, 3.3). Research is ongoing to develop better models of the hand and its passive properties such as impedance (Hajian & Howe, 1997) and joint torques (Kamper, Fischer, & Cruz, 2006; Kamper, Hornby, & Rymer, 2002; Kuo & Deshpande, 2010; Lee, Chen, & Kamper, 2009), which are affected by posture and muscle activity.

Estimation of passive properties of human limbs has been done previously via studies of mechanical impedance. Mechanical impedance can be thought of as a measure of how much a system resists movement when subjected to a force. Impedance itself can be broken down into three components: inertia ($I$) as resistance to acceleration, damping ($B$) as resistance to velocity, and stiffness ($K$) as resistance to displacement. Typically, impedance estimation is performed using small perturbations of an endpoint or a specific joint of a serial linkage, such as a human arm (Dolan, Friedman, & Nagurka, 1993; Flash & Mussa-Ivaldi, 1990; Gomi & Kawato, 1997; Gomi, Koike, & Kawato, 1992; Mussa-Ivaldi, Hogan, & Bizzi, 1985; Patel, 2013). The aforementioned studies rigidly attached the hand to the perturbation mechanism (usually a robot) with calcified bandages, straps, or magnets. This practice minimizes losses due to movement between the limb endpoint and the robot end-effector that imparts the perturbation.

Most studies employ small translational displacements of the endpoint in order to estimate the translational stiffness of the endpoint of a limb. However, activities of daily living often require physical interactions with the environment that require rotational stiffness as well (e.g., turning a knob). Further, early studies on translational stiffness were conducted using 2D perturbations. More recently, robots have been used to impose 3D translational perturbations that more accurately capture the effects of posture and muscle activity on 3D endpoint stiffness of the arm (Patel, 2013), for example.

In the present study, we investigate the translational and rotational stiffness of two serial linkages (thumb and index finger) that work in concert to grasp an object in a precision grip. Thus, stiffness properties reported here are for the precision grip-object system as a whole, as opposed to properties of specific digits. The objective of this study was to (i) estimate the translational and rotational stiffness of the precision grip-object system in 3D, and (ii) investigate the effects of grip force on stiffness of the system. To our knowledge, this is the first study of human grasp stiffness that involves more than one digit and estimates both translational and rotational stiffness.

## MATERIALS AND METHODS

**Equipment.** Seven consenting right-handed subjects with no history of neurological or hand impairment participated in this Arizona State University Institutional Review Board approved study. The subjects ranged in age from 25 to 35 years (3 male, 4 female).

An instrumented object housed two six degree-of-freedom force/torque transducers (Nano-17, ATI Industrial Automation) that were used to measure the fingertip forces and torques of the thumb and index finger independently at 2 kHz (Fig. 3.1). Each sensor was rigidly attached to a magnetic grip plate with a smooth Kapton Polymide (high friction) surface with coefficient of friction 0.63 (McMaster-Carr, 2012). The grip surfaces were parallel to one another and spaced 38 mm apart.

A Grass QP511 Quad Ace surface electromyography (EMG) system was used to collect data from four hand muscles (two intrinsic, two extrinsic) at 2 kHz. As seen in Figure 3.1, the four hand muscles that we investigated were the first dorsal interosseous (FDI, intrinsic, thumb and index finger), the abductor pollicis brevis (APB, intrinsic, thumb), the extensor digitorum communis (EDC, extrinsic, index finger), and the flexor pollicis longus (FPL, extrinsic, thumb).

Two Phantom haptic devices (Phantom Premium 1.5, SensAble Technologies) were used to administer 14 different translational perturbations and 14 different rotational perturbations (Fig. 3.2) that encompassed much of the hand-centric reference frame (Fig. 9): the distal-proximal (“d-p”) axis was directed away from and towards the subjects palm, the radial-ulnar (“r-u”) axis was aligned with the vertical axis of the grip plate, and the grip axis connected the two finger pads. Three different Phantom configurations were used to induce all the necessary perturbations. To ensure that the perturbations would be administered in the hand-centric reference frame, the position and orientation of the object was recorded using the magnetic position and orientation sensor (Fastrak, Polhemus) at 120 Hz. The position and orientation data for the object were transformed into the reference frames of the two Phantom robots such that perturbations commanded at the Phantom end-effectors would result in desired impulses in the hand-centric reference frame.

In order to minimize the pronation, supination, adduction, and abduction of the wrist, each subject’s arm and wrist were restrained by a vacuum positioning pillow (versa Form, Sammons Preston).

**Procedure.** Subjects were instructed to grasp the instrumented object between the thumb and index finger in a precision grasp and to gradually increase their grip force until both digits surpassed a specific threshold (15 N or 20 N). The grip threshold was provided to subjects as a continuously updated force trace on a computer monitor. Once the threshold was breached by both digits simultaneously, an impulse perturbation was applied to the object via the Phantoms. The type of impulse (rotational or translational), the direction (positive or negative), and the grip threshold (15 N or 20 N) was randomized.

Each combination of factors was tested four times. A mandatory 30 second rest period was given between blocks. In addition, subjects were instructed to notify the researcher if additional rest was necessary to avoid fatigue. To minimize time spent reconfiguring the experimental set-up (Fig. 3.3), all trials possible for a single configuration (Table 4.1) were randomized and conducted before changing the Phantom configuration. A total of 224 trials were performed per subject. Each impulse lasted for 60 ms and had a magnitude of 1.47 N for the translational cases and 50.5 N-mm for the rotational cases.

Table 4.1.

*Sample experimental trial block*

| Phantom Configuration | Axis | Direction | Type |
|---|---|---|---|
| 1 | GRIP | Negative | Rotation |
| 1 | All three | Combination | Translation |
| 1 | All three | Combination | Translation |
| 1 | All three | Combination | Translation |
| 1 | GRIP | Negative | Translation |
| 1 | All three | Combination | Translation |
| 1 | All three | Combination | Translation |
| 1 | All three | Combination | Translation |

**Data Analysis.** Position and orientation data for the object were transformed into the hand-centric reference frame using MATLAB (Mathworks) and used to determine the onset of the Phantom-imposed perturbation (t = 0 sec). All translational and rotational displacements were measured relative to the position and orientation of the object at the time point at which the impulse was imposed. Linear and angular velocity were determined by taking the first order difference of the displacement data. Linear and angular acceleration were determined by taking the first order difference of the velocity data.

Force and torque data were filtered using a fourth order, 30 Hz low-pass Butterworth filter (De Gregorio & Santos, 2013). The absolute value of the 3D forces and torques produced by the thumb and index finger were summed to determine the total restoring force and torque on the precision grip-object system).

***Impedance estimation.*** The impedance matrices (inertia *I*, damping *B*, stiffness *K*) of the grip-object system were estimated using the kinetic and kinematic data during each impulse. Data from the first 20ms and first 30 ms of the impulse were investigated. It was determined visually that trends in the 0-20 ms window (41 data points per subject) were preserved in the 0-30 ms window (61 data points per subject). Only the 0-20 ms window immediately following each impulse perturbation was used to estimate system impedance in order to minimize the effects of short-latency stretch reflexes (Brown, Rack, & Ross, 1982; Marsden, Merton, & Morton, 1976; Matthews, 1984a, 1984b; Thilmann, Schwarz, Töpper, Fellows, & Noth, 1991). Since the short impulse perturbation induced small movements of the system, we fit our data to the following models, as is common in perturbation studies of end-point impedance (Hajian & Howe, 1997; Tsuji & Kaneko, 1996).

$$F = I_T\ddot{x} + B_T\dot{x} + K_T x \tag{4.1}$$

$$T = I_R\ddot{\theta} + B_R\dot{\theta} + K_R\theta \tag{4.2}$$

where $I_T$, $B_T$, and $K_T$ are the 3 x 3 matrix representations of the inertia, damping, and stiffness of the grip-object system, respectively, for the translational impulse perturbations and $I_R$, $B_R$, and $K_R$ are the corresponding matrices for the rotational impulse perturbations. The 3D acceleration, velocity, and displacement vectors for translational impulses are represented by $\ddot{x}, \dot{x}$ and $x$, respectively. The 3D acceleration, velocity, and displacement vectors for rotational impulses are represented by $\ddot{\theta}, \dot{\theta}$ and $\theta$, respectively.

*F* is the 3 x 1 vector of restoring force while *T* is the 3 x 1 vector of restoring torque. Equations (4.1) and (4.2) can be rewritten in parameter identification form (Patel, 2013):

$$F = P_T Y_T \tag{4.3}$$

$$T = P_R Y_R \tag{4.4}$$

where $Y_T$ and $Y_R$ are 9x1 vectors of displacements defined as

$$Y_T = \begin{bmatrix} \ddot{x} \\ \dot{x} \\ x \end{bmatrix} \tag{4.5}$$

$$Y_R = \begin{bmatrix} \ddot{\theta} \\ \dot{\theta} \\ \theta \end{bmatrix} \tag{4.6}$$

$P_T$ and $P_R$ are the 3 x 9 matrices for the impedance parameters to be identified for the translational and rotational impulse perturbations, respectively:

$$P_T = \begin{bmatrix} I_T & B_T & K_T \end{bmatrix} \tag{4.7}$$

$$P_R = \begin{bmatrix} I_R & B_R & K_R \end{bmatrix} \tag{4.8}$$

By concatenating all *n* datapoints on a subject-specific basis, equations (4.3) and (4.4) were rewritten as

$$[F_1 \dots F_n] = P_T[Y_{T,1} \dots Y_{T,n}] \tag{4.9}$$

$$[T_1 \dots T_n] = P_R[Y_{R,1} \dots Y_{R,n}] \tag{4.10}$$

Using the right pseudo-inverse ($^\dagger$), a least-squares linear regression was performed to determine the parameter matrices $P_T$ and $P_R$.

$$P_T = [F_1 \dots F_n][Y_{T,1} \dots Y_{T,n}]^\dagger \tag{4.11}$$

$$P_R = [T_1 \dots T_n][Y_{R,1} \dots Y_{R,n}]^\dagger \tag{4.12}$$

The *I*, *B*, and *K* 3 x 3 submatrices were extracted from the appropriate 3 x 9 parameter matrix *P*. Given that the experiment was designed for impulse perturbations of position/ orientation as opposed to perturbations of velocity or acceleration, the *I* and *B* matrices were expected to be negligible. However, these matrices were not negligible, owing to large velocity and acceleration terms for the instrumented object after performing first order differences on the position/orientation data. In order to best estimate stiffness *K*, the parameter estimation was rerun without velocity, acceleration, damping, or inertia terms. The *K* matrix was then separated into symmetric (S) and anti-symmetric (A) components using the following method, demonstrated for the translational case.

$$K_T = K_T^S + K_T^A \tag{4.13}$$

where

$$K_T^S = \tfrac{1}{2}(K_T + K_T^T) \tag{4.14}$$

$$K_T^A = \tfrac{1}{2}(K_T - K_T^T) \tag{4.15}$$

Physically, the symmetric matrix is associated with conservative force fields and the anti-symmetric matrix is associated with losses in the system (Mussa-Ivaldi, Hogan, & Bizzi, 1985).

As the estimation of system impedance requires both displacement and force/torque data, the different sampling rates for each data stream (object position and orientation of data at 120 Hz, fingertip force and torque data at 2 kHz) had to be reconciled. To this end, we applied a linear interpolation between the points of the position data (approximately 8.3 ms apart) to match the number of data points for displacement and force/torque. We felt this was method was appropriate because, alternatively sub-sampling the load cell data would have resulted in only three data points to calculate the stiffnesses. Furthermore, the spring stiffness equation assumes a linear relationship between displacement and restoring force/torque. Data from all perturbation directions for a given grip force threshold were concatenated into a single *F*, *T*, or *Y* matrix as appropriate on a subject-specific basis (Eqns. 4.11 and 4.12).

***3D stiffness representation.*** Ellipsoids were created in order to visualize stiffness properties of the precision-grip object system relative to a hand-centric reference frame (d-p, r-u, and grip axes). Ellipsoids are described by their principal axes and the radii of those axes. These properties lend themselves well to visualization of stiffness as they produce an ellipsoid that is broadest in the direction of greatest stiffness, and narrowest in the direction of least stiffness.

The equation for an ellipsoid centered at the origin and whose principal axes are aligned with Cartesian axes can be represented as

$$\frac{x^2}{a^2} + \frac{y^2}{b^2} + \frac{z^2}{c^2} = 1 \qquad (4.16)$$

A more general equation for an ellipsoid is given by

$$(j - C)^T A (j - C) = 1 \qquad (4.17)$$

where $C$ is a vector representing the center of the ellipsoid with respect to the Cartesian origin, $j$ is a vector of all points forming the surface of the ellipsoid, and $A$ is a positive definite matrix whose eigenvectors define the directions of the principal axes of the ellipsoid and whose eigenvalues define the (squared) radii of the ellipsoid (O'Neill, 2013).

We consider the case of a unit sphere defined by small forces $F$

$$F^T F = 1 \tag{4.18}$$

Neglecting velocity and acceleration terms in Eqn. 4.1, we can define restoring forces $F$ as a function of the displacement $x$ and symmetric stiffness matrix $K^S$.

$$F = K^S x \tag{4.19}$$

Substituting Eqn. 4.19 into Eqn. 4.18 yields

$$x^T[(K^S)^T K^S]x = 1 \tag{4.20}$$

Eqn. 4.20, now in the form of Eqn. 4.17, represents an ellipsoid defined by the symmetric stiffness matrix $K^S$ (O'Neill, 2013) where $[(K^S)^T K^S]$ is equal to $A$. This method was used for both translational stiffness $K_T^S$ and rotational stiffness $K_R^S$.

Singular value decomposition (SVD) was performed on the matrix $[(K^S)^T K^S]$ in order to extract orthonormal eigenvectors and eigenvalues from the $V$ and $S$ matrices produced by the decomposition process, respectively.

$$K^S = USV^T \tag{4.21}$$

$$(K^S)^T K^S = VS^2V^T \tag{4.22}$$

where

$$V = \begin{bmatrix} p^1 & p^2 & p^3 \end{bmatrix} = \begin{bmatrix} p_{11} & p_{12} & p_{13} \\ p_{21} & p_{22} & p_{23} \\ p_{31} & p_{32} & p_{33} \end{bmatrix} \tag{4.23}$$

$$S = \begin{bmatrix} \lambda_1 & 0 & 0 \\ 0 & \lambda_2 & 0 \\ 0 & 0 & \lambda_3 \end{bmatrix} \tag{4.24}$$

The $V$ matrix of eigenvectors provided the directions of the principal axes of each ellipsoid (primary $p^1$, secondary $p^2$, and tertiary $p^3$) with respect to the hand centric reference frame. The $S$ matrix of eigenvalues was used to find the radii of the ellipsoid. The equatorial radii ($r_{e1}$ *and* $r_{e2}$) and polar radius $r_p$ associated with the principle axes were determined as follows:

$$r_{e1} = \sqrt{\lambda_1} \tag{4.25}$$

$$r_{e2} = \sqrt{\lambda_2} \tag{4.26}$$

$$r_p = \sqrt{\lambda_3} \tag{4.27}$$

**RESULTS**

**Stiffness analysis.** The stiffness ($K$) matrices were found and separated into symmetric and anti-symmetric components. Given our experimental design and standard practices (Hajian & Howe, 1997; F. A. Mussa-Ivaldi et al., 1985; Patel, 2013), the inertia and the damping components were assumed to be negligible (see Chapter 4 Materials and Methods).

Stiffness ellipsoids were created using the aforementioned methods for each of the seven subjects on an individual basis. The mean ± standard deviation (std) of the stiffness values for each case across subjects are reported in Tables 4.2 – 4.5, along with the stiffness ellipsoids from one representative subject (Figures 4.1 – 4.4) for the translational and rotational cases.

Translational stiffness was largest along the grip axis for both grip force threshold values (Fig. 4.1, Tables 4.2 and 4.3). As grip force threshold increased from 15 N to 20 N, the translational stiffness increased for the grip axis by 96%, decreased for the r-u axis by 19%, and stayed constant for the d-p axis (change of -0.01%). Regardless of these changes, the ranked order of stiffness remained the same for each grip force threshold. Translational stiffness was smallest along the r-u axis and largest along the grip axis (Figs. 4.1 and 4.2).

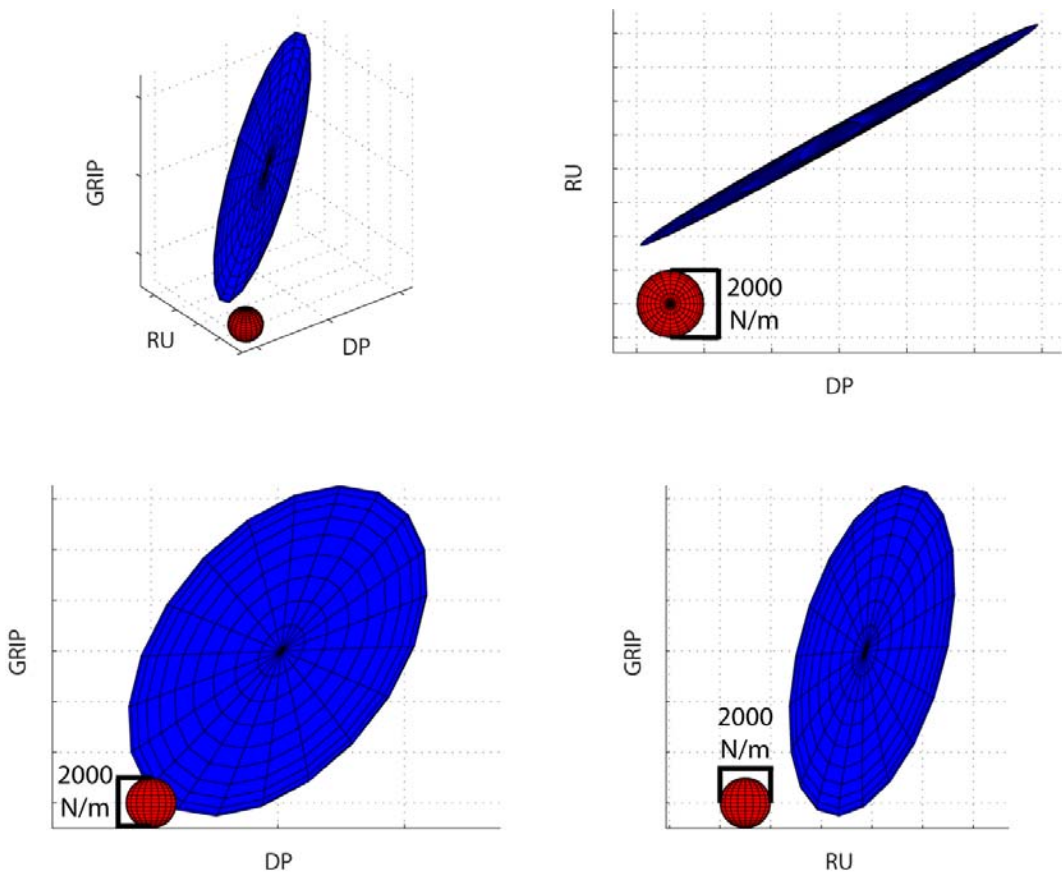


*Figure 4.1. Translational stiffness ellipsoid for 15 N grip force threshold (representative subject).* The translational stiffness ellipsoid is shown in various 2D and 3D views. The translational stiffness values were largest and smallest along the grip axis and r-u axis, respectively. The sphere represents a uniform stiffness of 2000 N/m in all directions for scale.

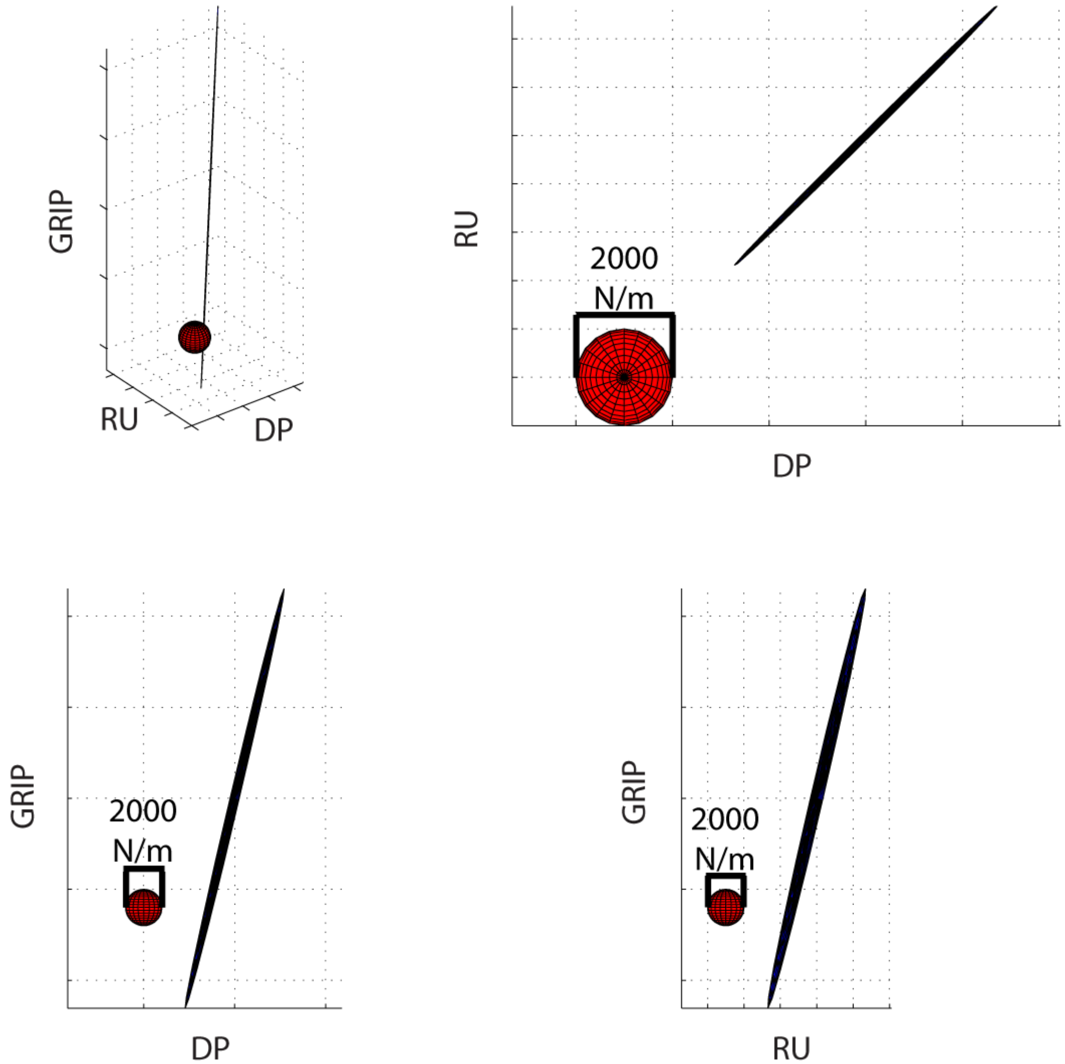

*Figure 4.2. Translational stiffness ellipsoid for 20 N grip force threshold (representative subject).* The translational stiffness ellipsoid is shown in various 2D and 3D views. The translational stiffness values were largest and smallest along the grip axis and r-u axis, respectively. The sphere represents a uniform stiffness of 2000 N/m in all directions for scale.

Rotational stiffness was largest about the r-u axis and smallest about the grip axis for both grip force thresholds (Figs. 4.3 and 4.4, Tables 4.4 and 4.5). Compared to the d-p and r-u axes, rotational stiffness was almost negligible about the grip axis for both grip force thresholds. As grip force threshold increased from 15 N to 20 N, the rotational stiffness increased about all axes (by 6% for the d-p axis, 6% for the r-u axis, and 700% for the grip axis), but remained small for the grip axis. The ranked order of rotational stiffness in the Cartesian frame did not change with grip force threshold.

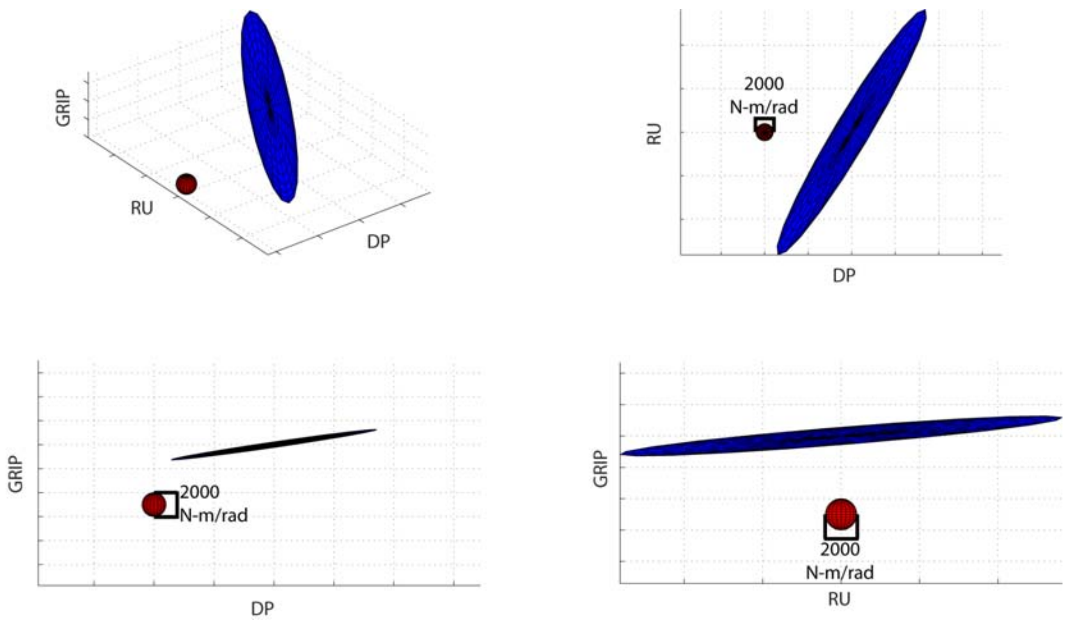


*Figure 4.3. Rotational stiffness ellipsoid for 15 N grip force threshold (representative subject).* The rotational stiffness ellipsoid is shown in various 2D and 3D views. The rotational stiffness values were largest and smallest along the r-u axis and grip axis, respectively. The sphere represents a uniform stiffness of 2000 N-m/rad in all directions for scale.

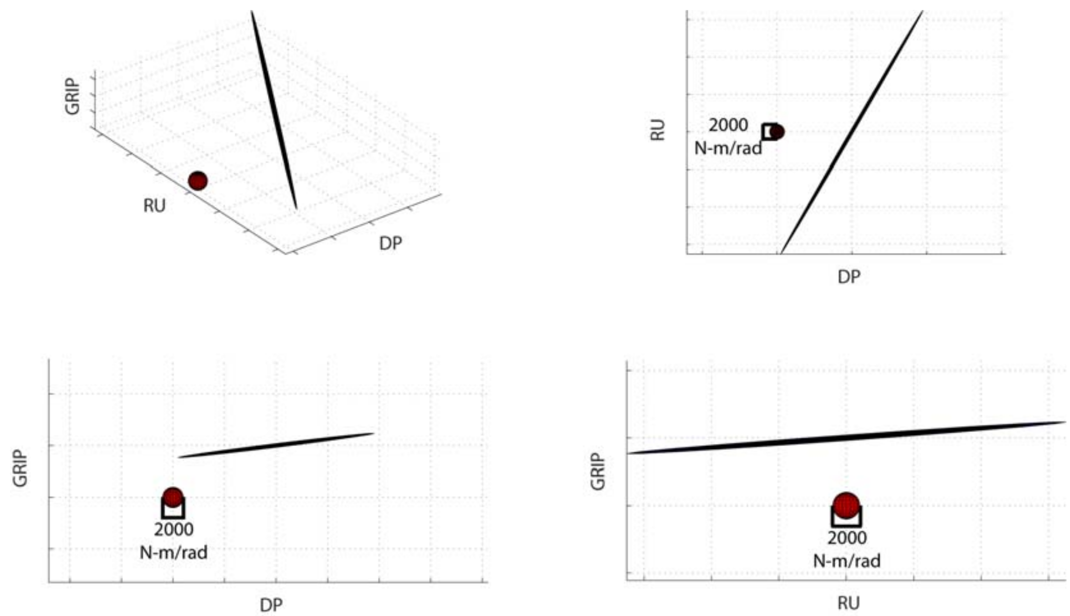


*Figure 4.4. Rotational stiffness ellipsoid for 20 N grip force threshold (representative subject).* The rotational stiffness ellipsoid is shown in various 2D and 3D views. The rotational stiffness values were largest and smallest along the r-u axis and grip axis, respectively. The sphere represents a uniform stiffness of 2000 N-m/rad in all directions for scale.

The symmetric stiffness matrix $K^S$ associated with the conservative force field is reported for pooled subject data for translational and rotational cases in Tables 4.2, 4.3, 4.4, and 4.5 along with the maximum value for $K^A$.

Table 4.2.

*Symmetric Translational Stiffness Matrix $K_T^S$ for the 15 N Grip Force Threshold (pooled data).* Stiffness values are reported as mean (std) in (N/m). The maximum value in the corresponding anti-symmetric stiffness matrix was $\boldsymbol{K^A_{max}}$ = 5765.9 N/m.

| | D-P | R-U | GRIP |
|---|---|---|---|
| **D-P** | **890.0 (717.8)** | 530.4 (302.5) | 5986.1 (3110.9) |
| **R-U** | 530.4 (302.5) | **256.5 (177.0)** | 2823.6 (1470.4) |
| **GRIP** | 5986.1 (3110.9) | 2823.6 (1470.4) | **3358.9 (2146.4)** |

Table 4.3.

*Symmetric Translational Stiffness Matrix $K_T^S$ for the 20 N Grip Force Threshold (pooled data).* Stiffness values are reported as mean (std) in (N/m). The maximum value in the corresponding anti-symmetric stiffness matrix was $\boldsymbol{K^A_{max}}$ = 5251.2 N/m.

| | D-P | R-U | GRIP |
|---|---|---|---|
| **D-P** | **889.9 (874.6)** | 389.5 (154.3) | 5656.5 (3839.5) |
| **R-U** | 389.5 (154.3) | **207.6 (138.4)** | 2603.2 (1159.4) |
| **GRIP** | 5656.5 (3839.5) | 2603.2 (1159.4) | **6578.4 (3500.9)** |

Table 4.4.

*Symmetric Rotational Stiffness Matrix $K_R^S$ for the 15 N Grip Force Threshold (pooled data).* Stiffness values are reported as mean (std) in (N-m/rad). The maximum value in the corresponding anti-symmetric stiffness matrix was $\boldsymbol{K^A_{max}}$ = 1167.0 N-m/rad.

| | **D-P** | **R-U** | **GRIP** |
|---|---|---|---|
| **D-P** | **7751.2 (3129.3)** | 9007.7 (3887.6) | 447.5 (232.9) |
| **R-U** | 9007.7 (3887.6) | **9993.6 (4972.6)** | 691.2 (568.0) |
| **GRIP** | 447.5 (232.9) | 691.2 (568.0) | **1.1 (4.8)** |

Table 4.5.

*Symmetric Rotational Stiffness Matrix $K_R^S$ for the 20 N Grip Force Threshold (pooled data).* Stiffness values are reported as mean (std) in (N-m/rad). The maximum value in the corresponding anti-symmetric stiffness matrix was $\boldsymbol{K^A_{max}}$ = 1309.7 N-m/rad.

| | **D-P** | **R-U** | **GRIP** |
|---|---|---|---|
| **D-P** | **8251.0 (3890.4)** | 9650.0 (2808.2) | 458.2 (295.3) |
| **R-U** | 9650.0 (2808.2) | **10616.2 (3641.1)** | 722.6 (384.8) |
| **GRIP** | 458.2 (295.3) | 722.6 (384.8) | **8.8 (19.2)** |

## DISCUSSION

**Translational stiffness of the precision grip-object system.** In both the subject-specific and pooled cases, translational stiffness was largest along the grip axis. As grip force threshold increased, translational stiffness decreased slightly for the r-u axis, but increased by two orders of magnitude for the d-p axis (Tables 4.2 and 4.3). The increase in translational stiffness along the grip axis with grip force threshold was not too surprising.

The increase in translational stiffness along the d-p axis may be related to concurrent flexion of finger joints as grip force is increased. Computer simulations suggest that extrinsic flexor muscles (flexor digitorum profundus and flexor digitorum superficialis) cause concurrent flexion of all three index finger joints (distal interphalangeal, proximal interphalangeal, metacarpophalangeal) (Kamper, Hornby, & Rymer, 2002). Index finger posture greatly affects transmission of muscle forces to joint torques. For instance, as the flexor digitorum superficialis is shortened, joint torques at the metacarpophalangeal joint are larger when the index finger is more flexed (Kamper, Fischer, & Cruz, 2006). Passive joint stiffness and damping are critical to the concurrent flexion of the index finger joints (S.-W. Lee et al., 2009). Thus, it is not unreasonable to expect that increases in grip force thresholds prescribed by the experimental task would require increased activity in extrinsic flexors that would, in turn, cause increases in joint torques and passive joint impedance. Given the orientation of the index finger in the precision grip posture, resistance to finger flexion/extension would directly affect resistance to translational displacements along the d-p axis.

The finding that grip force threshold did not really affect translational stiffness along the r-u axis is somewhat less intuitive. Translational displacements along the r-u axis would involve adduction/abduction of the index finger at the metacarpophalangeal joint. Given that the instructions to each subject were to achieve a prescribed grip force, it is likely that muscle activation was biased towards flexion/extension rather than adduction/abduction (Valero-Cuevas, Towles, & Hentz, 2000). Considering the orientation of the digits in the precision grip posture, increases in grip force would not necessarily affect resistance to translational displacements along the r-u axis. Furthermore, the kinematics of the precision grip posture are such that active resistance to translational displacements along the r-u axis is difficult to achieve.

**Rotational stiffness of the precision grip-object system.** In both the subject-specific and pooled cases, rotational stiffness was largest about the r-u and d-p axes and increased with increases in grip force threshold (Tables 4.3 and 4.4). Rotational stiffness about the grip axis was very small compared to rotational stiffness about the other two axes. Rotations about the grip axis induce rotational slip at the fingerpad (Kinoshita et al., 1997). Thus, without the use of the wrist, rotational perturbations about the grip axis cannot be corrected. Passive torsion of the fingerpad may be the primary mechanism for resisting rotational perturbations about the grip axis, and its contributions to rotational stiffness are likely to be small.

The large rotational stiffness about the r-u axis could be due to the fact that rotations about the r-u axis tend to flex (and “jam”) one digit while tending to extend the other digit. Given that the experimental task required isometric production of a specific grip force, flexion/extension of either digit is likely to be small. The large rotational stiffness about the d-p axis could also be related to the active maintenance of a constant posture for increased isometric grip forces. As grip force threshold increases, FDI activity  also likely increases (Valero-Cuevas et al., 2000), which could increase passive joint stiffness at the metacarpophangeal adduction/abduction joint. In turn, rotational displacements about the d-p axis would be increasingly resisted by the entire digits with increases in the grip force threshold.

The increase in rotational stiffness about the r-u axis may be related to the increase in translational stiffness along the d-p axis. If one were to break down the precision grip–object system, rotational displacements of the object would be related to opposing and potentially equal translational displacements at each fingertip. The concept is similar to how a couple is comprised of equal, opposing, parallel force vectors. If we think about rotational stiffness about the r-u axis as the combination of two opposing but potentially additive translational stiffnesses along the d-p axis, we see that rotational stiffness about the r-u axis and translational stiffness along the d-p would increase together with increases in grip force threshold, and for similar reasons.

**Potential losses in the precision-grip object system.** Physically, the anti-symmetric stiffness matrix represents stiffness associated with non-conservative forces that cause losses in the system. For small displacements of human arms that were physically (often rigidly) connected to perturbation mechanisms, losses in the system were typically small (Ferdinando A. Mussa-Ivaldi, Hogan, & Bizzi, 1985; Patel, 2013). In this study, some elements in the stiffness matrix $K^A$ associated with non-conservative forces were comparable to elements in the stiffness matrix $K^S$ associated with conservative forces (Tables 4.1 and 4.2). In our study, losses may have occurred due to the fact that the index finger and thumb were not rigidly attached to the object. Hence, small slips may have occurred between the digits and the instrumented object upon perturbation of the object. Any slip would not have been detected by the position and orientation sensor rigidly attached to the object. This may also help to explain why the translational stiffness was so low along the d-p axis for the 15 N grip force threshold. A smaller grip force would be more prone to slip of the object relative to the fingertips. Further investigation of the load cell data is needed to determine how much the center of pressure of each digit may have moved due to slip and/or shear of the fingerpads.

For the rotational stiffness case, elements in the anti-symmetric stiffness matrix were smaller than those in the symmetric stiffness matrix. However, not all anti-symmetric stiffness values were negligible. Since the index finger and thumb were not rigidly attached to the object, losses may have occurred due to roll of the fingerpad along the grip surface that would not have been accounted for by the position and orientation sensor attached to the object.

**CONCLUSION**

In this study, we investigate the translational and rotational stiffness of two serial linkages (thumb and index finger) that work in concert to grasp an object in a precision grip. Thus, stiffness properties reported here are for the precision grip-object system as a whole, as opposed to properties of specific digits. Further, this study was completed for rotational and translational stiffness estimations in 3D.

Translational stiffness increased with increasing grip force threshold along the d-p and grip axes. However, the stiffness decreased slightly along the r-u axis. It was hypothesized that the increase in translational stiffness along the d-p axis was due to the concurrent flexion of finger joints as grip force threshold increased, along with the posture of the digits for isometric force production in a precision grip.

Rotational stiffness increased with increasing grip force threshold about the d-p and r-u axes. The stiffness about the grip axis was very small compared to that about the other two axes. This finding makes sense given that rotational perturbations of an object about the grip axis are primarily resisted by torsion of the fingerpad while the digits themselves play larger resistive roles for rotations about the d-p and r-u axes.

We present a novel paradigm for estimating the passive properties of two-digit grasps. We suggest that 3D rotational stiffness is just as important to characterize as 3D translational stiffness. An understanding of translational and rotational stiffness of the precision grip-object system could provide insights into the strengths and weaknesses of grasps implemented by anthropomorphic artificial hands. In addition, the bimanual manipulation of an object between two arms shares certain aspects with the precision grip–object system studied here. It may be possible to characterize the stiffness of bimanual grasps in a similar manner.

# CHAPTER 5

# SUMMARY AND CONCLUSIONS

## MAJOR CONTRIBUTIONS

**Novel apparatus and experimental protocols** A novel experimental set-up was developed for the studies featured in Chapters 3 and 4 (Fig. 3.1). The set-up included two six-degree-of-freedom load cells, two Phantom haptic devices, a Fastrak magnetic position and orientation sensor, surface EMG for four muscles, and powered shutter goggles.

In order to record 3D fingertip forces and torques for each digit, the Phantom thimbles were replaced by a 3D printed, instrumented object which housed the load cells. The 3D printed object had four attachment points for the Phantom end-effectors which enabled translational and rotational perturbations for any 3D direction. Further, a Fastrak magnetic position and orientation sensor was rigidly mounted to the top of the 3D printed object. This sensor allowed for perturbations to be applied in a hand-centric reference frame (d-p, r-u, grip axes) regardless of the subject's hand posture. A flexible hose (Loc-Line) was used to easily bring the Fastrak transmitter and receiver within range of one another.

In order to test different random combinations of grip surface friction conditions quickly, a steel grip plate was attached to the working face of each load cell. Smooth grip surfaces (PTFE or Kapton Polymide) were affixed to magnetic strips with sticky backings so that low and high friction surfaces could be changed quickly and easily.

**Neural Control of Movement** For the past 20 years, most experiments investigating precision grip responses to unexpected perturbations have focused on grip responses when linear slip is induced by translational perturbations. Chapter 2 shows that the catch-up response exists for conditions other than pure linear slip. Further, it shows that the strength of the catch-up response scales such that rotations about the grip axis in the negative direction were stronger than those about the d-p axis.

In the follow-up study (Chapter 3) using robot-imposed perturbations, the temporal characteristics of the catch-up response (onset latency, duration) were robust to all experimental factors (smallest $p = 0.072$). However, we were unable to confirm all of the prior findings in the follow-up study. The spread of the data precluded any effects of perturbation axis on catch-up response strength, but catch-up response strength was occasionally affected by perturbation direction. The strength of the catch-up response was only affected by the axis of perturbation for translational perturbations. Translational perturbations along the grip axis were strongest while perturbations along the d-p axis were the weakest. Yet, catch-up responses elicited by translational perturbations away from the palm (positive d-p axis) were stronger than those for perturbations towards the palm. This finding was consistent with a previous study in which the catch-up response was stronger for “dangerous” directions (away from the palm of the hand, or with gravity) (Häger-Ross, Cole, & Johansson, 1996; Jones & Hunter, 1992).

Perhaps one of the more interesting results is the finding that surface roughness may be more salient than coefficient of friction of a smooth surface. Grip surface friction had no effect on catch-up response characteristics or preload normal and tangential forces. This result was surprising, as it was hypothesized that fingertip forces would scale independently according to grip surface frictional conditions (Edin, Westling, & Johansson, 1992). It may be that roughness, not necessarily coefficient of friction alone, is a salient property of grip surfaces.

**Significance for Robotics**. The characterization of human grip responses to unexpected perturbations may be of particular use to roboticists working on teleoperated systems. If something unexpected happens during a teleoperated task (e.g. – surgery, fixing a satellite, bomb defusal) an object could be lost from a robot's grasp before the human operator is aware of the problem or has time to command an appropriate response. With tactile feedback, a teleoperated robot could be programmed with context-dependent, low level reflexes that account for the passive properties of the end-effector, its kinematic workspace, and type and direction of a perturbation with respect to a hand-centric reference frame.

We present a novel paradigm for estimating the passive properties of two-digit grasps. We suggest that 3D rotational stiffness is just as important to characterize as 3D translational stiffness. An understanding of translational and rotational stiffness of the precision grip-object system could provide insights into the strengths and weaknesses of grasps implemented by anthropomorphic artificial hands. The experimental approach could inspire whole arm and hand studies to characterize the passive properties of bimanual grasps.

## FUTURE DIRECTIONS

**Grip responses to unexpected perturbations.** Perhaps one of the most interesting questions raised by these studies is whether grip surface friction conditions are perceived more easily with rough surfaces than smooth surfaces that have high coefficients of friction. In Chapter 3, we used smooth surfaces whose coefficient of friction differed by an order of magnitude ($\mu = 0.63$ for Kapton Polymide, $\mu = 0.05\text{-}0.1$ for PTFE) (McMaster-Carr, 2012). We elected to diverge from the traditional use of silk and sandpaper surfaces (Edin et al., 1992; Johansson & Westling, 1984; Westling & Johansson, 1984) in order to minimize discomfort to subjects from repeated perturbations. It would be interesting to rerun the experiment in Chapter 3 with unmatched pairings of smooth (silk) and rough (sandpaper) grip surfaces in order to see how preload fingertip forces and catch-up response strength may be affected.

Previous studies have been done on the spatial resolution of the fingerpad using grated surfaces (Johnson & Phillips, 1981; J. R. Phillips & Johnson, 1981; John R. Phillips & Johnson, 1981). These edge detection experiments inspire future research questions: Would a grated surface affect the preload normal and tangential forces? How would the catch-up response be affected? Does the direction of the grating with respect to the fingerpad or hand matter?

**Passive properties of the precision grip-object system.** The translational and rotational stiffness of the precision grip-object system was estimated without securing the digits rigidly to the grasped object (Chapter 4). The large values in the anti-symmetric translational stiffness matrices associated with non-conservative forces suggest that linear slip may have led to losses in the system that are otherwise neglected in traditional studies of impedance. To investigate the potential effects of the digit-object “attachment,” a novel object could be designed that would allow for Phantom thimbles to be fixed directly to the grip plates.

Given that finger posture is known to affect passive joint torques (Kamper, Fischer, & Cruz, 2006; Kamper, Hornby, & Rymer, 2002), posture is also likely to affect stiffness of the precision grip-object system. Inter-subject variability would make it difficult to prescribe specific joint angles, but the spacing between grip plates could be varied to test the effects of grip aperture on grasp stiffness. The distance between the grip axis and the palm of the hand could also be varied in order to alter subjects' grip postures. Posture could be constrained by using a test object designed to force digits into specific postures, or by monitoring joint angles in real-time with a motion capture system and imposing perturbations when the digits are in a specific posture. Further, if digit-specific joint angles were recorded using a marker-based motion capture system, it may be possible to estimate digit-specific stiffness properties. Finally, additional grip force threshold values could be tested in order to form a more complete picture of how stiffness ellipsoids scale, and possibly rotate, relative to a hand-centric reference frame.

By applying traditional methods of estimating end-effector stiffness, our study assumed that the stiffness of the precision grip-object system could be represented by an ellipsoid. However, an ellipsoid assumes an equatorial radius that is symmetric along the principal axes. It would be interesting to investigate individual digit stiffness during a precision grip given that differences in digit kinematics could cause the thumb to resist perturbations differently than the index finger. To this end, a novel test object could be designed in which an impulse perturbation was delivered independently to each digit during a precision grip. By tracking the displacements and restoring forces/torques for each digit independently, we could compare the digit-specific stiffness properties to those of the precision grip-object system.

The dynamic impedance of the precision grip-object system could also be studied. An experiment where the subject is instructed to rotate an object between thumb and fore-finger while an unexpected impulse perturbation is imposed would allow for an investigation of how rotational impedance changes during a task. Our novel experimental set-up could be used to both simulate a virtual knob and impose small displacements on the precision grip-object system.

The experimental approach used in Chapter 4 could potentially be extended to the entire upper limb in order to characterize the impedance of bimanual grasp. Different scenarios of bimanual grasp could be investigated, including robot-robot, robot-human, and human-human (same human or different humans) pairings. An understanding of the passive properties of bimanual grasps without rigid attachments could provide insights on how two agents might successfully complete a task such as cooperative movement of an object or object hand-off.

It is not known exactly how much of the catch-up response, as quantified using methods from the literature (De Gregorio & Santos, 2013; Johansson, Riso, Häger, & Bäckström, 1992), is due to passive mechanics and how much is due to an active response. It is likely that the passive and active contributions overlap temporally. It would be interesting to formulate a method for dissecting out the individual contributions over time. This can be tested by abandoning the assumption that stiffness is time invariant and estimating system impedance as a function of time as opposed to over a window of time (e.g., 0-30 ms).

REFERENCES


Allen, P. K., Ciocarlie, M. T., Goldfeder, C., & Dang, H. (2009). Low-dimensional data-driven grasping. *Proc. of the Robotics Science and Systems Conf.* Presented at the Robotics Science and Systems, Seattle, WA.

Argall, B. D., & Billard, A. G. (2010). A survey of Tactile Human–Robot Interactions. *Robotics and Autonomous Systems*, *58*(10), 1159–1176. doi:10.1016/j.robot.2010.07.002

Bekey, G., & Tomovic, R. (1986). Robot control by reflex actions. *Proc. of IEEE Intl Conf on Robotics and Automation* (Vol. 3, pp. 240–247). Presented at the IEEE Int'l Conf. on Robotics and Automation.

Bizzi, E., Dev, P., Morasso, P., & Polit, A. (1978). Effect of load disturbances during centrally initiated movements. *Journal of Neurophysiology*, *41*(3), 542.

Brown, T. I. H., Rack, P. M. H., & Ross, H. F. (1982). A range of different stretch reflex responses in the human thumb. *Journal of Physiology*, *332*(1), 101.

Cole, K. J., & Abbs, J. H. (1988). Grip force adjustments evoked by load force perturbations of a grasped object. *J Neurophysiol*, *60*(4), 1513–1522.

Cole, K. J., & Johansson, R. S. (1993). Friction at the digit-object interface scales the sensorimotor transformation for grip responses to pulling loads. *Exp Brain Res*, *95*(3), 523–532.

De Gregorio, M., Bair, K., & Santos, V. J. (2009). Kinematic and kinetic analyses of reflexive grip responses to rotational perturbations of an object in precision grasp. *Proc Neural Control of Movement Ann Mtg*. Waikoloa, HI.

De Gregorio, M., & Santos, V. J. (2010). Rotational object perturbations result in characteristic types of kinematic grip responses. *Proc Ann Mtg Amer Soc Biomech*. Providence, RI.

De Gregorio, M., & Santos, V. J. (2013a). Precision grip responses to unexpected rotational perturbations scale with axis of rotation. *Journal of Biomechanics*, *46*(6), 1098–1103. doi:10.1016/j.jbiomech.2013.01.017

De Gregorio, M., & Santos, V. J. (2013b). Precision grip responses to unexpected rotational perturbations scale with axis of rotation. *Journal of Biomechanics*, *46*(6), 1098–1103. doi:10.1016/j.jbiomech.2013.01.017

Di Fabio, R. P. (1987). Reliability of computerized surface electromyography for determining the onset of muscle activity. *Phys Ther*, *67*(1), 43 –48.

Dolan, J. M., Friedman, M. B., & Nagurka, M. L. (1993). Dynamic and loaded impedance components in the maintenance of human arm posture. *Systems, Man and Cybernetics, IEEE Transactions on*, *23*(3), 698–709.

Edin, B. B., Westling, G., & Johansson, R. S. (1992). Independent control of human finger-tip forces at individual digits during precision lifting. *Journal of Physiology*, *450*, 547–564.

Flanagan, J. R., Bowman, M. C., & Johansson, R. S. (2006). Control strategies in object manipulation tasks. *Current Opinion in Neurobiology*, *16*(6), 650–659.

Flash, T., & Mussa-Ivaldi, F. A. (1990). Human arm stiffness characteristics during maintenance of posture. *Experimental Brain Research*, (82), 315–326.

Fu, Q., Zhang, W., & Santello, M. (2010). Anticipatory planning and control of grasp positions and forces for dexterous two-digit manipulation. *Journal of Neuroscience*, *30*(27), 9117–9126.

Gomi, H., & Kawato, M. (1997). Human arm stiffness and equilibrium-point trajectory during multi-joint movement. *Biological Cybernetics*, *76*(3), 163–171. doi:10.1007/s004220050329

Gomi, H., Koike, Y., & Kawato, M. (1992). Human hand stiffness during discrete point-to-point multi-joint movement. *Engineering in Medicine and Biology Society, 1992 14th Annual International Conference of the IEEE* (Vol. 4, pp. 1628–1629). Retrieved from http://ieeexplore.ieee.org/xpls/abs_all.jsp?arnumber=5761956

Goodwin, A. W., Jenmalm, P., & Johansson, R. S. (1998). Control of grip force when tilting objects: effect of curvature of grasped surfaces and applied tangential torque. *Journal of Neuroscience*, *18*(24), 10724–10734.

Gordon, A. M., Forssberg, H., Johansson, R. S., & Westling, G. (1991). Integration of sensory information during the programming of precision grip: comments on the contributions of size cues. *Experimental Brain Research*, *85*(1). doi:10.1007/BF00230004

Gordon, A. M., Westling, G., Cole, K. J., & Johansson, R. S. (1993). Memory representations underlying motor commands used during manipulation of common and novel objects. *Journal of Neurophysiology*, *69*(6), 1789 – 1796.

Häger-Ross, C., Cole, K. J., & Johansson, R. S. (1996). Grip-force responses to unanticipated object loading: load direction reveals body-and gravity-referenced intrinsic task variables. *Exp Brain Res*, *110*(1), 142–150.

Häger-Ross, C., & Johansson, R. S. (1996). Nondigital afferent input in reactive control of fingertip forces during precision grip. *Exp Brain Res*, *110*(1), 131–141.

Hajian, A. Z., & Howe, R. D. (1997). Identification of Mechanical Impedance at the Humqan Finger Tip. *Journal of Biomechanical Engineering*, *119*, 109–114.

Hodges, P. W., & Bui, B. H. (1996). A comparison of computer-based methods for the determination of onset of muscle contraction using electromyography. *Electroen Clin Neuro*, *101*, 511–519.

Jenmalm, P., Dahlstedt, S., & Johansson, R. S. (2000). Visual and tactile information about object-curvature control fingertip forces and grasp kinematics in human dexterous manipulation. *J Neurophysiol*, *84*(6), 2984–2997.

Jenmalm, P., & Johansson, R. S. (1997). Visual and somatosensory information about object shape control manipulative fingertip forces. *J Neurosci*, *17*(11), 4486–4499.

Jenmalm, Per, Goodwin, A. W., & Johansson, R. S. (1998). Control of Grasp Stability When Humans Lift Objects With Different Surface Curvatures. *Journal of Neurophysiology*, *79*(4), 1643 –1652.

Johansson, R. S. (1996). Sensory control of dextrous manipulation in humans. In A. M. Wing, P. Haggard, & J. R. Flanagan (Eds.), *Hand and brain: the neurophysiology and psychology of hand movements*, (A.M. Wing, P. Haggard, J.R. Flanagan, eds) (pp. 381–414). San Diego: Academic.

Johansson, R. S., & Cole, K. J. (1994). Grasp stability during manipulative actions. *Canadian Journal of Physiology and Pharmacology*, *72*(5), 511–524.

Johansson, R. S., & Flanagan, J. R. (2008). Tactile sensory control of object manipulation in humans. In J. H. Kaas & E. Gardner (Eds.), *Handbook of the Senses* (Vol. 6: Somatosensation, pp. 67–86). San Diego: Academic Press. Retrieved from http://umu.diva-portal.org/smash/record.jsf?searchId=1&pid=diva2:208419

Johansson, R. S., & Flanagan, J. R. (2009). Coding and Use of Tactile Signals from the Fingertips in Object Manipulation Tasks. *Nature Reviews Neuroscience*.

Johansson, R. S., Häger, C., & Bäckström, L. (1992). Somatosensory control of precision grip during unpredictable pulling loads. III. Impairments during digital anesthesia. *Exp Brain Res*, *89*(1), 204.

Johansson, R. S., Häger, C., & Riso, R. (1992). Somatosensory control of precision grip during unpredictable pulling loads. II. Changes in load force rate. *Exp Brain Res*, *89*(1), 192–203. doi:10.1007/BF00229016

Johansson, R. S., Riso, R., Häger, C., & Bäckström, L. (1992). Somatosensory control of precision grip during unpredictable pulling loads. I. Changes in load force amplitude. *Exp Brain Res*, *89*(1), 181–191.

Johansson, R. S., & Westling, G. (1984). Roles of glabrous skin receptors and sensorimotor memory in automatic control of precision grip when lifting rougher or more slippery objects. *Experimental Brain Research*, *56*(3), 550–564.

Johansson, R. S., & Westling, G. (1987). Signals in tactile afferents from the fingers eliciting adaptive motor responses during precision grip. *Experimental Brain Research*, *66*, 141–154.

Johansson, R. S., & Westling, G. (1988). Programmed and triggered actions to rapid load changes during precision grip. *Experimental Brain Research*, *71*(1), 72–86.

Johnson, K. O., & Phillips, J. R. (1981). Tactile spatial resolution. I. Two-point discrimination, gap detection, grating resolution, and letter recognition. *J Neurophysiol*, *46*(6), 1177–1192.

Jones, L. A., & Hunter, I. W. (1992). Changes in pinch force with bidirectional load forces. *J Motor Behav*, *24*(2), 157–164.

Jordan, K., & Newell, K. (2004). Task goal and grip force dynamics. *Experimental Brain Research*, *156*(4), 451–457. doi:10.1007/s00221-003-1806-9

Kamper, D. G., Fischer, H. C., & Cruz, E. G. (2006). Impact of finger posture on mapping from muscle activation to joint torque. *Clinical Biomechanics*, *21*(4), 361–369. doi:10.1016/j.clinbiomech.2005.11.005

Kamper, D. G., Hornby, T. G., & Rymer, W. Z. (2002). Extrinsic flexor muscles generate concurrent flexion of all three finger joints. *Journal of Biomechanics*, *35*(12), 1581–1589.

Kinoshita, H., Bäckström, L., Flanagan, J. R., & Johansson, R. S. (1997). Tangential torque effects on the control of grip forces when holding objects with a precision grip. *Journal of Neurophysiology*, *78*(3), 1619 – 1630.

Kuo, P. H., & Deshpande, A. D. (2010a). Contribution of passive properties of muscle-tendon units to the metacarpophalangeal joint torque of the index finger. *Biomedical Robotics and Biomechatronics (BioRob), 2010 3rd IEEE RAS and EMBS International Conference on* (pp. 288–294).

Kuo, P. H., & Deshpande, A. D. (2010b). Contribution of passive properties of muscle-tendon units to the metacarpophalangeal joint torque of the index finger. *Proc IEEE Intl Conf on Biomedical Robotics and Biomechatronics* (pp. 288–294). Presented at the IEEE Intl Conf on Biomedical Robotics and Biomechatronics.

Lederman, S. J., & Klatzky, R. L. (1987). Hand Movements: A Window Into Haptic Object Recognition. *Cognitive Psychology*, *19*(3), 342–368.

Lee, M. H., & Nicholls, H. R. (1999). Tactile sensing for mechatronics—a state of the art survey. *Mechatronics*, *9*(1), 1–31.

Lee, S.-W., Chen, H., & Kamper, D. G. (2009). Transmission of musculotendon forces to the index finger. *Proc. of the Robotics Science and Systems Conf.* Presented at the Robotics Science and Systems, Seattle, WA.

Macefield, V. G., Häger-Ross, C., & Johansson, R. S. (1996). Control of grip force during restraint of an object held between finger and thumb: responses of cutaneous afferents from the digits. *Experimental Brain Research*, *108*(1), 155–171.

Macefield, V. G., & Johansson, R. S. (1996). Control of grip force during restraint of an object held between finger and thumb: responses of muscle and joint afferents from the digits. *Experimental Brain Research*, *108*(1), 172–184.

Marsden, C. D., Merton, P. A., & Morton, H. B. (1976). Stretch reflex and servo action in a variety of human muscles. *Journal of Physiology*, *259*(2), 531–560.

Matthews, P. B. (1984a). Evidence from the use of vibration that the human long-latency stretch reflex depends upon spindle secondary afferents. *Journal of Physiology*, *348*(1), 383.

Matthews, P. B. (1984b). The contrasting stretch reflex responses of the long and short flexor muscles of the human thumb. *Journal of Physiology*, *348*(1), 545–558.

McMaster-Carr. (2012). More About Plastics. McMaster-Carr Supply Company.

Mussa-Ivaldi, F. A., Hogan, N., & Bizzi, E. (1985a). Neural, mechanical, and geometric factors subserving arm posture in humans. *The Journal of Neuroscience*, *5*(10), 2732–2743.

Mussa-Ivaldi, F. A., Hogan, N., & Bizzi, E. (1985b). Neural, mechanical, and geometric factors subserving arm posture in humans. *The Journal of Neuroscience*, *5*(10), 2732–2743.

Napier, J. R. (1956). The prehensile movements of the human hand. *The Journal of Bone and Joint Surgery. British Volume*, *38-B*(4), 902–913.

O'Neill, G. (2013). *A study of 3D Human Arm Impedance Towards the Development of an EMG-Controlled Exoskeleton* (Master's Thesis). Arizona State University.

Patel, H. (2013). *Control of 3D Human Arm Impedance* (Master's Thesis). Arizona State University.

Pawluk, D. T., & Howe, R. D. (1999). Dynamic lumped element response of the human fingerpad. *Journal of Biomechanical Engineering*, *121*(2), 178–183.

Phillips, J. R., & Johnson, K. O. (1981). Tactile spatial resolution. III. A continuum mechanics model of skin predicting mechanoreceptor responses to bars, edges, and gratings. *J Neurophysiol*, *46*(6), 1204–1225.

Phillips, John R., & Johnson, K. O. (1981). Tactile spatial resolution. II. Neural representation of bars, edges, and gratings in monkey primary afferents. *J Neurophysiol*, *46*(6), 1192–1203.

Prattichizzo, D., & Trinkle, J. C. (2008). Grasping. In B. Siciliano & O. Khatib (Eds.), *Springer Handbook of Robotics*, (B. Siciliano and O. Khatib, eds.) (pp. 671–700). Berlin Heidelberg: Springer-Verlag. Retrieved from http://dx.doi.org/10.1007/978-3-540-30301-5_29

Santello, M., Flanders, M., & Soechting, J. F. (1998). Postural Hand Synergies for Tool Use. *Journal of Neuroscience*, *18*(23), 10105–10115.

Thilmann, A. F., Schwarz, M., Töpper, R., Fellows, S. J., & Noth, J. (1991). Different mechanisms underlie the long-latency stretch reflex response of active human muscle at different joints. *Journal of Physiology*, *444*(1), 631.

Tsuji, T., & Kaneko, M. (1996). Estimation and Modeling of Human Hand Impedance During Isometric Muscle Contraction. *ASME Dynamics Systems and Control Division* (Vol. 58).

UW Muscle Atlas. (n.d.). Retrieved July 29, 2013, from http://www.rad.washington.edu/academics/academic-sections/msk/muscle-atlas/upper-body/

Valero-Cuevas, F. J., Towles, J. D., & Hentz, V. R. (2000). Quantification of fingertip force reduction in the forefinger following simulated paralysis of extensor and intrinsic muscles. *Journal of biomechanics*, *33*(12), 1601–1609.

Westling, G., & Johansson, R. S. (1984). Factors influencing the force control during precision grip. *Experimental Brain Research*, *53*(2), 277–284.

Westling, G., & Johansson, R. S. (1987). Responses in glabrous skin mechanoreceptors during precision grip in humans. *Experimental Brain Research*, *66*(1), 128–140.

Wing, A. M., & Flanagan, J. R. (1998). Anticipating dynamic loads in handling objects. *Proc of the ASME Dynamic Systems and Control Division* (Vol. 64, pp. 139–143).

Yousef, H., Boukallel, M., & Althoefer, K. (2011). Tactile sensing for dexterous in-hand manipulation in robotics–A review. *Sensors and Actuators A: Physical*.

Zajac, F. E. (1989). Muscle and Tendon: Properties, models. scaling, and application to biomechanics and motor control. *Critical Reviews in Biomedical Engineering*, *17*(4), 359–411.

# APPENDIX A: INSTITUTIONAL REVIEW BOARD: CONSENT FORMS

## Consent Form for Chapter 2 Study

**INFORMED CONSENT FORM**

**Kinematic and kinetic analyses of reflexive grip responses to rotational perturbations of an object in precision grasp**

**INTRODUCTION**

The purposes of this form are to provide you (as a prospective research study participant) information that may affect your decision as to whether or not to participate in this research and to record the consent of those who agree to be involved in the study.

**RESEARCHERS**

The following researchers have invited your participation in this research study.

- *Principal Investigator:* Veronica J. Santos, PhD, Assistant Professor in the Ira A. Fulton School of Engineering at Arizona State University (ASU)
- Michael De Gregorio, M.S., Graduate Student at ASU
- Kevin Bair, Graduate Student at ASU
- Ruben Ponce Wong, Graduate Student at ASU
- Ryan Manis, Undergraduate Student at ASU
- Vi Nguyen, Undergraduate Student at ASU

**PARTICIPATION REQUIREMENTS**

In order to participate, you must be between the ages of 18 and 50 years, have no current impairment or history of impairment of your dominant hand, have no known neurological or neuromuscular disorders, be in general good health, and be proficient in English. If you do not meet these criteria, please inform a researcher.

**STUDY PURPOSE**

Several studies have shown that humans use fast, subconscious reflexes to maintain grasp of an object when the object is unexpectedly disturbed. These studies focused on fingertip forces that are typically associated with opening and closing the hand to loosen or tighten grip on an object (extension, flexion). However, little is known about fingertip motions and forces that are related to the spreading or gathering of fingertips (abduction, adduction), which are just as important for hand function. This study focuses on the motion and forces of human fingertips when an unexpected rotational disturbance is applied to a grasped object and the spreading or gathering of fingertips is required.

**DESCRIPTION OF RESEARCH STUDY**

If you decide to participate, then as a study participant you will join a study involving research on the reflexive responses of human hands to rotational disturbances. You will be asked questions about your general health and which hand you prefer to use for different daily tasks. The size, strength, and posture of your hand will be measured using devices commonly used in clinical settings. A medical-grade positioning pillow and Velcro straps will be used to comfortably secure your arm and wrist to a supportive tabletop. You are encouraged to notify a researcher immediately if the experimental set-up is uncomfortable at any time so the problem can be fixed.

In order to measure the motion of your hand during the study, digital video and special cameras will be used to track reflective dots that a researcher will attach to your hand with double-sided tape. A researcher will take still photos of your hand in order to measure your hand and the placement of the reflective dots. The digital video and still photos will be focused solely on your hand. No other parts of your body or identifying features (e.g., your face) will be videotaped or



ASU IRB
Approved
Sign QS for Carol Johnston
Date 5/20/10 - 2/24/11

photographed. The video will be used to validate our data analysis and to show representative examples of fingertip responses when disseminating the results of the study.

In order to measure how much you use your hand muscles during the study, a researcher will attach surface electromyography (EMG) electrodes to your hand. The electrodes, coated with medical-grade electrode cream, allow the researchers to "listen" to muscles in a non-invasive, painless manner. A researcher will squeeze your hand to find the best place to attach the electrodes to your hand with hypoallergenic medical tape.

For each 5 second trial, you will be asked to hold an object in mid-air using your thumb and index finger while you curl your other fingers towards your palm, as if making a fist. A disturbance will rotate the object at a random time during the 5 second trial. Your goal is to return the object to its initial upright position and to avoid dropping the object. You can imagine that the object is a small glass of water that you need to keep upright even when the glass is bumped. A researcher will record your fingertip responses for different types of disturbances, none of which will be large enough to hurt your hand. You will be able to rest your hand for 30 seconds between trials and you are encouraged to tell a researcher if you need lengthier, more frequent rest periods to keep your hand "fresh."

If you say YES, then your participation will last for approximately one hour for today's session in the Engineering Center E-Wing, Room 116A. If you say YES to an optional follow-up session tomorrow to study possible learning effects, then your participation tomorrow will last for approximately 30-45 minutes. Approximately 20 subjects will be participating in this study.

**RISKS**

As with any research, there is some possibility that you may be subject to risks that have not yet been identified. Potential risks that have been identified are addressed here:

| POTENTIAL RISK | HOW RISK IS MINIMIZED |
|---|---|
| **Temporary fatigue of your hand**<br>Your hand, specifically your thumb and index finger, might get tired from having to repeat the task. This may occur during the experiment and may last for approximately 30-60 minutes after completion of the experiment. There are no long term risks. | You will be able to rest your hand for 30 seconds between trials and you are encouraged to tell a researcher if you need lengthier, more frequent rest periods to keep your hand "fresh." You may withdraw from the experiment at any time without penalty if you feel uncomfortable. |
| **Allergic reaction to the experiment materials:**<br>• Conductive EMG electrode cream<br>• Hypoallergenic medical tape<br>• Double-sided tape | Allergic reactions are not expected given that the electrode cream and hypoallergenic medical tape are commonly used in clinical settings. The cream can be washed off with mild soap and water. You may inspect the ingredients in the electrode cream and test the cream and/or tape on your skin prior to the experiment. |
| **Brief pain as tape is removed at the conclusion of the experiment.** | The removal of the tape is similar to the removal of a small band-aid. You can choose whether you or a researcher will remove the tape. You may test the tape on your skin prior to the experiment. |

| POTENTIAL RISK (cont'd) | HOW RISK IS MINIMIZED (cont'd) |
|---|---|
| **Anxiety about the experimental methods or quality of your performance** | The researchers will answer any questions you may have about the experimental equipment and safety of the methods. Successful completion of the simple experimental task does not depend on hand strength or skill. |

**BENEFITS**

Although there may be no direct benefits to you, the possible benefits of your participation in the research are that the results of the study will enhance the scientific understanding of human grasp. This knowledge has practical applications for the advancement of prosthetic and robotic hands, which are currently no match for the dexterity of human hands.

**NEW INFORMATION**

If the researchers find new information during the study that would reasonably change your decision about participating, then they will provide this information to you.

**CONFIDENTIALITY**

All information obtained in this study is strictly confidential unless disclosure is required by law. The results of this research study may be used in reports, presentations, and publications, but the researchers will not identify you. In order to maintain confidentiality of your records, Dr. Santos or a member of her research team will assign you a random code. This code will be stamped on the last page of this informed consent form and will be used as the sole form of identification on all subsequent datasheets and filenames. Your anonymity is guaranteed by the use of the random code, which will be used to identify your data at all stages of collection, analysis, and publication or presentation.

This informed consent form (the only document that links your identity to your random code) will be stored in a locked filing cabinet in Dr. Santos' office (Engineering Research Center, Room 359). If you choose to participate in the optional follow-up session tomorrow, Dr. Santos will access this informed consent form to retrieve the random code assigned to you today. The code will be used as the sole form of identification on datasheets and filenames generated during tomorrow's session. Data files will be stored on computers in secure folders, accessible only by authorized researchers. Data will be retained for 3 years, after which, paper documents will be shredded and electronic documents will be deleted.

**WITHDRAWAL PRIVILEGE**

It is OK for you to say NO. Even if you say YES now, you are free to say NO later, and withdraw from the study at any time without penalty. Your decision will not affect your relationship with ASU or otherwise cause a loss of benefits to which you might otherwise be entitled. Participation in this study is entirely voluntary and nonparticipation or withdrawal from the study will not affect your grades or employment status.

**COSTS AND PAYMENTS**

The researchers want your decision about participating in the study to be absolutely voluntary. Yet they recognize that your participation may pose some cost or inconvenience. In order to compensate you for travel costs and/or infringement of your personal time, you will receive payment. You will receive $10 for participation in today's session. If you participate in an optional follow-up session tomorrow, you will receive an additional $5 for your participation. Should you choose to withdraw from the study, you will still receive $5 for your time. Your payment will be made in one lump sum. If you do not receive your payment today, you will be asked to provide your mailing address so that a check can be mailed to you within 2-4 weeks.

**COMPENSATION FOR ILLNESS AND INJURY**

If you agree to participate in the study, then your consent does not waive any of your legal rights. While no funds have been set aside to compensate you in the event of injury, the researchers do not foresee any risk of injury to you in this study.

**VOLUNTARY CONSENT**

Any questions you have concerning the research study or your participation in the study, before or after your consent, will be answered by the Principal Investigator: Veronica J. Santos, PhD, Assistant Professor in the Ira A. Fulton School of Engineering at ASU, Engineering Research Center, Room 359, (480) 965-3207.

If you have questions about your rights as a subject/participant in this research, or if you feel you have been placed at risk; you can contact the Chair of the Human Subjects Institutional Review Board, through the ASU Office of Research Integrity and Assurance, at (480) 965-6788.

This form explains the nature, demands, benefits and any risk of the project. By signing this form you agree knowingly to assume any risks involved. Remember, your participation is voluntary. You may choose not to participate or to withdraw your consent and discontinue participation at any time without penalty or loss of benefit. In signing this consent form, you are not waiving any legal claims, rights, or remedies. A copy of this consent form will be given (offered) to you.

Your signature below indicates that you consent to participate in the above study. By signing below, you are granting to the researchers the right to use your images (still photos or digital videos of your hand) and performance - whether recorded on or transferred to videotape, film, slides, and photographs - for presenting or publishing this research.

______________________ ______________________ __________

Subject's Signature Printed Name Date

**INVESTIGATOR'S STATEMENT**

"I certify that I have explained to the above individual the nature and purpose, the potential benefits and possible risks associated with participation in this research study, have answered any questions that have been raised, and have witnessed the above signature. These elements of Informed Consent conform to the Assurance given by Arizona State University to the Office for Human Research Protections to protect the rights of human subjects. I have provided (offered) the subject/participant a copy of this signed consent document."

______________________ ______________________ __________

Investigator's Signature Printed Name Date

## Consent Form for Chapter 3 and Chapter 4 Studies

SUBJECT CONSENT FORM

Collaborative Research: Sensory Integration and Sensorimotor Transformations for Dexterous Manipulation

*SCHOOL OF BIOLOGICAL AND HEALTH SYSTEMS ENGINEERING, ARIZONA STATE UNIVERSITY*

*************************************************************************************************

**INTRODUCTION**

The purposes of this form are to provide you (as a prospective research study participant) information that may affect your decision as to whether or not to participate in this research and to record the consent of those who agree to be involved in the study.

**RESEARCHERS**

Dr. Marco Santello, Ph.D., (Professor, School of Biological and Health Systems Engineering), Dr. Wei Zhang, Ph.D., (Postdoctoral Research Associate, School of Biological and Health Systems Engineering), Qiushi Fu, M.S., (Graduate Student Research Assistant, School of Biological and Health Systems Engineering), Jason Choi (Graduate Student Research Assistant, School of Biological and Health Systems Engineering), Daisuke Shibata, M.S. (Graduate Student Research Assistant Student, Kinesiology program), Dr. Veronica Santos, Ph.D. (Assistant Professor, School of Biological and Healthy Systems Engineering), Michael De Gregorio (Graduate Student Research Assistant, School of Biological and Health Systems Engineering), Dr. Pranav Parikh, Ph.D. (Postdoctoral Research Scholar, School of Biological and Health Systems Engineering), and Keivan Mojtahedi (Graduate Student, School of Biological and Health Systems Engineering have invited your participation in a research study.

**STUDY PURPOSE**

The purpose of the research is to obtain information about how sensory information from the fingertips is used during coordination of various movements of the hand. This information may be useful to professionals who work with people who have some form of physical disability and require therapy.

**DESCRIPTION OF RESEARCH STUDY**

If you decide to participate, then as a study participant you will join a study in which you will be asked to grasp a light-weight object (less than 2 pounds) with your whole hand while seated, and either squeeze lightly for several seconds, or to lift it a few inches above the table, hold it there for several seconds, and return it to the table. You will be asked to position your grasp on the object so that your thumb and each finger are placed over each pad. Certain properties of the object will be occasionally changed (such as center of mass, weight, or texture). In some instances you might be asked to position the fingertips of the thumb and index finger of one hand at a given distance from each other and then match that distance using the thumb and index fingertips of the other hand. Vision of both hands may not be allowed during this task. Additionally, you may be asked to squeeze a grip device with one or both hands while trying to match the fingertip distance of one hand using the fingertips of the other hand. If you say YES, depending on the tasks, your participation will last for 60-90 minutes during one session or for 2-3 hours over 2-day sessions, including instructions and rest periods between trials and tasks. In some instances the object may be a virtual object displayed on computer monitor, that you will grasp with the ends a three-hinge linkage system, which may in some instances automatically move the object. The linkage system can exert a movement on the object in any direction (up/down, forward/backward, and side-to-side). The linkage system can also rotate the object about any of these directions. In some instances you will be asked to resist the movements imposed by the linkage system and in other instances the linkage system will resist your movements. Properties of the movement and resistance may be changed (such as direction of resistance or movement, strength of the resistance or movement). Minimal force (< 1.5 lb) is exerted by the linkage system when it moves or resists your movement; therefore, you should not feel any discomfort. In other instances you will be asked to grasp and lift a cylindrical metal object (height: 16cm diameter: 5cm). You may be asked to close your eyes during portions of the experiment, including times in which you reach to and grasp the objects. For some of the experiments Phantom, surface electromyography (EMG) will used on the surface of the skin to measure the muscle activity from four hand

PAGE 3

muscles using self-adhesive skin electrodes. This will allow investigation of muscle coordination patterns with the robotic device. For EMG, you will be prepped for the application of surface EMG electrodes. This process begins by cleaning the areas that the electrodes will cover using and alcohol pad. Once the target regions are clean, the electrodes will be applied. During application, you may be asked to flex their hand in various ways to help in the identification of the appropriate muscles. For some instances, the grip strength will be measured using a pinch meter. You will be instructed to squeeze this meter with maximum strength. In some instances you may be asked to wear liquid crystal spectacles. The lenses of the goggles can change from transparent to opaque which removes your ability to see in front of you during various time points during the experiment. The object and If you consent, your hand and arm movements during each experimental session will be videotaped for the purpose of data and movement analysis. Experiments will be performed at the PEBE building in room 168 on the Tempe campus of Arizona State University. You may be excluded from this study if you do not meet the inclusion criteria based on screening tools to be completed. Approximately 300 subjects will be participating in this study.

**RISKS**

You should not participate in this study if you have any known neurological illness or orthopedic condition. Because you are in good health and have had no prior injury or health condition affecting your muscles, joints, or nerves, the risks of injury or discomfort in this research are minimal. There is a possibility that the linkage system will move you at an uncomfortable speed, however, several safety precautions have been implemented to reduce this risk. Specifically, the maximal speed of the movement imposed by the linkage system is set below human physiological limits. If these speeds are exceeded the linkage system is designed to immediately shutdown. Although your fingers you will be attached to the device via Velcro-like straps, you will be able to remove your fingers from the device if you feel any discomfort to let go of the object to protect yourself from potential discomfort, pain, or injury. Removal of self-adhesive surface EMG electrodes at the end of the experiment may cause some discomfort/pain, which will not last more than a few min. The metal cylindrical object is powered and connected to the USB port of a pc with proper shielding and grounding. The risk of getting static shock is no different than using metal objects in daily life. However, as with any research, there is some possibility that you may be subject to risks that have not yet been identified.

**BENEFITS**

If you are enrolled in kinesiology and related program and your instructor previously consents to give extra credit for your participation in this research, you will be eligible for extra credit even you are excluded from this study after coming to the laboratory. Otherwise this study will be of no direct benefit to you. However, your participation may contribute to a broader understanding of processes underlying hand function with implications for development of therapeutic intervention in people with impaired hand function due to injury or illness. You will not receive payment for your participation.

**NEW INFORMATION**

If the researchers find new information during the study that would reasonably change your decision about participating, then they will provide this information to you.

**CONFIDENTIALITY**

All information obtained in this study is strictly confidential unless disclosure is required by law. The results of this research study may be used in reports, presentations, and publications, but the researchers will not identify you. To ensure confidentiality, a code will be used instead of your name for data analysis. Your identity will not be associated with any published results. All characteristics that could identify you in the records, including the videotape, will be stored fully confidential in a locked filing cabinet in the principal investigator's office at Arizona State University. The videotape will be destroyed following the completion of the study.

**WITHDRAWAL PRIVILEGE**

It is ok for you to say no. Even if you say yes now, you are free to say no later, and withdraw from the study at any time. Your decision will not affect your relationship with Arizona State University or otherwise cause a loss of benefits to which you might otherwise be entitled.
Participation is voluntary and nonparticipation or withdrawal from the study will not affect your grade or employment status.

**COSTS AND PAYMENTS**
If you are not considering getting extra credits for your participation in the research, you will be eligible for monetary compensation. You will be paid $10 for every hour spend in the laboratory.

**COMPENSATION FOR ILLNESS AND INJURY**
If you agree to participate in the study, then your consent does not waive any of your legal rights. However, no funds have been set aside to compensate you in the event of injury.

**VOLUNTARY CONSENT**
Any questions you have concerning the research study or your participation in the study, before or after your consent, will be answered by Marco Santello, Ph.D., Neural Control of Movement Laboratory, School of Biological and Health Systems Engineering, PEBE room 107B, University of Arizona, (480) 965-8279.

If you have questions about your rights as a subject/participant in this research, or if you feel you have been placed at risk; you can contact the Chair of the Human Subjects Institutional Review Board, through the ASU Research Compliance Office, at 480-965 6788.

This form explains the nature, demands, benefits and any risk of the project. By signing this form you agree knowingly to assume any risks involved. Remember, your participation is voluntary. You may choose not to participate or to withdraw your consent and discontinue participation at any time without penalty or loss of benefit. In signing this consent form, you are not waiving any legal claims, rights, or remedies. A copy of this consent form will be given (offered) to you.

I ( ) consent to be video taped.

I ( ) do NOT consent to being video taped.

The written, video taped materials will be viewed only by the principal investigator and members of the research team.

Written, video taped materials

( ) may be viewed in an educational setting outside the research

( ) may NOT be viewed in an educational setting outside the research.

- My signature means that I agree to participate in this study.

_________________________ __________________ __________
Subject's Signature Printed Name Date

**INVESTIGATOR'S STATEMENT**
"I certify that I have explained to the above individual the nature and purpose, the potential benefits and possible risks associated with participation in this research study, have answered any questions that have been raised, and have witnessed the above signature. These elements of Informed Consent conform to the Assurance given by Arizona State University to the Office for Research Integrity and Assurance to protect the rights of human subjects. I have provided (offered) the subject/participant a copy of this signed consent document."

Signature of Investigator________________________ Date_______

ARIZONA STATE UNIVERSITY IRB
APPROVED BY IRB
DATE: 4/5/13 - 2/27/14
NAME: Dm

# APPENDIX B: DESIGN OF INSTRUMENTED OBJECT FOR HAPTIC ROBOT STUDIES

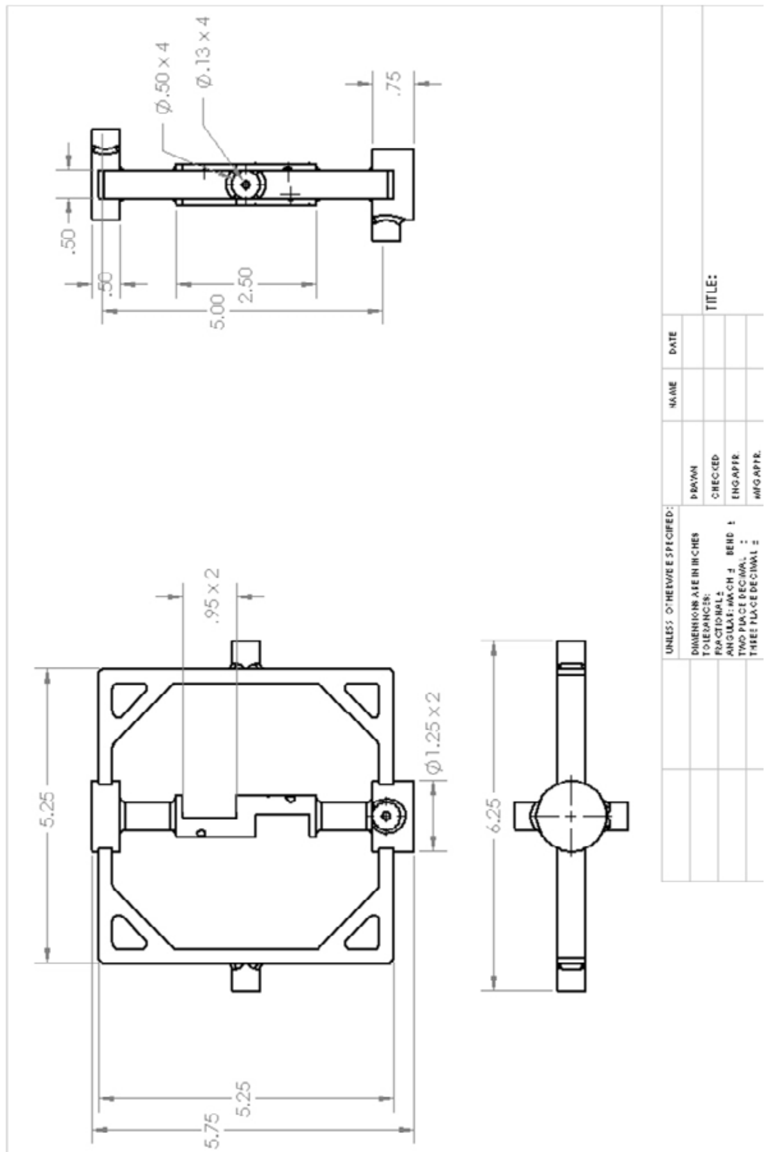

*Figure B.1.Production Drawing of Test Object.*

# APPENDIX C: STATISTICAL ANALYSES FOR PERTURBATION STUDIES

## Chapter 2 Statistics: Pooling by Digit

| Peak Normal Force - Both Digits | | | |
|---|---|---|---|
| | **p-Value** | **Decision** | **Check** |
| **p_dp_high_neg=** | 0.2057 | Not necessarily different | Cannot reject Ho |
| **p_dp_high_pos=** | 0.1839 | Not necessarily different | Cannot reject Ho |
| **p_dp_low_neg=** | 0.3263 | Not necessarily different | Cannot reject Ho |
| **p_dp_low_pos=** | 0.1965 | Not necessarily different | Cannot reject Ho |
| **p_ga_high_neg=** | 0.7176 | Not necessarily different | Cannot reject Ho |
| **p_ga_low_neg=** | 0.7697 | Not necessarily different | Cannot reject Ho |

| Time to Peak Normal Force - Both Digits | | | |
|---|---|---|---|
| | **p-Value** | **Decision** | **Check** |
| **p_dp_high_neg=** | 0.9118 | Not necessarily different | Cannot reject Ho |
| **p_dp_high_pos=** | 0.7517 | Not necessarily different | Cannot reject Ho |
| **p_dp_low_neg=** | 0.8228 | Not necessarily different | Cannot reject Ho |
| **p_dp_low_pos=** | 1 | Not necessarily different | Cannot reject Ho |
| **p_ga_high_neg=** | 0.2934 | Not necessarily different | Cannot reject Ho |
| **p_ga_low_neg=** | 0.8904 | Not necessarily different | Cannot reject Ho |

| Peak Normal Force Rate - Both Digits | | | |
|---|---|---|---|
| | **p-Value** | **Decision** | **Check** |
| **p_dp_high_neg=** | 0.2547 | Not necessarily different | Cannot reject Ho |
| **p_dp_high_pos=** | 0.4864 | Not necessarily different | Cannot reject Ho |
| **p_dp_low_neg=** | 0.0948 | Not necessarily different | Cannot reject Ho |
| **p_dp_low_pos=** | 0.904 | Not necessarily different | Cannot reject Ho |
| **p_ga_high_neg=** | 0.8497 | Not necessarily different | Cannot reject Ho |
| **p_ga_low_neg=** | 0.9768 | Not necessarily different | Cannot reject Ho |

| Time to Peak Normal Force Rate - Both digits | | | |
|---|---|---|---|
| | **p-Value** | **Decision** | **Check** |
| **p_dp_high_neg=** | 0.1412 | Not necessarily different | Cannot reject Ho |
| **p_dp_high_pos=** | 0.079 | Not necessarily different | Cannot reject Ho |
| **p_dp_low_neg=** | 0.2086 | Not necessarily different | Cannot reject Ho |
| **p_dp_low_pos=** | 0.1385 | Not necessarily different | Cannot reject Ho |
| **p_ga_high_neg=** | 0.7176 | Not necessarily different | Cannot reject Ho |
| **p_ga_low_neg=** | 0.5814 | Not necessarily different | Cannot reject Ho |

## Chapter 2 Statistics: Effect of Perturbation Direction

| Peak Normal Force | | | |
|---|---|---|---|
| DIRECTION (OMM and AXIS CONSTANT) | | | |
| | p-Value | Decision | Check |
| p_dp_high= | 0.7018 | Not Necessarily Different | Cannot reject Ho |
| p_dp_low= | 0.3512 | Not Necessarily Different | Cannot reject Ho |

| Time to Peak Normal Force | | | |
|---|---|---|---|
| DIRECTION (OMM and AXIS CONSTANT) | | | |
| | p-Value | Decision | Check |
| p_dp_high= | 0.6976 | Not Necessarily Different | Cannot reject Ho |
| p_dp_low= | 0.6107 | Not Necessarily Different | Cannot reject Ho |

| Peak Normal Force Rate | | | |
|---|---|---|---|
| DIRECTION (OMM and AXIS CONSTANT) | | | |
| | p-Value | Decision | Check |
| p_dp_high= | 0.5506 | Not Necessarily Different | Cannot reject Ho |
| p_dp_low= | 0.9902 | Not Necessarily Different | Cannot reject Ho |

| Time to Peak Normal Force Rate | | | |
|---|---|---|---|
| DIRECTION (OMM and AXIS CONSTANT) | | | |
| | p-Value | Decision | Check |
| p_dp_high= | 0.543 | Not Necessarily Different | Cannot reject Ho |
| p_dp_low= | 0.2365 | Not Necessarily Different | Cannot reject Ho |

| Catch-up Response Strength | | | |
|---|---|---|---|
| DIRECTION (OMM and AXIS CONSTANT) | | | |
| | p-Value | Decision | Check |
| p_dp_high= | 0.5209 | Not Necessarily Different | Cannot reject Ho |
| p_dp_low= | 0.7873 | Not Necessarily Different | Cannot reject Ho |

| Catch-up Response Duration | | | |
|---|---|---|---|
| DIRECTION (OMM and AXIS CONSTANT) | | | |
| | p-Value | Decision | Check |
| p_dp_high= | 0.5724 | Not Necessarily Different | Cannot reject Ho |
| p_dp_low= | 0.5447 | Not Necessarily Different | Cannot reject Ho |

## Chapter 2 Statistics: Effect of Object Moment Magnitude

| Peak Normal Force | | | |
|---|---|---|---|
| OMM (DIRECTION and AXIS CONSTANT) | | | |
| | p-Value | Decision | Check |
| p_dp_pos= | 0.24 | Not necessarily different | Cannot reject Ho |
| p_dp_neg= | 0.1024 | Not necessarily different | Cannot reject Ho |
| p_ga_neg= | 0.1164 | Not necessarily different | Cannot reject Ho |

| Time to Peak Normal Force | | | |
|---|---|---|---|
| OMM (DIRECTION and AXIS CONSTANT) | | | |
| | p-Value | Decision | Check |
| p_dp_pos= | 0.3236 | Not necessarily different | Cannot reject Ho |
| p_dp_neg= | 0.0625 | Not necessarily different | Cannot reject Ho |
| p_ga_neg= | 0.3264 | Not necessarily different | Cannot reject Ho |

| Peak Normal Force Rate | | | |
|---|---|---|---|
| OMM (DIRECTION and AXIS CONSTANT) | | | |
| | p-Value | Decision | Check |
| p_dp_pos= | 0.0226 | Different | Distributions are different |
| p_dp_neg= | 0.11 | Not necessarily different | Cannot reject Ho |
| p_ga_neg= | 0.1657 | Not necessarily different | Cannot reject Ho |

| Time to Peak Normal Force Rate | | | |
|---|---|---|---|
| OMM (DIRECTION and AXIS CONSTANT) | | | |
| | p-Value | Decision | Check |
| p_dp_pos= | 0.1371 | Not necessarily different | Cannot reject Ho |
| p_dp_neg= | 0.4808 | Not necessarily different | Cannot reject Ho |
| p_ga_neg= | 0.9024 | Not necessarily different | Cannot reject Ho |

| Catch-up Response Strength | | | |
|---|---|---|---|
| OMM (DIRECTION and AXIS CONSTANT) | | | |
| | p-Value | Decision | Check |
| p_dp_pos= | 0.0325 | Different | Distributions are different |
| p_dp_neg= | 0.1356 | Not necessarily different | Cannot reject Ho |
| p_ga_neg= | 0.1478 | Not necessarily different | Cannot reject Ho |

| Catch-up Response Duration | | | |
|---|---|---|---|
| OMM (DIRECTION and AXIS CONSTANT) | | | |
| | **p-Value** | **Decision** | **Check** |
| **p_dp_pos=** | 0.6442 | Not necessarily different | Cannot reject Ho |
| **p_dp_neg=** | 0.1282 | Not necessarily different | Cannot reject Ho |
| **p_ga_neg=** | 0.4598 | Not necessarily different | Cannot reject Ho |

## Chapter 2 Statistics: Effect of Perturbation Axis

| Peak Normal Force | | | |
|---|---|---|---|
| AXIS (DIRECTION and OMM CONSTANT) | | | |
| | **p-Value** | **Decision** | **Check** |
| **p_axis_low=** | 0.0104 | Different | Distributions are different |
| **p_axis_high=** | 0.0058 | Different | Distributions are different |

| Time to Peak Normal Force | | | |
|---|---|---|---|
| AXIS (DIRECTION and OMM CONSTANT) | | | |
| | **p-Value** | **Decision** | **Check** |
| **p_axis_low=** | 0.0526 | Not Necessarily Different | Cannot reject Ho |
| **p_axis_high=** | 0.4074 | Not Necessarily Different | Cannot reject Ho |

| Peak Normal Force Rate | | | |
|---|---|---|---|
| AXIS (DIRECTION and OMM CONSTANT) | | | |
| | **p-Value** | **Decision** | **Check** |
| **p_axis_low=** | 0.0147 | Different | Distributions are different |
| **p_axis_high=** | 0.0104 | Different | Distributions are different |

| Time to Peak Normal Force Rate | | | |
|---|---|---|---|
| AXIS (DIRECTION and OMM CONSTANT) | | | |
| | **p-Value** | **Decision** | **Check** |
| **p_axis_low=** | 0.5478 | Not Necessarily Different | Cannot reject Ho |
| **p_axis_high=** | 0.8971 | Not Necessarily Different | Cannot reject Ho |

| Catch-up Response Strength | | | |
|---|---|---|---|
| AXIS (DIRECTION and OMM CONSTANT) | | | |
| | **p-Value** | **Decision** | **Check** |
| **p_axis_low=** | 0.024 | Different | Distributions are different |
| **p_axis_high=** | 0.0094 | Different | Distributions are different |

| Catch-up Response Duration | | | |
|---|---|---|---|
| AXIS (DIRECTION and OMM CONSTANT) | | | |
| | **p-Value** | **Decision** | **Check** |
| **p_axis_low=** | 0.1809 | Not Necessarily Different | Cannot reject Ho |
| **p_axis_high=** | 0.5216 | Not Necessarily Different | Cannot reject Ho |

## Chapter 3 Statistics: Pooling by Digit

| Catch-up Start Time | | | |
|---|---|---|---|
| | **p-Value** | **Decision** | **Check** |
| **p_DPpos_rot=** | 0.817 | Not Necessarily Different | Cannot reject Ho |
| **p_DPneg_rot=** | 0.525 | Not Necessarily Different | Cannot reject Ho |
| **p_RUpos_rot=** | 0.285 | Not Necessarily Different | Cannot reject Ho |
| **p_RUneg_rot=** | 0.241 | Not Necessarily Different | Cannot reject Ho |
| **p_GRIPpos_rot=** | 0.529 | Not Necessarily Different | Cannot reject Ho |
| **p_GRIPneg_rot=** | 0.255 | Not Necessarily Different | Cannot reject Ho |
| **p_DPpos_lin=** | 0.582 | Not Necessarily Different | Cannot reject Ho |
| **p_DPneg_lin=** | 0.844 | Not Necessarily Different | Cannot reject Ho |
| **p_RUpos_lin=** | 0.609 | Not Necessarily Different | Cannot reject Ho |
| **p_RUneg_lin=** | 0.903 | Not Necessarily Different | Cannot reject Ho |
| **p_GRIPpos_lin=** | 0.088 | Not Necessarily Different | Cannot reject Ho |
| **p_GRIPneg_lin=** | 0.736 | Not Necessarily Different | Cannot reject Ho |

| Peak Normal Force | | | |
|---|---|---|---|
| | **p-Value** | **Decision** | **Check** |
| **p_DPpos_rot=** | 0.7489 | Not Necessarily Different | Cannot reject Ho |
| **p_DPneg_rot=** | 0.8856 | Not Necessarily Different | Cannot reject Ho |
| **p_RUpos_rot=** | 0.2827 | Not Necessarily Different | Cannot reject Ho |
| **p_RUneg_rot=** | 0.2137 | Not Necessarily Different | Cannot reject Ho |
| **p_GRIPpos_rot=** | 0.831 | Not Necessarily Different | Cannot reject Ho |
| **p_GRIPneg_rot=** | 0.9292 | Not Necessarily Different | Cannot reject Ho |
| **p_DPpos_lin=** | 0.3605 | Not Necessarily Different | Cannot reject Ho |
| **p_DPneg_lin=** | 0.8988 | Not Necessarily Different | Cannot reject Ho |
| **p_RUpos_lin=** | 0.7031 | Not Necessarily Different | Cannot reject Ho |
| **p_RUneg_lin=** | 0.4732 | Not Necessarily Different | Cannot reject Ho |
| **p_GRIPpos_lin=** | 0.1656 | Not Necessarily Different | Cannot reject Ho |
| **p_GRIPneg_lin=** | 0.7156 | Not Necessarily Different | Cannot reject Ho |

| Peak Normal Force Rate | | | |
|---|---|---|---|
| | **p-Value** | **Decision** | **Check** |
| **p_DPpos_rot=** | 0.6037 | Not Necessarily Different | Cannot reject Ho |
| **p_DPneg_rot=** | 0.6271 | Not Necessarily Different | Cannot reject Ho |
| **p_RUpos_rot=** | 0.2577 | Not Necessarily Different | Cannot reject Ho |
| **p_RUneg_rot=** | 0.6969 | Not Necessarily Different | Cannot reject Ho |
| **p_GRIPpos_rot=** | 0.9196 | Not Necessarily Different | Cannot reject Ho |
| **p_GRIPneg_rot=** | 0.9881 | Not Necessarily Different | Cannot reject Ho |
| **p_DPpos_lin=** | 0.7458 | Not Necessarily Different | Cannot reject Ho |
| **p_DPneg_lin=** | 0.7397 | Not Necessarily Different | Cannot reject Ho |
| **p_RUpos_lin=** | 0.4738 | Not Necessarily Different | Cannot reject Ho |
| **p_RUneg_lin=** | 0.6217 | Not Necessarily Different | Cannot reject Ho |
| **p_GRIPpos_lin=** | 0.3446 | Not Necessarily Different | Cannot reject Ho |
| **p_GRIPneg_lin=** | 0.9303 | Not Necessarily Different | Cannot reject Ho |

| Preload Radial Force | | | |
|---|---|---|---|
| | **p-Value** | **Decision** | **Check** |
| **p_DPpos_rot=** | 0.8644 | Not Necessarily Different | Cannot reject Ho |
| **p_DPneg_rot=** | 0.8438 | Not Necessarily Different | Cannot reject Ho |
| **p_RUpos_rot=** | 0.8695 | Not Necessarily Different | Cannot reject Ho |
| **p_RUneg_rot=** | 0.9165 | Not Necessarily Different | Cannot reject Ho |
| **p_GRIPpos_rot=** | 0.7558 | Not Necessarily Different | Cannot reject Ho |
| **p_GRIPneg_rot=** | 0.5375 | Not Necessarily Different | Cannot reject Ho |
| **p_DPpos_lin=** | 0.623 | Not Necessarily Different | Cannot reject Ho |
| **p_DPneg_lin=** | 0.9481 | Not Necessarily Different | Cannot reject Ho |
| **p_RUpos_lin=** | 0.7206 | Not Necessarily Different | Cannot reject Ho |
| **p_RUneg_lin=** | 0.4702 | Not Necessarily Different | Cannot reject Ho |
| **p_GRIPpos_lin=** | 0.7392 | Not Necessarily Different | Cannot reject Ho |
| **p_GRIPneg_lin=** | 0.9324 | Not Necessarily Different | Cannot reject Ho |

| Catch-up Duration | | | |
|---|---|---|---|
| | **p-Value** | **Decision** | **Check** |
| **p_DPpos_rot=** | 0.7275 | Not Necessarily Different | Cannot reject Ho |
| **p_DPneg_rot=** | 0.5729 | Not Necessarily Different | Cannot reject Ho |
| **p_RUpos_rot=** | 0.9053 | Not Necessarily Different | Cannot reject Ho |
| **p_RUneg_rot=** | 0.1563 | Not Necessarily Different | Cannot reject Ho |
| **p_GRIPpos_rot=** | 0.4624 | Not Necessarily Different | Cannot reject Ho |
| **p_GRIPneg_rot=** | 0.5324 | Not Necessarily Different | Cannot reject Ho |
| **p_DPpos_lin=** | 0.5612 | Not Necessarily Different | Cannot reject Ho |
| **p_DPneg_lin=** | 0.1843 | Not Necessarily Different | Cannot reject Ho |
| **p_RUpos_lin=** | 0.9747 | Not Necessarily Different | Cannot reject Ho |
| **p_RUneg_lin=** | 0.1929 | Not Necessarily Different | Cannot reject Ho |
| **p_GRIPpos_lin=** | 0.8891 | Not Necessarily Different | Cannot reject Ho |
| **p_GRIPneg_lin=** | 0.6421 | Not Necessarily Different | Cannot reject Ho |

| Time to Peak Normal Force | | | |
|---|---|---|---|
| | **p-Value** | **Decision** | **Check** |
| **p_DPpos_rot=** | 0.4861 | Not Necessarily Different | Cannot reject Ho |
| **p_DPneg_rot=** | 0.5818 | Not Necessarily Different | Cannot reject Ho |
| **p_RUpos_rot=** | 0.9461 | Not Necessarily Different | Cannot reject Ho |
| **p_RUneg_rot=** | 0.1154 | Not Necessarily Different | Cannot reject Ho |
| **p_GRIPpos_rot=** | 0.6199 | Not Necessarily Different | Cannot reject Ho |
| **p_GRIPneg_rot=** | 0.3692 | Not Necessarily Different | Cannot reject Ho |
| **p_DPpos_lin=** | 0.6356 | Not Necessarily Different | Cannot reject Ho |
| **p_DPneg_lin=** | 0.321 | Not Necessarily Different | Cannot reject Ho |
| **p_RUpos_lin=** | 0.9564 | Not Necessarily Different | Cannot reject Ho |
| **p_RUneg_lin=** | 0.2298 | Not Necessarily Different | Cannot reject Ho |
| **p_GRIPpos_lin=** | 0.9991 | Not Necessarily Different | Cannot reject Ho |
| **p_GRIPneg_lin=** | 0.5563 | Not Necessarily Different | Cannot reject Ho |

| Time to Peak Normal Force Rate | | | |
|---|---|---|---|
| | **p-Value** | **Decision** | **Check** |
| **p_DPpos_rot=** | 0.4551 | Not Necessarily Different | Cannot reject Ho |
| **p_DPneg_rot=** | 0.8291 | Not Necessarily Different | Cannot reject Ho |
| **p_RUpos_rot=** | 0.079 | Not Necessarily Different | Cannot reject Ho |
| **p_RUneg_rot=** | 0.3636 | Not Necessarily Different | Cannot reject Ho |
| **p_GRIPpos_rot=** | 0.0314 | Different | Distributions are different |
| **p_GRIPneg_rot=** | 0.8092 | Not Necessarily Different | Cannot reject Ho |
| **p_DPpos_lin=** | 0.0529 | Not Necessarily Different | Cannot reject Ho |
| **p_DPneg_lin=** | 0.2807 | Not Necessarily Different | Cannot reject Ho |
| **p_RUpos_lin=** | 0.8947 | Not Necessarily Different | Cannot reject Ho |
| **p_RUneg_lin=** | 0.3457 | Not Necessarily Different | Cannot reject Ho |
| **p_GRIPpos_lin=** | 0.5965 | Not Necessarily Different | Cannot reject Ho |
| **p_GRIPneg_lin=** | 0.8447 | Not Necessarily Different | Cannot reject Ho |

| Preload Grip Force | | | |
|---|---|---|---|
| | **p-Value** | **Decision** | **Check** |
| **p_DPpos_rot=** | 0.4656 | Not Necessarily Different | Cannot reject Ho |
| **p_DPneg_rot=** | 0.4045 | Not Necessarily Different | Cannot reject Ho |
| **p_RUpos_rot=** | 0.9896 | Not Necessarily Different | Cannot reject Ho |
| **p_RUneg_rot=** | 0.5273 | Not Necessarily Different | Cannot reject Ho |
| **p_GRIPpos_rot=** | 0.5649 | Not Necessarily Different | Cannot reject Ho |
| **p_GRIPneg_rot=** | 0.5931 | Not Necessarily Different | Cannot reject Ho |
| **p_DPpos_lin=** | 0.434 | Not Necessarily Different | Cannot reject Ho |
| **p_DPneg_lin=** | 0.3791 | Not Necessarily Different | Cannot reject Ho |
| **p_RUpos_lin=** | 0.8023 | Not Necessarily Different | Cannot reject Ho |
| **p_RUneg_lin=** | 0.6236 | Not Necessarily Different | Cannot reject Ho |
| **p_GRIPpos_lin=** | 0.4814 | Not Necessarily Different | Cannot reject Ho |
| **p_GRIPneg_lin=** | 0.6473 | Not Necessarily Different | Cannot reject Ho |

## Chapter 3 Statistics: Effect of Perturbation Direction

| Catch-up Start Time | | | |
|---|---|---|---|
| | **p-Value** | **Decision** | **Check** |
| **p_DP_HH_rot=** | 0.545 | Not Necessarily Different | Cannot reject Ho |
| **p_DP_HL_rot=** | 0.325 | Not Necessarily Different | Cannot reject Ho |
| **p_DP_LH_rot=** | 0.345 | Not Necessarily Different | Cannot reject Ho |
| **p_RU_HH_rot=** | 0.009 | Different | Distributions are different |
| **p_RU_HL_rot=** | 0.520 | Not Necessarily Different | Cannot reject Ho |
| **p_RU_LH_rot=** | 0.364 | Not Necessarily Different | Cannot reject Ho |
| **p_GRIP_HH_rot=** | 0.130 | Not Necessarily Different | Cannot reject Ho |
| **p_GRIP_HL_rot=** | 0.791 | Not Necessarily Different | Cannot reject Ho |
| **p_GRIP_LH_rot=** | 0.344 | Not Necessarily Different | Cannot reject Ho |
| **p_DP_HH_lin=** | 0.545 | Not Necessarily Different | Cannot reject Ho |
| **p_DP_HL_lin=** | 0.226 | Not Necessarily Different | Cannot reject Ho |
| **p_DP_LH_lin=** | 0.325 | Not Necessarily Different | Cannot reject Ho |
| **p_RU_HH_lin=** | 0.677 | Not Necessarily Different | Cannot reject Ho |
| **p_RU_HL_lin=** | 0.880 | Not Necessarily Different | Cannot reject Ho |
| **p_RU_LH_lin=** | 0.880 | Not Necessarily Different | Cannot reject Ho |
| **p_GRIP_HH_lin=** | 0.364 | Not Necessarily Different | Cannot reject Ho |
| **p_GRIP_HL_lin=** | 0.677 | Not Necessarily Different | Cannot reject Ho |
| **p_GRIP_LH_lin=** | 0.112 | Not Necessarily Different | Cannot reject Ho |

| Peak Normal Force | | | |
|---|---|---|---|
| | **p-Value** | **Decision** | **Check** |
| **p_DP_HH_rot=** | 0.9353 | Not Necessarily Different | Cannot reject Ho |
| **p_DP_HL_rot=** | 0.304 | Not Necessarily Different | Cannot reject Ho |
| **p_DP_LH_rot=** | 0.8287 | Not Necessarily Different | Cannot reject Ho |
| **p_RU_HH_rot=** | 0.2448 | Not Necessarily Different | Cannot reject Ho |
| **p_RU_HL_rot=** | 0.0483 | Different | Distributions are different |
| **p_RU_LH_rot=** | 0.9138 | Not Necessarily Different | Cannot reject Ho |
| **p_GRIP_HH_rot=** | 0.6849 | Not Necessarily Different | Cannot reject Ho |
| **p_GRIP_HL_rot=** | 0.7455 | Not Necessarily Different | Cannot reject Ho |
| **p_GRIP_LH_rot=** | 0.6263 | Not Necessarily Different | Cannot reject Ho |
| **p_DP_HH_lin=** | 0.4819 | Not Necessarily Different | Cannot reject Ho |
| **p_DP_HL_lin=** | 0.1167 | Not Necessarily Different | Cannot reject Ho |
| **p_DP_LH_lin=** | 0.1368 | Not Necessarily Different | Cannot reject Ho |
| **p_RU_HH_lin=** | 0.4328 | Not Necessarily Different | Cannot reject Ho |
| **p_RU_HL_lin=** | 0.1517 | Not Necessarily Different | Cannot reject Ho |
| **p_RU_LH_lin=** | 0.4328 | Not Necessarily Different | Cannot reject Ho |
| **p_GRIP_HH_lin=** | 0.0935 | Not Necessarily Different | Cannot reject Ho |
| **p_GRIP_HL_lin=** | 0.766 | Not Necessarily Different | Cannot reject Ho |
| **p_GRIP_LH_lin=** | 0.2559 | Not Necessarily Different | Cannot reject Ho |

| Peak Normal Force Rate | | | |
|---|---|---|---|
| | **p-Value** | **Decision** | **Check** |
| **p_DP_HH_rot=** | 1 | Not Necessarily Different | Cannot reject Ho |
| **p_DP_HL_rot=** | 0.9784 | Not Necessarily Different | Cannot reject Ho |
| **p_DP_LH_rot=** | 0.5885 | Not Necessarily Different | Cannot reject Ho |
| **p_RU_HH_rot=** | 0.9138 | Not Necessarily Different | Cannot reject Ho |
| **p_RU_HL_rot=** | 0.062 | Not Necessarily Different | Cannot reject Ho |
| **p_RU_LH_rot=** | 0.6073 | Not Necessarily Different | Cannot reject Ho |
| **p_GRIP_HH_rot=** | 0.8077 | Not Necessarily Different | Cannot reject Ho |
| **p_GRIP_HL_rot=** | 0.7251 | Not Necessarily Different | Cannot reject Ho |
| **p_GRIP_LH_rot=** | 0.6849 | Not Necessarily Different | Cannot reject Ho |
| **p_DP_HH_lin=** | 0.0265 | Different | Distributions are different |
| **p_DP_HL_lin=** | 0.0161 | Different | Distributions are different |
| **p_DP_LH_lin=** | 0.0032 | Different | Distributions are different |
| **p_RU_HH_lin=** | 0.6652 | Not Necessarily Different | Cannot reject Ho |
| **p_RU_HL_lin=** | 0.8711 | Not Necessarily Different | Cannot reject Ho |
| **p_RU_LH_lin=** | 0.8287 | Not Necessarily Different | Cannot reject Ho |
| **p_GRIP_HH_lin=** | 0.4488 | Not Necessarily Different | Cannot reject Ho |
| **p_GRIP_HL_lin=** | 0.6849 | Not Necessarily Different | Cannot reject Ho |
| **p_GRIP_LH_lin=** | 0.9569 | Not Necessarily Different | Cannot reject Ho |

| Preload Radial Force | | | |
|---|---|---|---|
| | **p-Value** | **Decision** | **Check** |
| **p_DP_HH_rot=** | 0.9138 | Not Necessarily Different | Cannot reject Ho |
| **p_DP_HL_rot=** | 0.6456 | Not Necessarily Different | Cannot reject Ho |
| **p_DP_LH_rot=** | 0.4017 | Not Necessarily Different | Cannot reject Ho |
| **p_RU_HH_rot=** | 0.6456 | Not Necessarily Different | Cannot reject Ho |
| **p_RU_HL_rot=** | 0.9353 | Not Necessarily Different | Cannot reject Ho |
| **p_RU_LH_rot=** | 0.8924 | Not Necessarily Different | Cannot reject Ho |
| **p_GRIP_HH_rot=** | 0.6263 | Not Necessarily Different | Cannot reject Ho |
| **p_GRIP_HL_rot=** | 0.5885 | Not Necessarily Different | Cannot reject Ho |
| **p_GRIP_LH_rot=** | 0.4171 | Not Necessarily Different | Cannot reject Ho |
| **p_DP_HH_lin=** | 0.8498 | Not Necessarily Different | Cannot reject Ho |
| **p_DP_HL_lin=** | 0.6652 | Not Necessarily Different | Cannot reject Ho |
| **p_DP_LH_lin=** | 0.9138 | Not Necessarily Different | Cannot reject Ho |
| **p_RU_HH_lin=** | 0.372 | Not Necessarily Different | Cannot reject Ho |
| **p_RU_HL_lin=** | 0.8711 | Not Necessarily Different | Cannot reject Ho |
| **p_RU_LH_lin=** | 0.7868 | Not Necessarily Different | Cannot reject Ho |
| **p_GRIP_HH_lin=** | 0.766 | Not Necessarily Different | Cannot reject Ho |
| **p_GRIP_HL_lin=** | 0.7251 | Not Necessarily Different | Cannot reject Ho |
| **p_GRIP_LH_lin=** | 0.7251 | Not Necessarily Different | Cannot reject Ho |

| Catch-up Response Duration | | | |
|---|---|---|---|
| | **p-Value** | **Decision** | **Check** |
| **p_DP_HH_rot=** | 0.2447 | Not Necessarily Different | Cannot reject Ho |
| **p_DP_HL_rot=** | 0.6652 | Not Necessarily Different | Cannot reject Ho |
| **p_DP_LH_rot=** | 0.7867 | Not Necessarily Different | Cannot reject Ho |
| **p_RU_HH_rot=** | 0.3104 | Not Necessarily Different | Cannot reject Ho |
| **p_RU_HL_rot=** | 0.5427 | Not Necessarily Different | Cannot reject Ho |
| **p_RU_LH_rot=** | 0.2914 | Not Necessarily Different | Cannot reject Ho |
| **p_GRIP_HH_rot=** | 0.2083 | Not Necessarily Different | Cannot reject Ho |
| **p_GRIP_HL_rot=** | 0.675 | Not Necessarily Different | Cannot reject Ho |
| **p_GRIP_LH_rot=** | 0.6167 | Not Necessarily Different | Cannot reject Ho |
| **p_DP_HH_lin=** | 0.4248 | Not Necessarily Different | Cannot reject Ho |
| **p_DP_HL_lin=** | 0.8498 | Not Necessarily Different | Cannot reject Ho |
| **p_DP_LH_lin=** | 0.6263 | Not Necessarily Different | Cannot reject Ho |
| **p_RU_HH_lin=** | 0.072 | Not Necessarily Different | Cannot reject Ho |
| **p_RU_HL_lin=** | 0.0215 | Different | Distributions are different |
| **p_RU_LH_lin=** | 0.4017 | Not Necessarily Different | Cannot reject Ho |
| **p_GRIP_HH_lin=** | 0.0398 | Different | Distributions are different |
| **p_GRIP_HL_lin=** | 0.0425 | Different | Distributions are different |
| **p_GRIP_LH_lin=** | 0.6263 | Not Necessarily Different | Cannot reject Ho |

| Time to Peak Normal Force | | | |
|---|---|---|---|
| | **p-Value** | **Decision** | **Check** |
| **p_DP_HH_rot=** | 0.3104 | Not Necessarily Different | Cannot reject Ho |
| **p_DP_HL_rot=** | 0.7868 | Not Necessarily Different | Cannot reject Ho |
| **p_DP_LH_rot=** | 0.3369 | Not Necessarily Different | Cannot reject Ho |
| **p_RU_HH_rot=** | 0.0787 | Not Necessarily Different | Cannot reject Ho |
| **p_RU_HL_rot=** | 0.3437 | Not Necessarily Different | Cannot reject Ho |
| **p_RU_LH_rot=** | 0.9569 | Not Necessarily Different | Cannot reject Ho |
| **p_GRIP_HH_rot=** | 0.1298 | Not Necessarily Different | Cannot reject Ho |
| **p_GRIP_HL_rot=** | 0.5885 | Not Necessarily Different | Cannot reject Ho |
| **p_GRIP_LH_rot=** | 0.5338 | Not Necessarily Different | Cannot reject Ho |
| **p_DP_HH_lin=** | 0.5075 | Not Necessarily Different | Cannot reject Ho |
| **p_DP_HL_lin=** | 0.6948 | Not Necessarily Different | Cannot reject Ho |
| **p_DP_LH_lin=** | 0.6652 | Not Necessarily Different | Cannot reject Ho |
| **p_RU_HH_lin=** | 0.0858 | Not Necessarily Different | Cannot reject Ho |
| **p_RU_HL_lin=** | 0.0483 | Different | Distributions are different |
| **p_RU_LH_lin=** | 0.2036 | Not Necessarily Different | Cannot reject Ho |
| **p_GRIP_HH_lin=** | 0.072 | Not Necessarily Different | Cannot reject Ho |
| **p_GRIP_HL_lin=** | 0.0601 | Not Necessarily Different | Cannot reject Ho |
| **p_GRIP_LH_lin=** | 0.372 | Not Necessarily Different | Cannot reject Ho |

| Time to Peak Normal Force Rate | | | |
|---|---|---|---|
| | **p-Value** | **Decision** | **Check** |
| **p_DP_HH_rot=** | 0.008 | Different | Distributions are different |
| **p_DP_HL_rot=** | 0.0133 | Different | Distributions are different |
| **p_DP_LH_rot=** | 0.0128 | Different | Distributions are different |
| **p_RU_HH_rot=** | 0.1198 | Not Necessarily Different | Cannot reject Ho |
| **p_RU_HL_rot=** | 0.00061943 | Different | Distributions are different |
| **p_RU_LH_rot=** | 0.8924 | Not Necessarily Different | Cannot reject Ho |
| **p_GRIP_HH_rot=** | 0.5792 | Not Necessarily Different | Cannot reject Ho |
| **p_GRIP_HL_rot=** | 0.7972 | Not Necessarily Different | Cannot reject Ho |
| **p_GRIP_LH_rot=** | 0.1988 | Not Necessarily Different | Cannot reject Ho |
| **p_DP_HH_lin=** | 0.4651 | Not Necessarily Different | Cannot reject Ho |
| **p_DP_HL_lin=** | 0.0764 | Not Necessarily Different | Cannot reject Ho |
| **p_DP_LH_lin=** | 0.2134 | Not Necessarily Different | Cannot reject Ho |
| **p_RU_HH_lin=** | 0.0833 | Not Necessarily Different | Cannot reject Ho |
| **p_RU_HL_lin=** | 0.0018 | Different | Distributions are different |
| **p_RU_LH_lin=** | 0.0035 | Different | Distributions are different |
| **p_GRIP_HH_lin=** | 0.4569 | Not Necessarily Different | Cannot reject Ho |
| **p_GRIP_HL_lin=** | 0.5161 | Not Necessarily Different | Cannot reject Ho |
| **p_GRIP_LH_lin=** | 0.8286 | Not Necessarily Different | Cannot reject Ho |

| Preload Grip Force | | | |
|---|---|---|---|
| | **p-Value** | **Decision** | **Check** |
| **p_DP_HH_rot=** | 0.6652 | Not Necessarily Different | Cannot reject Ho |
| **p_DP_HL_rot=** | 0.7251 | Not Necessarily Different | Cannot reject Ho |
| **p_DP_LH_rot=** | 0.7455 | Not Necessarily Different | Cannot reject Ho |
| **p_RU_HH_rot=** | 0.5885 | Not Necessarily Different | Cannot reject Ho |
| **p_RU_HL_rot=** | 0.8498 | Not Necessarily Different | Cannot reject Ho |
| **p_RU_LH_rot=** | 0.9138 | Not Necessarily Different | Cannot reject Ho |
| **p_GRIP_HH_rot=** | 0.3577 | Not Necessarily Different | Cannot reject Ho |
| **p_GRIP_HL_rot=** | 0.4819 | Not Necessarily Different | Cannot reject Ho |
| **p_GRIP_LH_rot=** | 0.6652 | Not Necessarily Different | Cannot reject Ho |
| **p_DP_HH_lin=** | 0.8924 | Not Necessarily Different | Cannot reject Ho |
| **p_DP_HL_lin=** | 0.5338 | Not Necessarily Different | Cannot reject Ho |
| **p_DP_LH_lin=** | 0.4819 | Not Necessarily Different | Cannot reject Ho |
| **p_RU_HH_lin=** | 0.9353 | Not Necessarily Different | Cannot reject Ho |
| **p_RU_HL_lin=** | 0.8287 | Not Necessarily Different | Cannot reject Ho |
| **p_RU_LH_lin=** | 0.6456 | Not Necessarily Different | Cannot reject Ho |
| **p_GRIP_HH_lin=** | 0.8924 | Not Necessarily Different | Cannot reject Ho |
| **p_GRIP_HL_lin=** | 0.7455 | Not Necessarily Different | Cannot reject Ho |
| **p_GRIP_LH_lin=** | 0.5518 | Not Necessarily Different | Cannot reject Ho |

## Chapter 3 Statistics: Effect of Perturbation Axis

| Catch-up Start Time | | | |
|---|---|---|---|
| | p-Value | Decision | Check |
| p_rot_HH= | 0.253 | Not Necessarily Different | Cannot reject Ho |
| p_rot_HL= | 0.207 | Not Necessarily Different | Cannot reject Ho |
| p_rot_LH= | 0.916 | Not Necessarily Different | Cannot reject Ho |
| p_lin_HH= | 0.074 | Not Necessarily Different | Cannot reject Ho |
| p_lin_HL= | 0.279 | Not Necessarily Different | Cannot reject Ho |
| p_lin_LH= | 0.385 | Not Necessarily Different | Cannot reject Ho |

| Peak Normal Force | | | |
|---|---|---|---|
| | p-Value | Decision | Check |
| p_rot_HH= | 0.188 | Not Necessarily Different | Cannot reject Ho |
| p_rot_HL= | 0.162 | Not Necessarily Different | Cannot reject Ho |
| p_rot_LH= | 0.066 | Not Necessarily Different | Cannot reject Ho |
| p_lin_HH= | 0.001 | Different | Distributions are different |
| p_lin_HL= | 0.086 | Not Necessarily Different | Cannot reject Ho |
| p_lin_LH= | 0.002 | Different | Distributions are different |

| Time to Peak Normal Force (Catch-up End) | | | |
|---|---|---|---|
| | p-Value | Decision | Check |
| p_rot_HH= | 0.206 | Not Necessarily Different | Cannot reject Ho |
| p_rot_HL= | 0.033 | Different | Distributions are different |
| p_rot_LH= | 0.020 | Different | Distributions are different |
| p_lin_HH= | 0.709 | Not Necessarily Different | Cannot reject Ho |
| p_lin_HL= | 0.872 | Not Necessarily Different | Cannot reject Ho |
| p_lin_LH= | 0.296 | Not Necessarily Different | Cannot reject Ho |

| Peak Normal Force Rate | | | |
|---|---|---|---|
| | **p-Value** | **Decision** | **Check** |
| **p_rot_HH=** | 0.176 | Not Necessarily Different | Cannot reject Ho |
| **p_rot_HL=** | 0.785 | Not Necessarily Different | Cannot reject Ho |
| **p_rot_LH=** | 0.379 | Not Necessarily Different | Cannot reject Ho |
| **p_lin_HH=** | 0.000 | Different | Distributions are different |
| **p_lin_HL=** | 0.005 | Different | Distributions are different |
| **p_lin_LH=** | 0.000 | Different | Distributions are different |

| Time to Peak Normal Force Rate | | | |
|---|---|---|---|
| | **p-Value** | **Decision** | **Check** |
| **p_rot_HH=** | 0.149 | Not Necessarily Different | Cannot reject Ho |
| **p_rot_HL=** | 0.119 | Not Necessarily Different | Cannot reject Ho |
| **p_rot_LH=** | 0.000 | Different | Distributions are different |
| **p_lin_HH=** | 0.060 | Not Necessarily Different | Cannot reject Ho |
| **p_lin_HL=** | 0.011 | Different | Distributions are different |
| **p_lin_LH=** | 0.052 | Not Necessarily Different | Cannot reject Ho |

| Preload Radial Force | | | |
|---|---|---|---|
| | **p-Value** | **Decision** | **Check** |
| **p_rot_HH=** | 0.565 | Not Necessarily Different | Cannot reject Ho |
| **p_rot_HL=** | 0.771 | Not Necessarily Different | Cannot reject Ho |
| **p_rot_LH=** | 0.596 | Not Necessarily Different | Cannot reject Ho |
| **p_lin_HH=** | 0.974 | Not Necessarily Different | Cannot reject Ho |
| **p_lin_HL=** | 0.851 | Not Necessarily Different | Cannot reject Ho |
| **p_lin_LH=** | 0.963 | Not Necessarily Different | Cannot reject Ho |

| Preload Grip Force | | | |
|---|---|---|---|
| | **p-Value** | **Decision** | **Check** |
| **p_rot_HH=** | 0.769 | Not Necessarily Different | Cannot reject Ho |
| **p_rot_HL=** | 0.512 | Not Necessarily Different | Cannot reject Ho |
| **p_rot_LH=** | 0.873 | Not Necessarily Different | Cannot reject Ho |
| **p_lin_HH=** | 0.743 | Not Necessarily Different | Cannot reject Ho |
| **p_lin_HL=** | 0.898 | Not Necessarily Different | Cannot reject Ho |
| **p_lin_LH=** | 0.549 | Not Necessarily Different | Cannot reject Ho |

| Catch-up Duration | | | |
|---|---|---|---|
| | **p-Value** | **Decision** | **Check** |
| **p_rot_HH=** | 0.171 | Not Necessarily Different | Cannot reject Ho |
| **p_rot_HL=** | 0.019 | Different | Distributions are different |
| **p_rot_LH=** | 0.021 | Different | Distributions are different |
| **p_lin_HH=** | 0.667 | Not Necessarily Different | Cannot reject Ho |
| **p_lin_HL=** | 0.847 | Not Necessarily Different | Cannot reject Ho |
| **p_lin_LH=** | 0.161 | Not Necessarily Different | Cannot reject Ho |

# APPENDIX D: COPYRIGHT PERMISSIONS

Licensee: Michael De Gregorio

License Date: Jul 15, 2013

License Number: 3190301260601

Publication: Journal of Biomechanics

Title: Precision grip responses to unexpected rotational perturbations scale with axis of rotation

Type Of Use: reuse in a thesis/dissertation